AD NUMBER

AD884048

NEW LIMITATION CHANGE

TO

Approved for public release, distribution unlimited

FROM

Distribution authorized to U.S. Gov't. agencies only; Test and Evaluation; APR 1971. Other requests shall be referred to Naval Ship Systems Command, Attn: OOV11, Washington, DC 20360.

AUTHORITY

USNSSC ltr, 4 Jun 1974

THE UNIVERSITY OF TEXAS AT AUSTIN

ARL-TR-71-16
19 April 1971

Copy No. 11

SCATTERING AND PROPAGATION OF ACOUSTIC WAVES IN THE PRESENCE OF ROUGH, PENETRABLE BOUNDARIES

FINAL REPORT UNDER CONTRACT N00024-70-C-1279
1 April 1970 - 31 March 1971

Michael L. Boyd, Roy L. Deavenport
Patrick J. Welton

NAVAL SHIP SYSTEMS COMMAND
Contract N00024-70-C-1279
Proj. Ser. No. SF 11552001, Task 8118

UNCLASSIFIED, FOUO

Security Classification

DOCUMENT CONTROL DATA - R & D

(Security classification of title, body of abstract and indexing annotation must be entered when the overall report is classified)

1 ORIGINATING ACTIVITY (Corporate author)	2a. REPORT SECURITY CLASSIFICATION
Applied Research Laboratories The University of Texas at Austin Austin, Texas 78712	UNCLASSIFIED, FOUO 2b GROUP ---

3 REPORT TITLE

SCATTERING AND PROPAGATION OF ACOUSTIC WAVES IN THE PRESENCE OF ROUGH, PENETRABLE BOUNDARIES

4 DESCRIPTIVE NOTES (Type of report and inclusive dates)

Final Report under Contract N00024-70-C-1279, 1 April 1970 - 31 March 1971

5 AUTHOR(S) (First name, middle initial, last name)

Michael L. Boyd, Roy L. Deavenport, Patrick J. Welton

6 REPORT DATE	7a TOTAL NO OF PAGES	7b NO OF REFS
19 April 1971	130	60

8a CONTRACT OR GRANT NO	9a. ORIGINATOR'S REPORT NUMBER(S)
N00024-70-C-1279 b PROJECT NO SF 11552001, Task 8118	ARL-TR-71-16
c. d	9b OTHER REPORT NO(S) (Any other numbers that may be assigned this report)

10 DISTRIBUTION STATEMENT

Distribution limited to U. S. Government agencies only; TEST AND EVALUATION, 13 May 1971. Other requests for this document must be referred to NAVSHIPS 00V1

11 SUPPLEMENTARY NOTES	12 SPONSORING MILITARY ACTIVITY
---	Naval Ship Systems Command Department of the Navy Washington, D. C. 20360

13 ABSTRACT

In this report, the reflection and scattering models and the propagation model including the effects of realistic ocean boundaries are further developed. (U-FOUO)

A brief introduction which includes a short history of the scattering and propagation work performed at ARL, and the considerations which motivated the research represented in this report is given in Chapter I. In Chapter II, the theoretical foundations of the scattering by acoustically penetrable surfaces are presented. The formulas developed in Chapter II are used in Chapter III to investigate the effects of various realistic ocean bottoms on the performance of bottom bounce sonars. Once the effect of a known bottom on the signal can be predicted, the problem of predicting the physical properties of the bottom from the signals it returns becomes manageable. Certain relevant aspects of this problem are discussed Chapter IV, specifically, the prediction of the forward reflected signal from measurements of the backscattered signal. In Chapter V, propagation in a surface duct with realistic boundaries is treated, and the attenuation per mode due to boundary roughness is calculated for the Epstein model. Finally, the preliminary work on the experimental measurements of the scattering by acoustically penetrable, rough surfaces is presented in Appendix A. (U-FOUO)

DD FORM 1 NOV 1473 (PAGE 1)

N 0101-807-6801

UNCLASSIFIED, FOUO

Security Classification

14 KEY WORDS	LINK A		LINK B		LINK C	
	ROLE	WT	ROLE	WT	ROLE	WT
Rough Surface						
Reflection Coefficients						
Rough Attenuating Bottom						
Potential Theory						
Sonar Systems						
Ccean Bottom Parameters						
Surface Duct Propagation						
Green's Function						

ARL-TR-71-16
19 April 1971

SCATTERING AND PROPAGATION OF ACOUSTIC WAVES IN THE PRESENCE OF ROUGH, PENETRABLE BOUNDARIES

FINAL REPORT UNDER CONTRACT N00024-70-C-1279
1 April 1970 - 31 March 1971

Michael L. Boyd
Roy L. Deavenport
Patrick J. Welton

NAVAL SHIP SYSTEMS COMMAND
Contract N00024-70-C-1279
Proj. Ser. No. SF 11552001, Task 8118

APPLIED RESEARCH LABORATORIES
THE UNIVERSITY OF TEXAS AT AUSTIN
AUSTIN, TEXAS 78712

ABSTRACT

In this report, the reflection and scattering models and the propagation model including the effects of realistic ocean boundaries are further developed.

A brief introduction which includes a short history of the scattering and propagation work performed at ARL and the considerations which motivated the research represented in this report is given in Chapter I. In Chapter II, the theoretical foundations of the scattering by acoustically penetrable surfaces are presented. The formulas developed in Chapter II are used in Chapter III to investigate the effects of various realistic ocean bottoms on the performance of bottom bounce sonars. Once the effect of a known bottom on the signal can be predicted, the problem of predicting the physical properties of the bottom from the signals it returns becomes manageable. Certain relevant aspects of this problem are discussed in Chapter IV, specifically, the prediction of the forward reflected signal from measurements of the backscattered signal. In Chapter V, propagation in a surface duct with realistic boundaries is treated, and the attenuation per mode due to boundary roughness is calculated for the Epstein model. Finally, the preliminary work on the experimental measurements of the scattering by acoustically penetrable, rough surfaces is presented in Appendix A.

TABLE OF CONTENTS

TABLE OF CONTENTS (Cont'd)

I. INTRODUCTION

The detection, localization, and classification of targets in the ocean environment require extensive and detailed knowledge of the propagation of acoustic energy in the ocean. Typically, sonar operation is a complex problem involving the propagation of sound in an inhomogeneous medium with imperfect boundaries (a perfect boundary is a plane, acoustically impenetrable surface). As a consequence of the medium inhomogeneity and the boundary imperfections, two related limitations on sonar operation arise. Due to the inhomogeneity of the ocean, so called "shadow zones" and sound channels exist in the ocean. The propagation of signals into a shadow zone or in sound channels depends in a very complicated manner on the ocean surface and bottom. The effects of the imperfect ocean boundaries are seen as losses in the strength of the returned signal and as reverberation returns. The bottom bounce mode and the surface duct mode are two examples of sonar operational modes which are required to obtain coverage of certain regions of the ocean volume, but which, nevertheless, are limited by the ocean boundaries.

The development of more effective sonars requires increased knowledge of the physical nature of the ocean surface, the bottom, the water between these surfaces, and the effect of these factors on the propagation of sound. Accordingly, extensive full scale sea tests have been conducted to study the ocean environment, the acoustic scattering properties of the ocean surface and bottom, and long range propagation in the ocean.

Full scale experiments at sea are an invaluable source of data for typical conditions that might be expected in an operational situation. Environmental conditions, surface wave structure, and bottom composition and roughness can only be obtained by in situ measurement. However, the generally uncontrolled sea conditions and lack of precise knowledge of the test geometry can introduce ambiguities when particular aspects of scattering or propagation theory are to be investigated. In response to these difficulties measurements using models where the geometry and the physical composition and topography of the boundary surfaces could be precisely controlled were initiated.

In view of the complex and entangled effects of the medium and its boundaries, the treatment of acoustic propagation in the ocean is greatly facilitated by separating it into two problems. The first problem is the study of propagation in an inhomogeneous medium with perfectly reflecting plane boundaries. The second problem deals with propagation in a homogeneous medium with imperfect boundaries, that is, the reflection and scattering problem. The reflection and scattering problem is further simplified by separating the effects due to the topography of the boundary and the effects due to the acoustic penetrability of the boundary, which depends on the physical composition of the boundary media.

In 1961, a research program was initiated at Applied Research Laboratories to investigate experimentally and theoretically the reflection and scattering of sound from the ocean boundaries. The first studies conducted under this program involved the reflection of sound by plane layered sediments of the type usually found in abyssal plain areas and the scattering of sound by a pressure release sinusoidal surface. These studies were performed under Contract NObsr-72627 and resulted in very satisfactory agreement between the experimental and theoretical results.

Upon completion of these investigations, the study of the scattering properties of pressure release randomly rough surfaces was undertaken. This work was done under Contracts NObsr-93127, N00024-68-C-1112, and N00024-68-C-1275 and covered the period from January 1967 to April 1970. The experimental program resulted in the measurement of the forward, specular, and backscattering properties at the frequencies 100, 200, and 500 kHz of four rough surfaces with different rms heights. The frequency-roughness regimes investigated represent the extremes of the cases where the wavelength is much greater than the roughness to the case where the wavelength is very much less than the roughness.

The theoretical investigations conducted under this program have resulted in a totally new and very powerful formulation of scattering problems. The theory which is now available gives very good agreement for all cases of forward and specular scattering and predicts the way in which the range behavior of scattering depends on roughness. The theory had previously proved inadequate for backscattering predictions at low grazing angles. This defect in the theory has now been corrected.

This final report is a summary of the research on acoustically penetrable rough surface scattering and propagation in a surface duct with a realistically rough boundary. This work was performed under Contract N00024-70-C-1279 from 1 April 1970 to 31 March 1971. The work done under this contract represents an effort to combine the topographical and physiological effects of the bottom into a unified scattering treatment. Further, the surface duct propagation study is an attempt to incorporate a realistically rough boundary into the propagation model.

This final report is composed of the following sections. A brief introduction to the report has been given in Chapter I. The

theoretical foundations of scattering by penetrable surfaces are presented in Chapter II. In Chapter III, the formulas developed in Chapter II are used to investigate the effects of various realistic ocean bottoms on the operation of bottom bounce sonars. Once the effect of a known bottom on the signal can be predicted, the problem of predicting the physical properties of the bottom from the signals it returns becomes manageable. Certain relevant aspects of this problem are discussed in Chapter IV, specifically, the prediction of the forward reflected signal from measurements of the backscattered signal. In Chapter V, the propagation in a surface duct with realistic boundaries is treated, and the attenuation per mode due to boundary roughness is calculated for the Epstein model. Finally, the preliminary work on the experimental measurements of the scattering by acoustically penetrable, rough surfaces is presented in Appendix A.

The theoretical and experimental methods developed in these investigations should prove useful in the choice of some of the operational characteristics of present and future sonar systems. In addition, further understanding of the limitations imposed by the properties of the boundaries on detection and localization capabilities of modern sonars should result from these studies. Another important consequence of these investigations is the verification or improvement of mathematical models being used in numerous computer simulation studies of optimum sonar operation.

II. REFLECTION COEFFICIENTS FOR A ROUGH, ACOUSTICALLY PENETRABLE SURFACE

A. Introduction

It was pointed out in Chapter I that the scattering behavior of the ocean boundaries depends on both the topography and the physical composition of the boundary. The topography controls the scattering while the physical composition of the boundaries determines the acoustic penetrability of a surface, and as will be seen later, the two effects interact. On some boundaries, for example the water-air interface, the acoustic impedance is so large that practically all of the sound remains trapped in the ocean; consequently, the scattering depends entirely on the surface topography (including bubbles, etc.). On the other hand, the problem of scattering at the ocean bottom requires for its solution the inclusion of the effects of both the topography and the physical composition of the bottom. The scattering due to topography alone has a very extensive literature and is now thought to be well understood. However, very little is known about the effect of the acoustic penetrability of the boundary on scattering. Most of the literature available treats only the single interface case and does not give a very good account of the interrelation of the topography and acoustic penetrability of the scattering surface. In this section of the final report, the effect of the acoustic penetrability of the ocean bottom will be incorporated into the scattering integral developed earlier in the program, and the interaction of the topography with the penetrability will be discussed.

Historically the problem of calculating the scattered pressure from an acoustically penetrable interface, such as the ocean bottom, has been treated in a number of ways. The most common method has been to assume that the pressure scattered by the acoustically penetrable interface is given by the pressure scattered from a perfectly reflecting surface modified by a suitable reflection coefficient to account for the penetration losses. The form of the reflection coefficient is determined by the boundary conditions at the surface, and its value is determined by the local geometry (local slope of the surface). If the surface is plane or suitably smooth, the local geometry is the same everywhere on the surface and the reflection coefficient is usually assumed to be the Rayleigh coefficient. It should be pointed out that to arrive at the Rayleigh coefficient it is necessary to assume that the incoming radiation is a plane wave and that the outgoing (reflected) wave is radiated in the local specular direction. This assumption is inconsistent with the integral equation of scattering which is based only on wave mechanics (as opposed to ray theory). It will be shown that the restriction on the outgoing wave can be easily removed in the context of the potential formulation, and in the limit $kr \gg 1$ (k is the wave number and r is the separation distance of the source and surface), this formulation results in a reflection coefficient identical to the Rayleigh coefficient for the single rough interface case.

For smooth surfaces, it is usually assumed that the reflection coefficient can be removed from the scattered pressure integral. Since the slopes are small, the local value of the reflection coefficient may be everywhere approximated by the value of Rayleigh coefficient referenced to the mean plane, and this coefficient can be removed from the integral as a constant. When this is done, the remaining integral can be evaluated in a straightforward manner, and it gives the expression for the field scattered by a pressure release surface. However, if the surface is rough, the boundary conditions are only given locally,

so the value of the reflection coefficient varies from point to point on the surface. Thus, the reflection coefficient cannot be removed from the integral for the scattered pressure except in an averaged form. Due to the large rms roughness of the surfaces considered in this program, a treatment of the reflection coefficient within the context of the scattered pressure integral has been pursued. This basic approach has been modified in several ways to give expressions for the reflection coefficient. These results will be discussed later in this section and may be generally classified as the series, the exact, and the stationary phase expressions. In addition, the reflection coefficient given by Kuo[1] is included in this section for the sake of comparison.

B. Formal Development

The reflection coefficients presented in this section were all calculated for the same sets of bottom parameters. The parameters used were those given by Mackenzie[2] for four separate coastal bottom samples (these data were originally published by Hamilton et al.[3]). The samples used in this section were: sample number 13 (sand-silt-clay), sample number 27 (clayey fine silt), sample number 28 (silty very fine sand), and sample number 32 (sand). The attenuations for these samples at 30 kHz were 5.61, 1.42, 2.63, and 4.48 dB per foot, respectively.

1. Kuo's Reflection Coefficient

The reflection coefficient given by E. Y. T. Kuo is presented in this section because it is a fairly well known result which can serve as a basis for comparison with other reflection coefficients.[1]

The coefficients are calculated for a backscattering geometry on the assumption of a single interface and are given by

$$\mathcal{R}(\gamma) = \frac{\rho_2 c_2 \gamma - \rho_1 c_1 \eta}{\rho_2 c_2 \gamma + \rho_1 c_1 \eta} + 2 \frac{(1-\gamma^2)\rho_2 c_2^2 (\rho_2 - \rho_1)}{(\rho_2 c_2 \gamma + \rho_1 c_1 \eta)} \quad , \tag{1}$$

where

$$\eta = \left[1 - \left(\frac{c_2}{c_1} \right)^2 (1-\gamma^2) \right]^{1/2} \quad , \tag{2}$$

and

$$\gamma = \sin\Phi \quad .$$

Here, Φ is the receiver grazing angle, ρ_1 and c_1 are the density and sound velocity in the first medium (water), and ρ_2 and c_2 are the density and sound velocity in the second medium (bottom). This coefficient is restricted to fairly smooth surfaces. The coefficient given by Eq. (1) was evaluated using the parameters of all four bottom samples, with the results shown in Dwg. AS-71-213. Near normal incidence these curves approach the value of the Rayleigh coefficient; however, at low grazing angles they become quite large. Although these coefficients, when used in conjunction with Kuo's scattering coefficients, give fairly good fits to some backscatter data, it is thought that reflection coefficients that have average magnitudes greater than unity over large ranges of grazing angle must be regarded as nonphysical. At any given grazing angle a reflection coefficient could, without violating any energy considerations, have a magnitude greater than unity due to focusing effects. However, to exhibit this behavior over a large range of grazing angles implies a large radius of curvature of the mean plane, which is inconsistent with the assumptions that have already been made about the nature of the surface. In conclusion, to

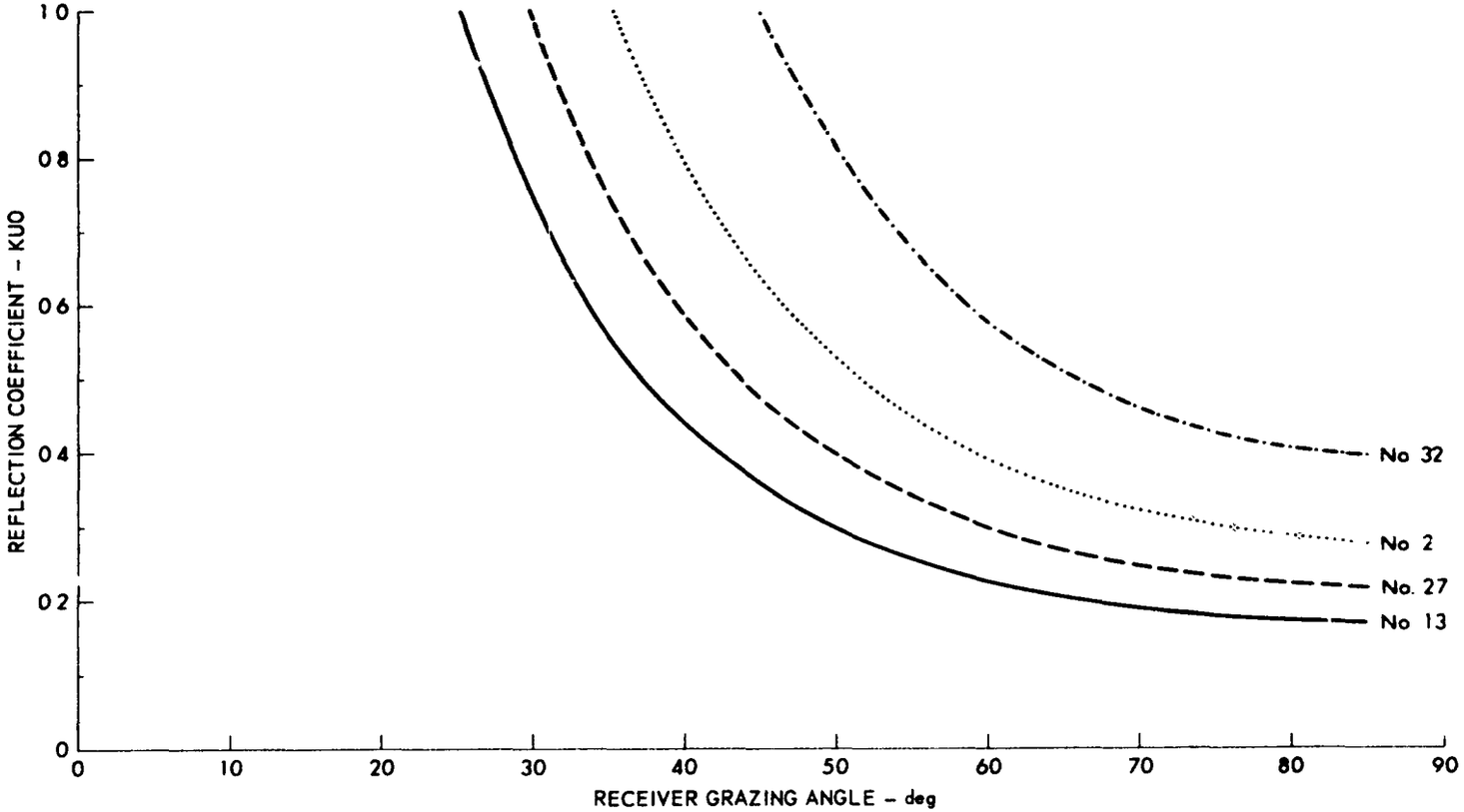

ARL - UT
AS-71-213
MLB - RFO
3 - 30 - 71

KUO'S REFLECTION COEFFICIENT FOR BACKSCATTERING
GEOMETRY FOR FOUR BOTTOM SAMPLES

understand the relatively good agreement of Kuo's results with experimental data, it is necessary to consider the entire expression for the scattered field. The separation of the scattering coefficient from the reflection coefficient does not appear to be consistent because, ir the limit of rigid or pressure release surfaces, the reflection coefficient obviously does not give the correct values. Thus, Kuo's result does not conform to the generally accepted definition of a reflection coefficient and can only be meaningful in the context of his scattering theory.

2. The Calculation of the Pressure Density in the Case of Penetrable Interfaces

a. Single Interface

In the introduction to this section it was pointed out that the adjustment of the boundary conditions to account for the acoustic penetrability of the scattering interface has usually been done by incorporating the Rayleigh reflection coefficient $R(\varphi_i)$ into the scattered pressure

$$p_s = R(\varphi_i)p_i \quad .$$

Further, it was stated that this method is inconsistent with the wave mechanics viewpoint of the integral equation. It is a simple matter to avoid this inconsistency by starting with the potential expression for the reflected or scattered field and then determining the unknown pressure density on the surface.

Consider the geometry in Dwg. AS-70-795. The line indicated by p_i connects the source Q and the surface point N. The line labeled p_R connects the surface point N to the receiver at A.

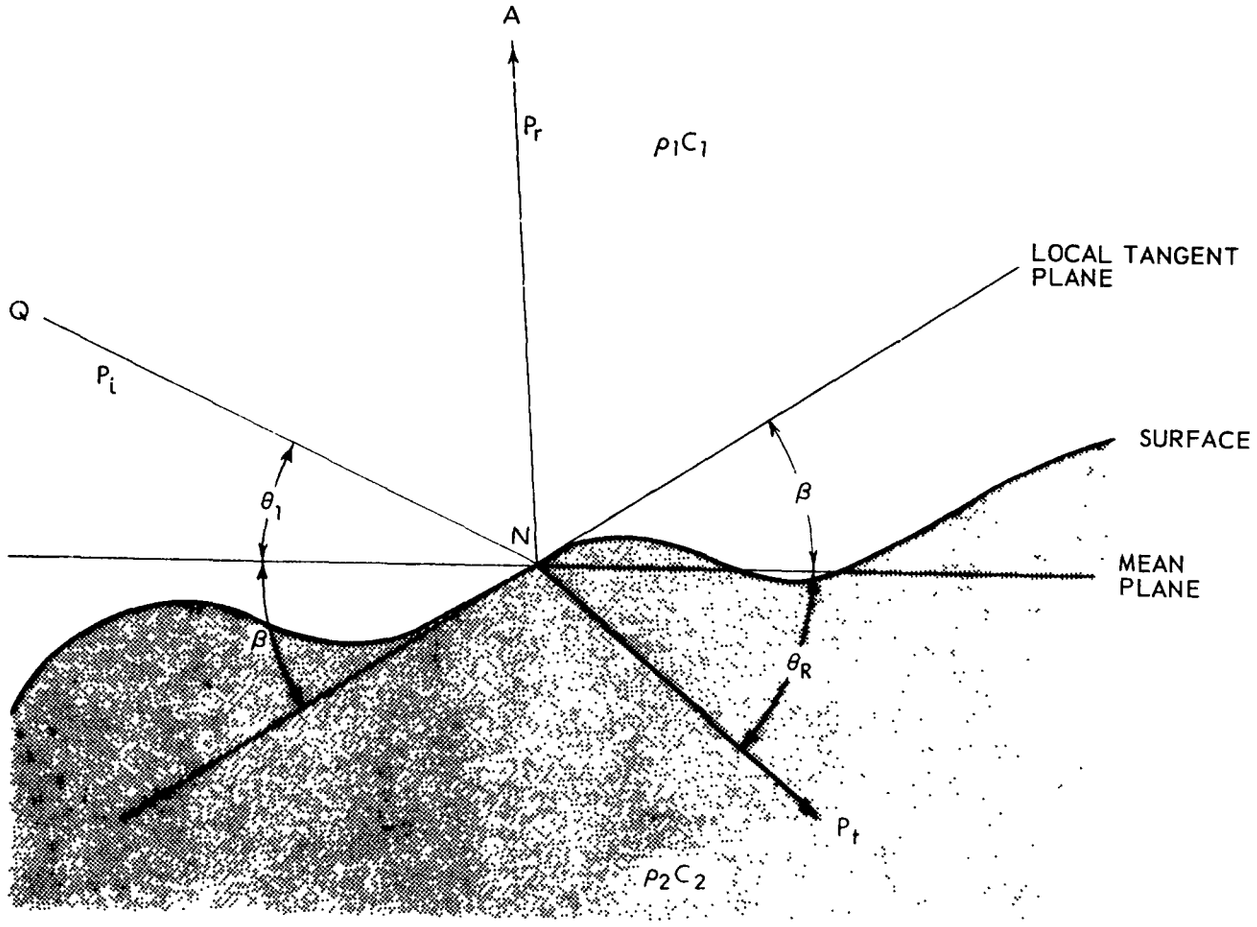

ACOUSTICALLY PENETRABLE ROUGH SURFACE GEOMETRY
SINGLE INTERFACE CASE

ARL - UT
AS-70-795
PJW - ORS
7 - 3 - 70

Then the incident pressure density at N due to the source at Q is given by

$$p_i(N) = \frac{e^{ik_1 r_o}}{r_o} \quad , \tag{3}$$

where $r_o = |QN|$. The reflected or scattered field, $p_R(A)$, at the receiver A, due to the distribution of pressure on the surface, is given by

$$p_R(A) = \iint_S \mu \frac{\partial}{\partial n} \left(\frac{e^{ik_1 r_1}}{r_1} \right) dS \quad , \tag{4}$$

where μ is some as yet unspecified pressure density (potential) on the side of the surface towards A, here $r_1 = |AN|$, k_1 is the wave number in the upper medium, and n is the outward normal with respect to the surface.

The problem is to calculate the reflected or scattered pressure $p_R(A)$ at A. The calculation of $p_R(A)$ could be performed if μ were known; hence, the problem reduces to that of determining μ.

Consider Eq. (4); if the field point A is allowed to approach the boundary point N, then Eq. (4) becomes

$$p_R(N) = 2\pi\mu(N) + \iint_S \mu \frac{\partial}{\partial n} \left(\frac{e^{ik_1 r_s}}{r_s} \right) dS \quad , \tag{5}$$

where the integral term represents the multiple scattering term. If it is assumed that as a first approximation $p_R(N) \cong Rp_i(N)$,

where R is some unknown constant, then Eq. (5) may be solved by iteration yielding

$$p_R(N) = Rp_i(N) + \frac{1}{2\pi} \iint_S Rp_i(N') \frac{\partial}{\partial n} \left(\frac{e^{-ik_1 r_s}}{r_s} \right) dS \quad . \qquad (6)$$

If multiple scattering is negligible, then Eq. (6) may be approximated as

$$p_R(N) \cong Rp_i(N) \quad , \qquad (7)$$

and then

$$\mu \cong \frac{R}{2\pi} p_i(N) \quad . \qquad (8)$$

It may be said that Eqs. (7) and (8) are fairly obvious, but in obtaining them in this manner, it is clear that they are approximations and that the method of performing the exact calculation is indicated.

The problem has now been reduced to finding R, which is some pressure density coefficient. It will now be expedient to collect certain quantities which will prove useful in the calculation of R.

The pressure transmitted through the interface is also an outgoing wave, and it is given by

$$p_T = \iint_S \omega \frac{\partial}{\partial n} \left(\frac{e^{ik_2 r_2}}{r_2} \right) dS \quad , \qquad (9)$$

where

p_T is taken at some field point B in the lower medium,

ω is the pressure density on the lower side of the surface,

$r_2 = |NB|$,

k_2 is the wave number in medium 2, and

n is the outward normal with respect to the surface.

Using the same analysis as in Eq. (4), it is easily seen that

$$p_T \cong T p_i(N)$$

$$\omega \cong \frac{T}{2\pi} p_i(N) \quad , \tag{10}$$

where T is again some unknown constant.

Now, for penetrable, liquid boundary media, the boundary condition is the continuity of the pressure across the boundary interface. A consequence of this condition is Snell's Law

$$\vec{k}_1 \cdot \hat{t} = \vec{k}_2 \cdot \hat{t} \quad , \tag{11}$$

where k_1 and k_2 are the wave vectors in media 1 and 2, and $\hat{t}$ is the unit tangent at point N of the boundary. If the interface were perfectly plane, then Eq. (11) reduces to

$$k_1 \cos\theta_1 = k_2 \cos\theta_2 \quad ,$$

which is the usual expression of Snell's Law.

The boundary condition itself is not sufficient to uniquely determine μ; however, a further condition is obtained at the boundary from the hydrodynamic equation of continuity. This equation implies that if the interface remains intact, then the normal component of the velocity is continuous across the interface.

It is well known that for a homogeneous medium the velocity fields are easily related to the pressure fields. In fact, the normal component of the velocity field φ_j in the jth medium is related to the pressure p_j by the simple expression

$$\varphi_j = \frac{1}{\rho_j} \frac{\partial p_j}{\partial n} \quad , \tag{12}$$

where ρ_j is the static density of jth medium.

The pressure densities μ and ω are related similarly to the normal component of the surface velocity density χ

$$\chi_j = \frac{1}{\rho_j} \frac{\partial \mu_j}{\partial n} \quad .$$

The application of the boundary condition and the continuity condition gives the two following independent equations:

$$p_i(N) + p_R(N) = p_T(N) \quad ,$$

and (13)

$$\varphi_i(N) + \varphi_R(N) = \varphi_T(N) \quad .$$

Substituting Eq. (12) into Eqs. (3), (4), and (9), respectively, and distinguishing between outgoing and incoming waves give the following

expressions for the normal component of the incident, reflected and transmitted velocity fields:

$$\varphi_i(N) = \frac{ik_1}{\rho_1}\frac{\partial r_o}{\partial n}\left[1 - \frac{1}{ik_1 r_o}\right] p_i \quad ,$$

$$\varphi_R(N) = -R\,\frac{ik_1}{\rho_1}\frac{\partial r_o}{\partial n}\left[1 - \frac{1}{ik_1 r_o}\right] p_i \quad , \tag{14}$$

and

$$\varphi_T(N) = T\,\frac{ik_2}{\rho_2}\frac{\partial r_2}{\partial n}\left[1 - \frac{1}{ik_2 r_o}\right] p_i \quad .$$

The quantity $k_1 \partial r_o/\partial n$ can be identified as $\vec{k}_1 \cdot \hat{n}$, the component of the wave vector in medium 1 which is locally normal to the surface. Hence,

$$k_{n1} = k_1 \frac{\partial r_o}{\partial n} = k_1 \sin(\theta_1 + \beta) \quad , \tag{15}$$

where β is the inclination of the local slope to the mean plane. Similarly, the term $k_2 \partial r_2/\partial n$ can be identified as the normal component of the wave vector in medium 2. Further using Snell's Law, this component is uniquely determined as

$$k_{n2} = k_2 \frac{\partial r_2}{\partial n} = k_2 \sin(\theta_2 + \beta) \quad . \tag{16}$$

Substituting Eqs. (7), (10), and (14) into Eq. (13) and solving for R give the pressure density, μ,

$$\mu = \frac{1}{2\pi} R p_i(N) \quad ,$$

where

$$R = \frac{\rho_2 k_{n1}\left[1 - \frac{1}{ik_1 r_o}\right] - \rho_1 k_{n2}\left[1 - \frac{1}{ik_2 r_o}\right]}{\rho_2 k_{n1}\left[1 - \frac{1}{ik_1 r_o}\right] + \rho_1 k_{n2}\left[1 - \frac{1}{ik_2 r_o}\right]} \quad . \tag{17}$$

In the limit as $k_1 r_o \gg 1$ and $k_2 r_o \gg 1$, Eq. (17) has the same form as the Rayleigh reflection coefficient for a single interface. Equation (17) has certain inherent advantages over the Rayleigh reflection coefficient. First of all, since the reflected or transmitted fields were given in terms of an integral equation which required only the incident pressure density on the surface, no condition on the reflected or transmitted field arises. For example, the condition of specularity of the locally reflected field is not present; this is in accordance with the usual wave mechanics viewpoint. Second, it was not necessary to make the appeal to the tangent plane approximation. Further, the theory utilized spherical waves and contained no requirement that the surface be in the farfield of the source. Realistically, for most sources, the surface should be far enough removed so that nearfield source behavior can be neglected in the pressure density on the surface.

From the preceding derivation, it is clear that, for a source removed many wavelengths from a penetrable surface, a suitable approximation for the surface pressure potential, μ, is given by modifying the incident pressure density $p_i(N)$ by the factor R. Further this factor R is equivalent to the Rayleigh reflection coefficient but does not contain the explicit assumption of specularity to determine the surface pressure density of the reflected field.

b. Double Interface

It was just shown that, for a single rough interface, the Rayleigh reflection coefficient referenced with respect to the local incident angle will be the correct result if multiple scattering among features on the interface is negligible. However, in the case of two rough interfaces the correct result will not be obtained by assuming the two interface Rayleigh reflection coefficient and by modifying it to include the local incident angles as has been done by Clay.[4,5] The only other paper to treat scattering by rough layers is by Krishen and Koepsel.[6] They recognize the inadequacy of Clay's method and attempt to account for the scattering between layers. They assume that each layer is in the farfield of the other and use Eckart's[7] method to obtain the scattered pressure at one interface due to the presence of the other rough interface. Further, they assume that the Rayleigh reflection coefficients are valid at each interface and proceed on the basis of this assumption. Several objections can be raised to their method. First, Eckart's method does not lead to the correct expression for the pressure scattered or transmitted by a rough surface. Further, for the reasons mentioned previously, it is not intuitively obvious that the Rayleigh reflection coefficients should be applied to the scattering at each interface.

The pressure at some receiver A above a rough surface is given by the potential integral in Eq. (4). In the case where the water-bottom interface is acoustically penetrable and contains another interface at some deeper depth, the pressure density, μ, at the water-sediment interface must include the interaction and interference effects due to the sub-bottom reflections. The geometry is shown in Dwg. AS-71-354.

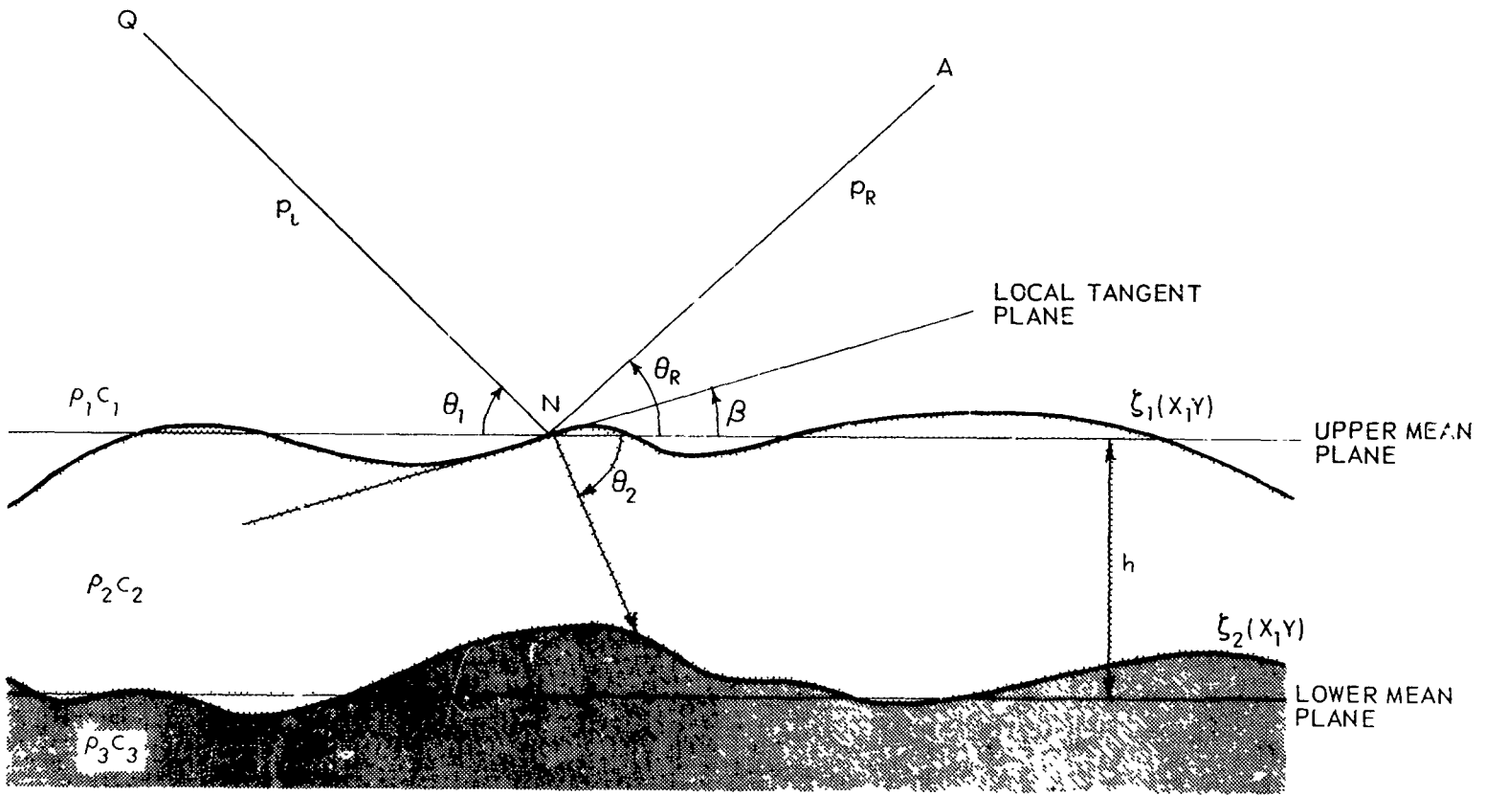

ACOUSTICALLY PENETRABLE ROUGH SURFACE GEOMETRY
DOUBLE INTERFACE CASE

The method used to calculate the equivalent pressure density due to a double interface is identical to the method used for the single interface, but in addition it will rely heavily on the calculation of the scattered pressure given in previous final reports. This method allows the integration over the lower scattering interface to be bypassed.

Assume that the two interfaces are represented by the stochastic processes $z_1 = \zeta_1(x,y)$ and $z_2 = \zeta_2(x,y)$ and that the mean planes of the two processes are parallel and separated by the vertical distance h. Assume further that

$$\zeta_1^{MAX} \quad , \quad \zeta_2^{MAX} < h$$

and that the insonified area of the surface is much greater than h^2 and also includes many correlation lengths. From these conditions it may then be assumed that the pressure density (or normal velocity field density) at any point on the lower interface is the sum of the contributions from a region of the upper interface which is many correlation lengths in size. The significance of these assumptions is that now the equivalent pressure density must be calculated in terms of the <u>average</u> pressure densities and normal velocity densities contributed by the lower interface; that is, the averages are taken <u>before</u> calculating the equivalent surface potential. In general, taking the averages of the expressions used to derive the equivalent pressure density is much easier than taking the average of the equivalent pressure density itself. It should be recognized, however, that if the contributing surfaces have dimensions of only fractions of a correlation length, then the equivalent pressure density must be calculated first and the average of this quantity taken.

Using these assumptions, the equivalent pressure density in the case of a double interface is found to be

$$\mu = Rp_i \quad , \tag{18}$$

where

$$R = \frac{R_{12} + \Delta R_{23} e^{-i2k_2 \sin\theta_2 h}}{1 + \Delta R_{12} R_{23} e^{-i2k_2 \sin\theta_2 h}} \quad . \tag{19}$$

The quantities R_{12} and R_{23} are the reflection coefficients which would exist at interfaces 1 and 2, respectively, if medium 2 were infinite in extent; they are given by Eq. (17). R_{23} is calculated using the average pressures at interface 2. Finally, Δ is the term which arises because part of the pressure at interface 1 has been scattered upwards by the lower interface.

If it is assumed that the upper interfacc has mild slopes, then Δ is given by

$$\Delta = \left\langle (1 - \eta_2 \cot\theta_2)\, e^{-i\eta_2 k_2 h\cos\theta_2 + i\eta_2 \zeta' k_2 \cos\theta_2} \right\rangle \quad ,$$

where η_2 is the local slope of the lower interface, and ζ' is the variation of the separation of the interfaces about the mean value h. Performing the average indicated in the previous expression yields

$$\Delta = \left(1 - i \cot\theta_2 \frac{s^2 k_2 \cos\theta_2 h}{\left[1 + s^2\sigma^2 k_2^2 \cos^2\theta_2\right]^{3/2}} \right) e^{-\frac{s^2 k_2^2 \cos^2\theta_2 h^2}{2\left(1 + s^2\sigma^2 k_2^2 \cos^2\theta_2\right)}} \quad , \tag{20}$$

where s is the rms value of the lower interface slopes, and σ is the rms value of the fluctuation of the interface separation ζ' about the mean value h.

Clearly, in the limit of two plane, parallel interfaces $\Delta \to 1$ (since s and $\sigma \to 0$) and R approaches the Rayleigh reflection coefficient for the two interface case. However, it must be noted that Eq. (19) can not be obtained by simply taking the Rayleigh reflection coefficient and referencing it with respect to the local geometry. To obtain a valid expression for the equivalent pressure density in the case of a double interface, it is necessary to start with the appropriate pressure expressions and boundary conditions.

It should be emphasized that R [Eq. (19)] is not a constant, but rather is a function of the local geometry of the upper interface. This dependence is contained in the R_{12} terms, which are simply the reflection coefficients for interface 1 referenced to the local geometry. Consequently, R_{12} is a function of the slopes of the upper interface and must be used in conjunction with the scattering integral exactly as the single interface reflection coefficient shown in Eq. (20).

c. Summary

In this portion [Section B] of Chapter II, the effect of the surface configuration and physical composition on the boundary value (i.e., the equivalent pressure density) used in the scattering integrals has been calculated. This work was motivated by the need to determine the boundary values in a manner which was consistent with the integral equation of scattering and, consequently, required no assumptions about the direction of propagation of the reflected or scattered field. For the case of a single interface, it was found

that if the source was many wavelengths from the surface, the correct boundary value for a rough, acoustically penetrable surface is given by multiplying the incident pressure density by the Rayleigh reflection coefficient referenced with respect to the local slope. In the event there is another rough interface underlying the water-bottom interface, the equivalent pressure density on the bottom must include the scattering and interference effects of the sub-bottom interface. However, it was found that these effects could not be accounted for by simply referencing the two interface Rayleigh reflection coefficient to the local slope because this does not account for the scattering by the sub-bottom.

The scattering and interference effects of the sub-bottom can be properly accounted for in the context of the potential theory while simultaneously avoiding any restrictions on the direction of propagation of the waves scattered at the water-bottom interface.

The single and double interface pressure density coefficients (reflection coefficients) given by Eqs. (17) and (19) depend upon the local slopes of the scattering surface. Hence, these expressions must be retained in the scattering integral, and averaged over the interface slopes along with the other slope dependent terms. The remainder of Chapter II is devoted to methods of calculating the averages over the surface slopes when the scattering interface is acoustically penetrable. In addition, since the slopes play an important role in both the scattering and the acoustic penetration of an interface, considerable attention is given to the interaction of these two effects on the basis of their slope dependence.

3. Series Evaluation of the Rayleigh Coefficient

In order to treat surfaces with fairly large rms roughness, an evaluation of the reflection coefficient within the integral for

the scattered pressure was carried out for a single interface. Using this approach, the conditions under which the reflection coefficient can be separated from the scattered pressure integral were examined. The series expression which results from this method was evaluated for various roughnesses and for the same four bottom samples used in the evaluation of Kuo's reflection coefficient.

The scattered pressure at point A is given by the integral

$$p_s(A) = \iint_S \mu(N) \frac{\partial}{\partial n} \left(\frac{e^{ik_1 r_1}}{r_1} \right) dS \quad , \tag{21}$$

where

μ is pressure density at the variable point N on the surface,

n is the outward normal to the surface, and

r_1 is defined in Dwg. AS-68-1100.

The value of μ on the boundary is given by

$$\mu(N) = \frac{1}{2\pi} R p_i(N) \quad , \tag{22}$$

where p_i is the value of the incident pressure on the surface and R is the reflection coefficient given by Eq. (17) or Eq. (19), which will later be shown to be a function of the local slope of the surface. If it is now assumed that the incident pressure is of the form

$$p_i = D_o \frac{e^{ikr_o}}{r_o} \quad , \tag{23}$$

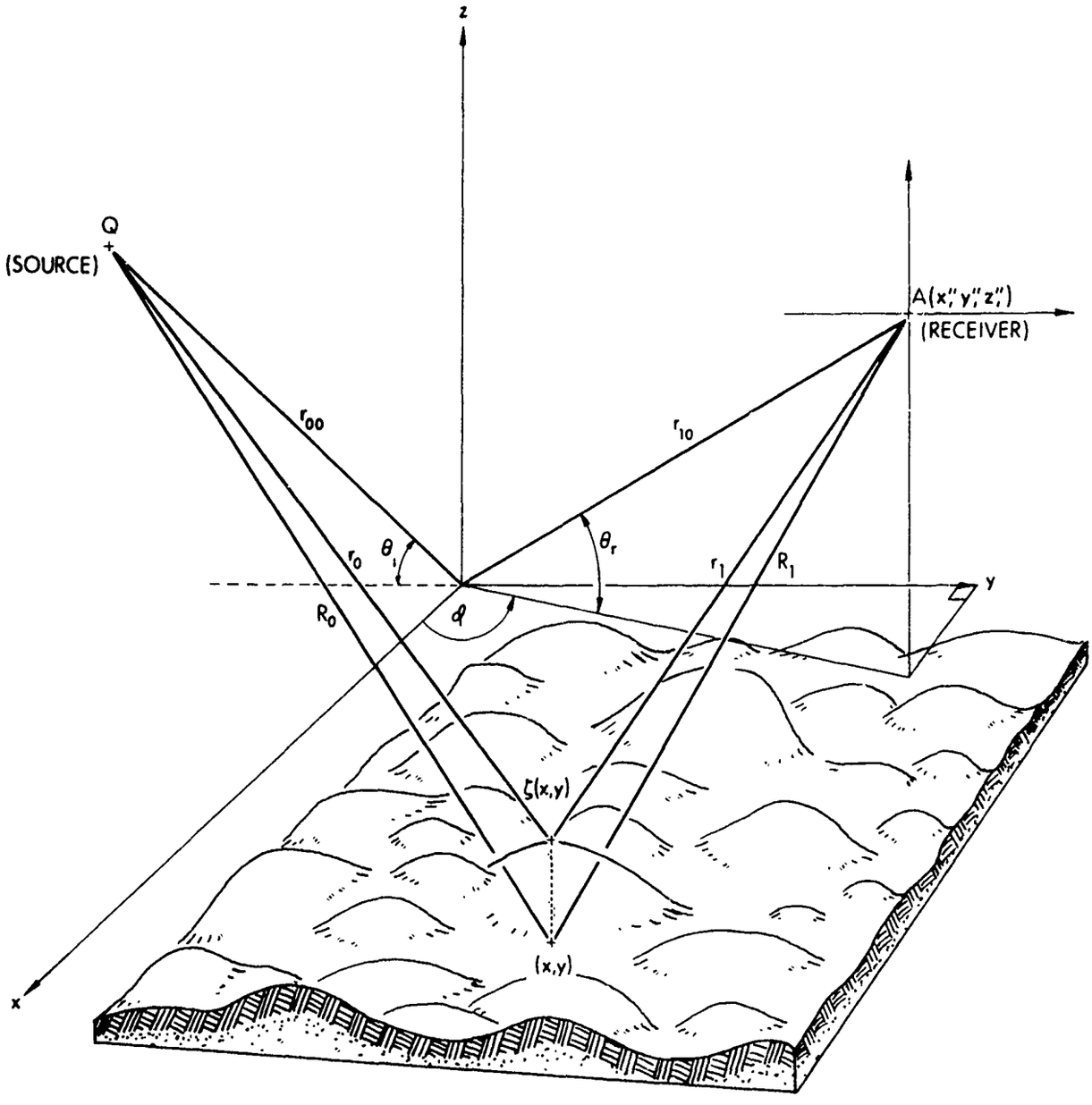

SCATTERING GEOMETRY

DRL - UT
AS-68-1100
KEH - RFO
9 - 6 - 68

then it is obvious that

$$\mu(N) = \frac{RD_o}{2\pi} \frac{e^{ikr_o}}{r_o} \quad , \tag{24}$$

and

$$p_s(A) = \frac{-1}{2\pi} \iint_S RD_o \left(\frac{e^{ikr_o}}{r_o}\right) \frac{\partial}{\partial n} \left(\frac{e^{ikr_1}}{r_1}\right) dS \quad . \tag{25}$$

It is shown in the Final Report under Contract N00024-69-C-1275 that this integral becomes

$$p_s(A) = \frac{-ik}{2\pi} \iint_\Sigma D_o R \left(\frac{e^{ik(R_o+R_1)}}{R_o R_1}\right) e^{-ik\gamma\zeta} \left(\zeta_x \hat{e}_x + \zeta_y \hat{e}_y - \hat{e}_z\right) \cdot \hat{e}_1 \, dxdy \, , \tag{26}$$

where

$$\gamma = \sin\theta_1 + \sin\theta_r \quad , \tag{27}$$

and $\hat{e}_1$ is a unit vector directed along line R_1. If it is assumed that

$$\begin{aligned} \hat{e}_x \cdot \hat{e}_1 &= 0 \quad , \\ \hat{e}_y \cdot \hat{e}_1 &= \cos\theta_r \quad , \\ \hat{e}_z \cdot \hat{e}_1 &= \sin\theta_r \quad , \end{aligned} \tag{28}$$

then

$$\left(\zeta_x \hat{e}_x + \zeta_y \hat{e}_y - \hat{e}_z\right) \cdot \hat{e}_1 = -\sin\theta_r + \zeta_y \cos\theta_r \quad . \tag{29}$$

The integral for the scattered pressure becomes

$$p_s(A) = \frac{-ik}{2\pi} \iint_S D_o \left(\frac{e^{ik(R_o+R_1)}}{R_o R_1} \right) e^{-ik\gamma\zeta} \left[R(-\sin\theta_r + \zeta_y \cos\theta_r) \right] dxdy \quad . \tag{30}$$

At this point a suitable expression for the reflection coefficient R must be given. Referring to Dwg. AS-70-795, p. 11, the single interface reflection coefficient is given by

$$R(\Phi_1, \Phi_2) = \frac{\rho_2 c_2 \sin\Phi_1 - \rho_1 c_1 \sin\Phi_2}{\rho_2 c_2 \sin\Phi_1 + \rho_1 c_1 \sin\Phi_2} \quad , \tag{31}$$

where Eqs. (15) and (16) have been substituted into Eq. (17), k has been replaced by $\frac{\omega}{c}$, and $\Phi_1 = \theta_1 + \beta$ and $\Phi_2 = \theta_2 + \beta$. This is the standard Rayleigh reflection coefficient referenced to an infinite plane oriented at an angle β to the mean plane. Application of Snell's Law to the formula is accomplished through the substitution

$$\sin\Phi_2 = \sqrt{1 - \cos^2\Phi_2} = \frac{1}{N}\sqrt{N^2 - \cos^2\Phi_1} \quad , \tag{32}$$

where $N = \frac{c_1}{c_2}$ is the acoustic index of refraction. Applying Eq. (32) to Eq. (31) gives

$$R(\theta_1+\beta) = \frac{\rho_2 c_2 \sin(\theta_1+\beta) - \frac{\rho_1 c_1}{N}\sqrt{N^2 - \cos^2(\theta_1+\beta)}}{\rho_2 c_2 \sin(\theta_1+\beta) + \frac{\rho_1 c_1}{N}\sqrt{N^2 - \cos^2(\theta_1+\beta)}} \quad . \tag{33}$$

Expanding $\sin(\theta_1+\beta)$ and $\cos(\theta_1+\beta)$ and using various trigonometric identities, Eq. (33) may be arranged into the form

$$R(\theta_1,\eta) = \frac{A + B\eta - C\sqrt{D\eta^2 + E\eta + F}}{A + B\eta + C\sqrt{D\eta^2 + E\eta + F}} \quad , \tag{34}$$

where

$$\eta = \tan\beta \quad , \tag{35}$$

$$A = \rho_2 c_2 \sin\theta_1 \quad ,$$

$$B = \rho_2 c_2 \cos\theta_1 \quad ,$$

$$C = \frac{\rho_1 c_1}{N} \quad , \tag{36}$$

$$D = N^2 - \sin^2\theta_1 \quad ,$$

$$E = \sin^2\theta_1 \quad , \text{ and}$$

$$F = N^2 - \cos^2\theta_1 \quad .$$

Since η is the tangent of β, it is obvious from Dwg. AS-70-795 that β is just the slope of the local tangent plane with respect to the mean plane. Because the formulation is restricted to the plane of incidence ($\hat{e}_x \cdot \hat{e}_1 = 0$), it may be assumed that $\eta = \zeta_y$. Using this result in the original pressure integral gives

$$p_s(A) = \frac{-ik}{2\pi} \iint_S D_o \left(\frac{e^{ik(R_o+R_1)}}{R_o R_1} \right) e^{-ik\gamma\zeta} \left[R(\theta_1,\eta)(-\sin\theta_r + \eta\cos\theta_r) \right] dxdy \quad , \tag{37}$$

where $R(\theta_1,\eta)$ is given by Eq. (34).

It is now obvious why the reflection coefficient cannot be separated from the integral for the scattered pressure a priori. The dependence of R upon η, a quantity which appears within the integral, places restrictions on the separation. Here it is recognized that ζ and η are random variables and that $p_s(A)$ must be replaced by the ensemble average $\langle p_s(A)\rangle$. If it is assumed that the surface height, ζ, and the surface slope, η, are independent, then the integral for $\langle p_s(A)\rangle$ takes on the simple form

$$\langle p_s(A)\rangle = \frac{-ik}{2\pi}\iint_S D_o\left(\frac{e^{ik(R_o+R_1)}}{R_oR_1}\right)\left\langle e^{ik\gamma\zeta}\right\rangle\left\langle R(\theta_1,\eta)(-\sin\theta_r+\eta\cos\theta_r)\right\rangle dxdy \quad . \tag{38}$$

To separate an effective reflection coefficient (in an averaged form) from the integral it must also be assumed that η is stationary so that

$$\langle p_s(A)\rangle = -\left\langle R(\theta_1,\eta)(1-\eta\cot\theta_r)\right\rangle\left(\frac{-ik}{2\pi}\right)\iint_S D_o\sin\theta_r\left(\frac{e^{ik(R_o+R_1)}}{R_oR_1}\right) \cdot \left\langle e^{ik\gamma\zeta}\right\rangle dxdy \quad . \tag{39}$$

Since ζ is also stationary, its expectation value may also be removed from the integral, leaving only a form which is immediately recognized as the pressure reflected from a plane surface, p_r,

$$\langle p_s(A)\rangle = -\left[\langle R(\theta_1,\eta)\rangle - \cot\theta_r\langle\eta R(\theta_1,\eta)\rangle\right]\langle e^{ik\gamma\zeta}\rangle p_r \quad . \tag{40}$$

Assuming a Gaussian distribution of heights, the average over ζ gives

$$\langle p_s(A)\rangle = -\left[\langle R(\theta_1,\eta)\rangle - \cot\theta_r \langle \eta R(\theta_1,\eta)\rangle\right] e^{-g/2} p_r \quad . \qquad (41)$$

where $g = (k\gamma\sigma)^2$ and σ is the rms height value.

The expression in brackets in Eq. (41) may be regarded as an effective reflection coefficient which has been averaged along with the slope terms in the integral for the scattered pressure and then separated from the integral in an averaged form. The expectation values $\langle R\rangle$ and $\langle \eta R\rangle$ are still quite difficult to evaluate directly due to the complex form of R. In order to evaluate these expressions, $R(\theta_1,\eta)$ is expanded in a Maclaurin series;

$$R(\theta_1,\eta) = R\,|_{\eta=0} + \frac{\partial R}{\partial \eta}\bigg|_{\eta=0} \eta + \frac{\partial^2 R}{\partial \eta^2}\bigg|_{\eta=0} \frac{\eta^2}{2!} + \ldots \quad , \qquad (42)$$

where

$$R\,|_{\eta=0} = \frac{A - C\sqrt{F}}{A + C\sqrt{F}} = \frac{\rho_2 c_2 \sin\theta_1 - \frac{\rho_1 c_1}{N}\sqrt{N^2 - \cos^2\theta_1}}{\rho_2 c_2 \sin\theta_1 + \frac{\rho_1 c_1}{N}\sqrt{N^2 - \cos^2\theta_1}} \quad ,$$

$$\frac{\partial R}{\partial \eta}\bigg|_{\eta=0} = \frac{2C\left(B\sqrt{F} - \frac{AF}{2\sqrt{F}}\right)}{\left(A+C\sqrt{F}^2\right)} \quad , \qquad (43)$$

$$\frac{\partial^2 R}{\partial \eta^2}\bigg|_{\eta=0} = \frac{\left[A+C\sqrt{F}\right]\left[\frac{2BCE-2AD-BE}{2\sqrt{F}}\right] - 4C\left[B\sqrt{F} - \frac{AE}{2\sqrt{F}}\right]\left[B + \frac{CE}{2\sqrt{F}}\right]}{(A+C\sqrt{F})^3} \quad .$$

The first term of this series is equivalent to the Rayleigh reflection coefficient for a plane surface. This series expansion of $R(\theta_1,\eta)$ has been widely used in rough surface scattering literature (Refs. 8-14). Using this expansion the evaluation of the reflection coefficient is straightforward and is given by

$$\left[\langle R\rangle - \cot\theta_r\langle\eta R\rangle\right] = \left[R(1 - \langle\eta\rangle\cot\theta_r) + R'(\langle\eta\rangle - \langle\eta^2\rangle\cot\theta_r) + \frac{R''}{2}(\langle\eta^2\rangle - \langle\eta^3\rangle\cot\theta_r) + \ldots\right] \quad , \tag{44}$$

where R and its derivatives are evaluated at $\eta=0$.

The only expectation values to be calculated are of the form

$$\langle\eta^\ell\rangle = \int_{-\tan\theta_1}^{\infty} \eta^\ell P(\eta)d\eta \quad , \tag{45}$$

where the lower limit of $-\tan\theta_1$ represents a simple shadowing consideration for backscattering geometry. In forward and specular scattering the upper limit is replaced by the tangent of the receiver angle. For a Gaussian distribution of surface slopes and for ℓ, an odd integer, Eq. (45) becomes

$$\langle\eta^\ell\rangle = \frac{1}{2\sqrt{2\pi}s}\left(\frac{1}{2s^2}\right)^{-\left(\frac{\ell+1}{2}\right)}\Gamma\left(\frac{\ell+1}{2}, \frac{\tan^2\theta_1}{2s^2}\right) \quad , \tag{46}$$

where s is the rms value of the surface slope and Γ is the incomplete gamma function. Similarly for ℓ even,

$$\langle \eta^{\ell} \rangle = \frac{1}{2\sqrt{2\pi}s} \left(\frac{1}{2s^2}\right)^{-\left(\frac{\ell+1}{2}\right)} \left[\Gamma\left(\frac{\ell+1}{2}, \frac{\tan^2\theta_1}{2s^2}\right) + 2\gamma\left(\frac{\ell+1}{2}, \frac{\tan^2\theta_1}{2s^2}\right) \right] \quad . \tag{47}$$

For the forward and specular scattering cases the expectation values of η contain additional incomplete gamma functions depending on θ_r. These expectation values may be easily calculated and combined with the values of R, R', R", etc., to find the value of the effective reflection coefficient $[\langle R \rangle - \cot\theta_r \langle \eta R \rangle]$.

It should be noted here that the expression $[\langle R \rangle - \cot\theta_r \langle \eta R \rangle]$, which has been called the effective reflection coefficient, actually contains terms which arise from the exact treatment of the surface slopes in the scattered pressure integral as well as from the penetrability of the surface. The rigorous treatment of the surface slopes produces the term $(-\sin\theta_r + \eta\cos\theta_r)$ in the integrand of Eq. (30). This term is a result of the scattering process and is independent of the penetrability of the surface. Averaging this term together with R is necessary because they both depend on η, but this averaging results in an effective reflection cofficient in which effects of scattering are combined with effects of penetrability. To see this more clearly, it is only necessary to examine the behavior of the effective reflection coefficient for an impenetrable rough surface. For a pressure release surface $R(\theta_1, \eta) = -1$, so the effective reflection coefficient is given by

$$[1 - \cot\theta_r \langle \eta \rangle] \quad .$$

If $\langle\eta\rangle$ is calculated according to Eq. (41) with the appropriate limits on the integral for each scattering geometry, the results are given by

$$[1 - \cot\theta_r\langle\eta\rangle]_{\text{SPECULAR}} = 1 \quad ,$$

$$[1 - \cot\theta_r\langle\eta\rangle]_{\text{BACKSCATTER}} = \left[1 - \cot\theta_r\left(\frac{s}{\sqrt{2\pi}}\right)e^{-\frac{\tan^2\theta_r}{2s^2}}\right] \quad , \tag{48}$$

and

$$[1 - \cot\theta_r\langle\eta\rangle]_{\text{FORWARD SCATTER}} = \left[1 - \cot\theta_r\left(\frac{s}{\sqrt{2\pi}}\right)\left(e^{-\frac{\tan^2\theta_r}{2s^2}} - e^{-\frac{\tan^2\theta_i}{2s^2}}\right)\right] .$$

These results are shown for various values of S(rms slope) in Dwg. AS-71-294 for backscattering geometry and in Dwg. AS-71-295 for forward scattering geometry. This expression represents the contribution to the effective reflection coefficient that is due solely to the scattering process. In Dwg. AS-71-295, curves corresponding to the larger values of s were not plotted because they all lie quite close to the s = 0.5 curve. Realistic values of the rms slope of the ocean bottoms are generally quite small. For the model surfaces used in this program the rms slopes range from s = 0.1 to s = 0.3. From Dwgs. AS-71-294 and AS-71-295 it is obvious that for these small slope values, the slope dependent term is very nearly unity except at very low grazing angles. Since this scattering contribution can be calculated exactly, a true reflection coefficient, which depends only upon the penetrability of the bottom, may be defined as

$$\bar{R} = \frac{[\langle R\rangle - \cot\theta_r\langle\eta R\rangle]}{[1 - \cot\theta_r\langle\eta\rangle]} \quad , \tag{49}$$

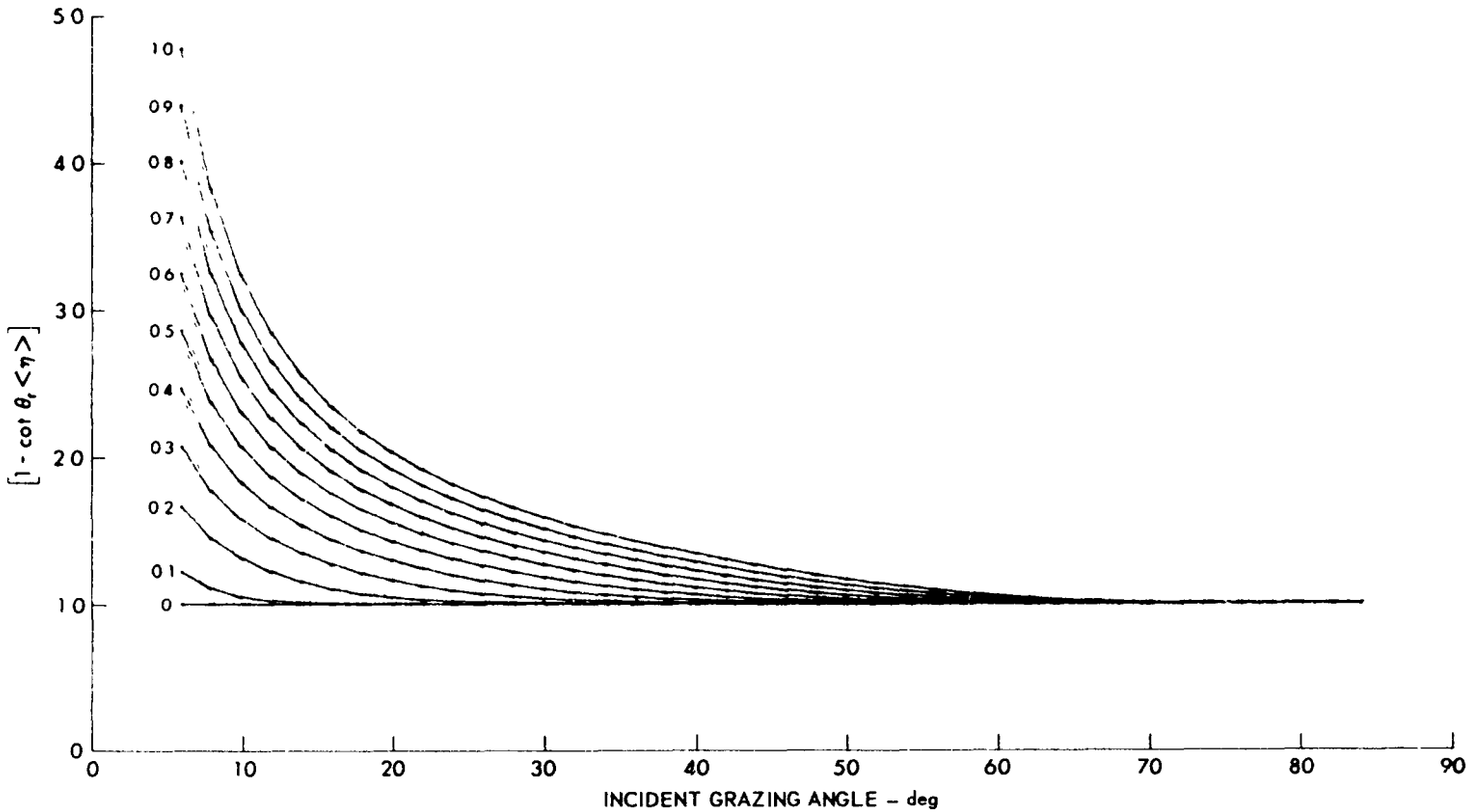

ARL - UT
AS-71-294
MLB - RFO
3 - 30 - 71

SLOPE DEPENDENT TERM ($[1 - \cot\theta_r < \eta >]$) OF THE SCATTERED PRESSURE FOR AN IMPENETRABLE SURFACE AND BACKSCATTERING GEOMETRY FOR VARIOUS VALUES OF THE rms SLOPE

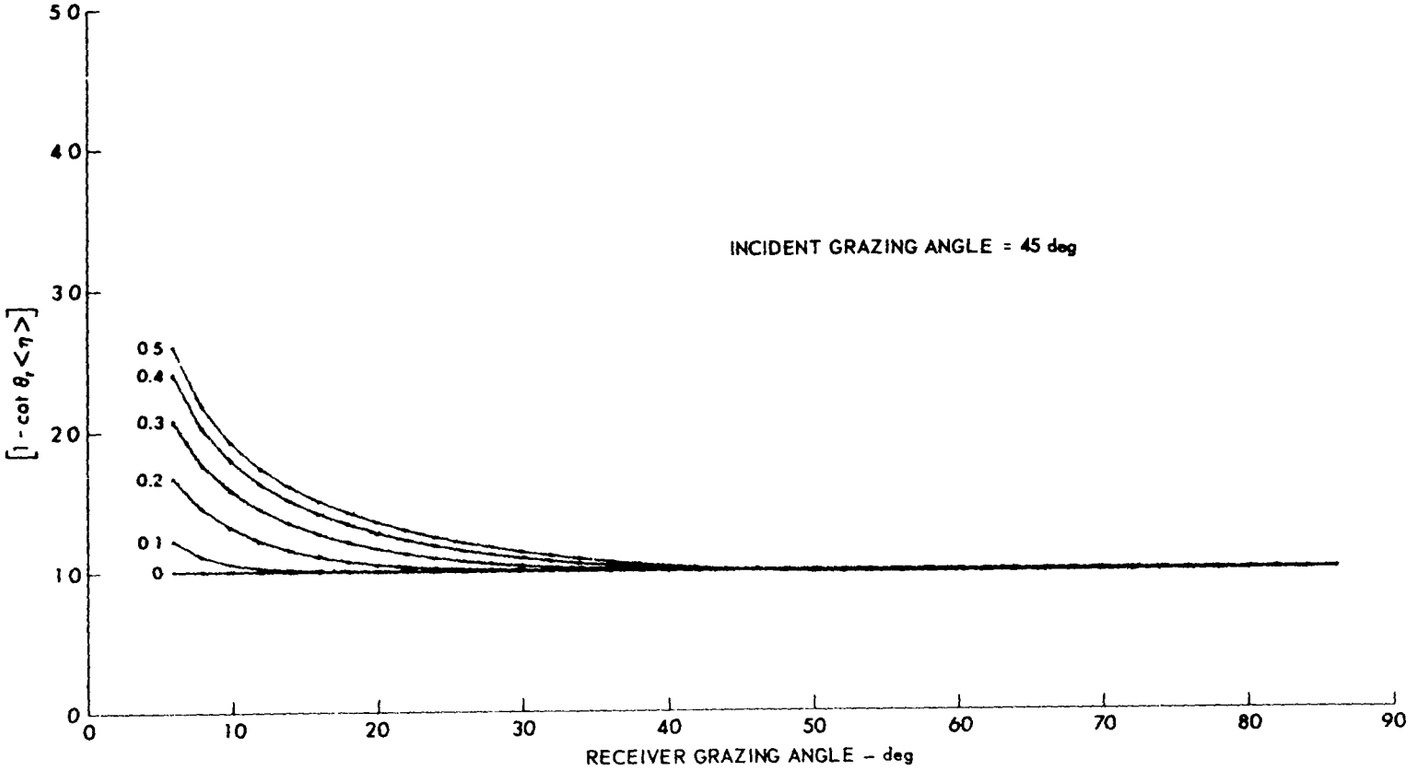

ARL - UT
AS-71-295
MLB - RFO
3 - 30 - 71

SLOPE DEPENDENT TERM ([1 – cot θ_r $<\eta>$]) OF THE SCATTERED PRESSURE FOR AN IMPENETRABLE SURFACE AND FORWARD SCATTERING GEOMETRY FOR VARIOUS VALUES OF THE *rms* SLOPE

where the expression in the numerator is the effective reflection coefficient and the expression in the denominator has been shown to be the scattering contribution to the effective reflection coefficient. Using this result the scattered pressure for a Gaussian distribution of heights if given by

$$p_s = \bar{R} \left[1 - \cot\theta_r \langle\eta\rangle\right] e^{-g/2} p_r \quad ,$$

where $\bar{R}$ depends only upon the penetrability and obviously is unity for an impenetrable or pressure release surface. Because the slope dependent term $[1 - \cot\theta_r \langle\eta\rangle]$ is nearly unity, for the cases considered here it will be assumed that the effective reflection coefficient provides an adequate approximation to the true reflection coefficient given by Eq. (49).

The effective reflection coefficient $[\langle R\rangle - \cot\theta_r \langle\eta R\rangle]$ will now be evaluated for a penetrable surface under the assumption that it adequately approximates the true reflection coefficient and thus represents the change in the scattered pressure due to the penetrability of the bottom.

To allow for attenuation in the bottom the velocity c_2 must be complex with an imaginary part that is proportional to the attenuation. This makes the constants A, B, C, D, and F in the expressions for R, R', R", etc., complex, and hence the entire effective reflection coefficient is a complex quantity. Plots of the magnitude of this coefficient for various bottoms with several values of the rms slope are given in this section.

Drawings AS-71-24, AS-71-25, and AS-71-26 show the reflection coefficients for various source and receiver geometries for Mackenzie's sample number 32 at a frequency of 5 kHz. The measured attenuation

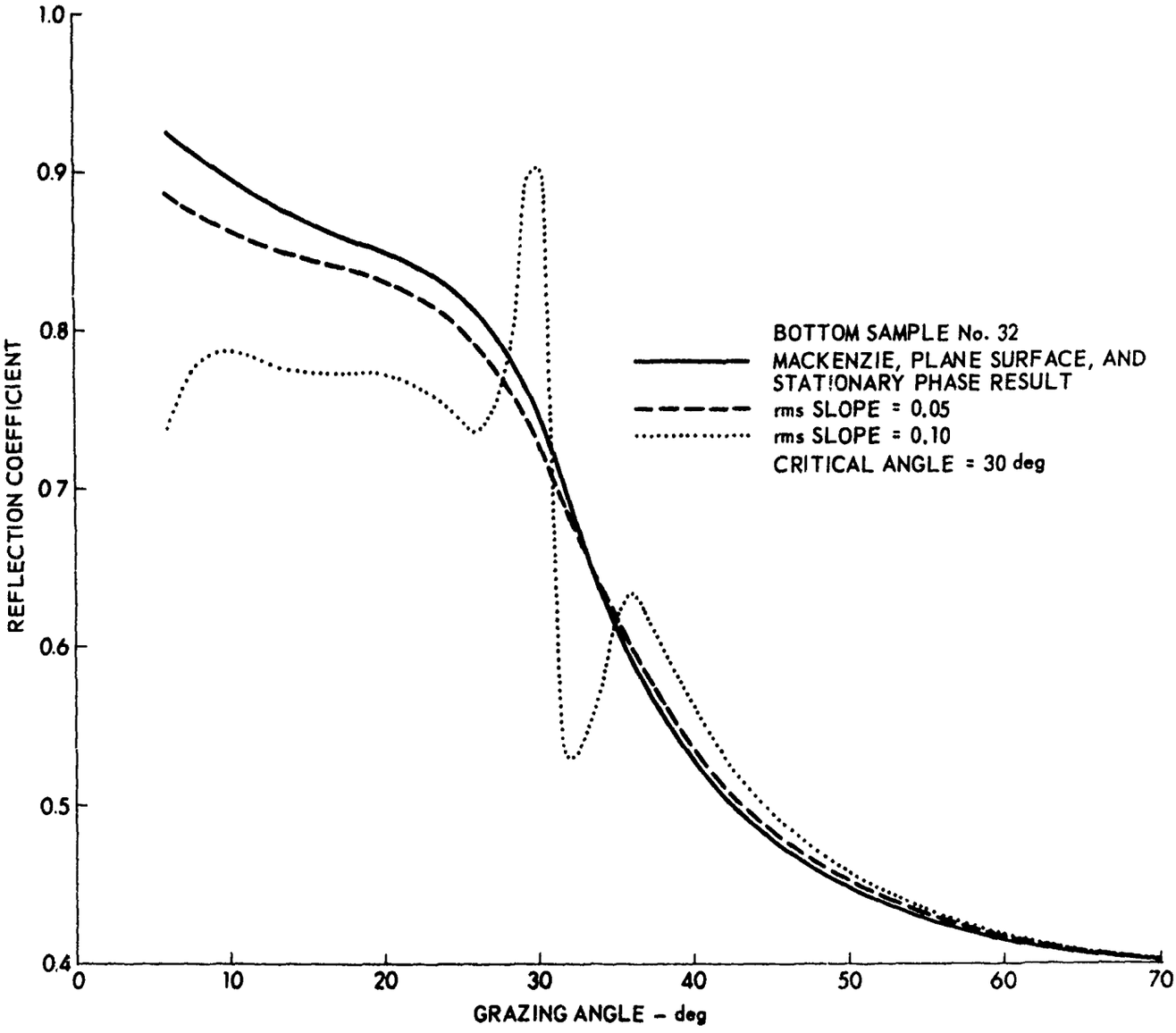

REFLECTION COEFFICIENT vs INCIDENT GRAZING ANGLE
FOR SPECULAR SCATTERING GEOMETRY

ARL - UT
AS-71-24
MLB - RFO
1 - 15 - 71

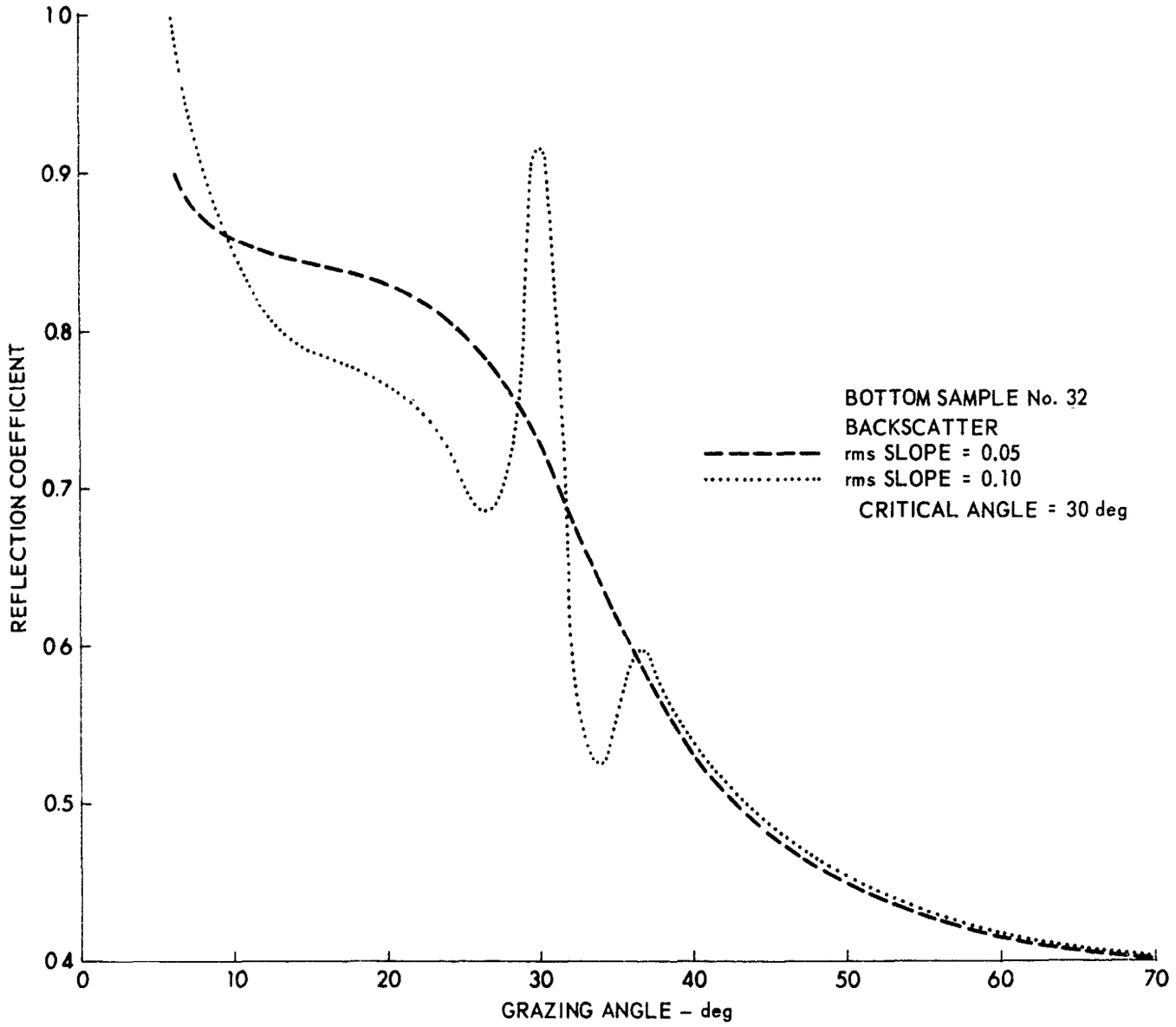

REFLECTION COEFFICIENT vs INCIDENT GRAZING ANGLE
FOR BACKSCATTERING GEOMETRY

ARL - UT
AS-71-25
MLB - RFO
1 - 15 - 71

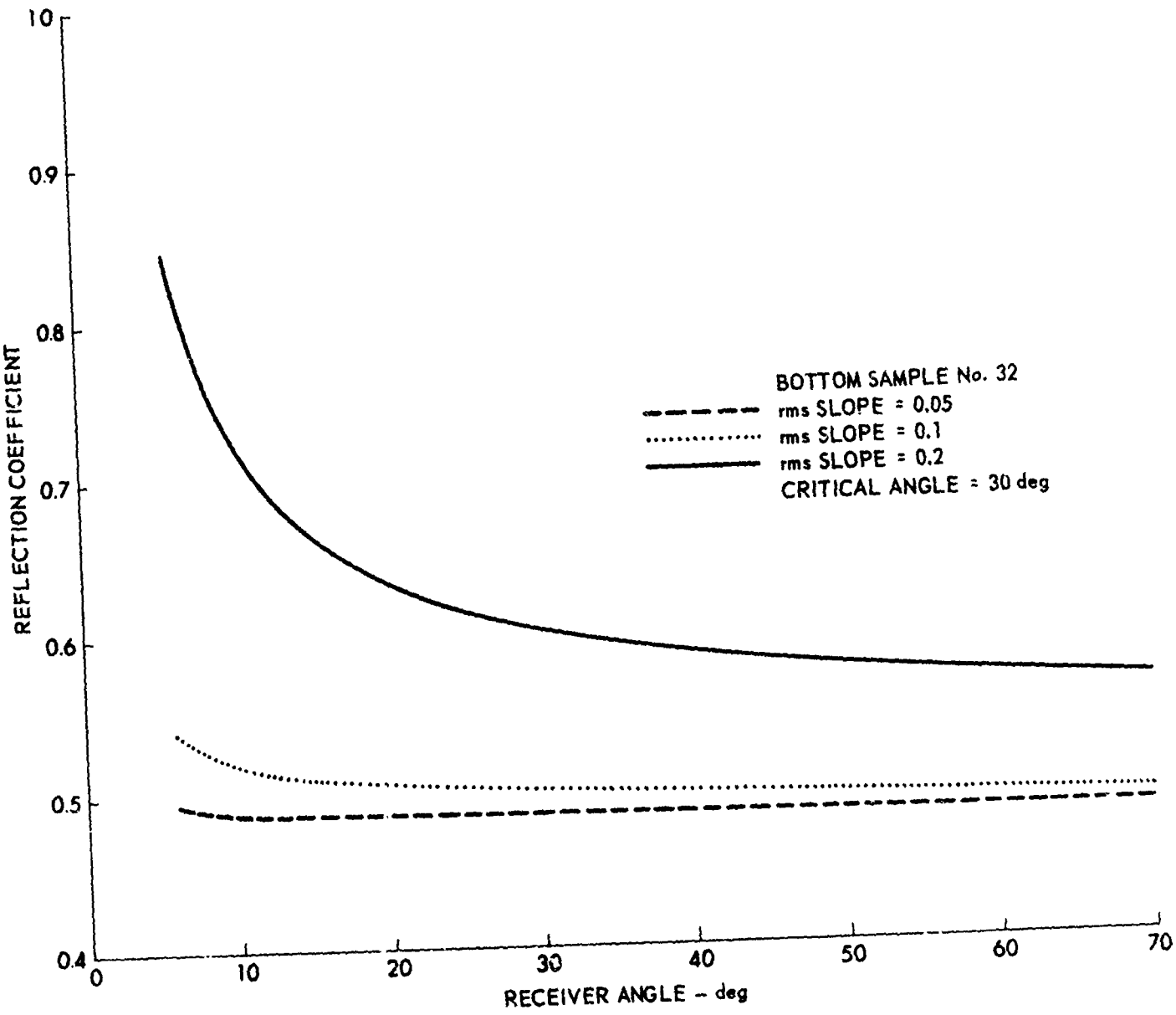

REFLECTION COEFFICIENT vs RECEIVER ANGLE FOR FORWARD SCATTERING GEOMETRY WITH A 45 deg INCIDENT GRAZING ANGLE

ARL - UT
AS-71-26
MLB - RFO
1 - 15 - 71

of 4.48 dB per ft at 30 kHz was extrapolated to 5 kHz assuming that attenuation varied as the square root of the frequency. Drawing AS-71-24 shows the magnitude of the effective reflection coefficient plotted versus grazing angle for a specular scattering geometry ($\theta_r = \theta_1$). In the limit of no roughness the first term in the series expansion of $R(\theta,\eta)$ is the only nonzero term. This term is just Mackenzie's original result for a plane attenuating surface and is plotted as a solid line in Dwg. AS-71-24. The dashed line represents a small rms slope of 0.05 and shows little deviation from the zero slope term. The dotted line represents a larger rms slope value of 0.10 and exhibits large fluctuations in the region around the critical angle which occurs at a grazing angle of 30 deg for this surface. The failure near the critical angle is a problem inherent in the formulation of this method and will be discussed later. Similar results are obtained for back-scatter and are shown in Dwg. AS-71-25. Here the plane surface term has no meaning and is not plotted. The forward scatter curves shown in Dwg. AS-71-26 are typical and have no fluctuations as long as the incident grazing angle is not in the region immediately around the critical angle. Similar results are shown in Dwgs. AS-71-214 and AS-71-215 for bottom sample number 28, which exhibits a critical angle near 10 deg. The forward scatter curves were not plotted since, for these rms roughness values, the forward scatter coefficient was very nearly a constant (R=0.29). Samples number 27 and 13 do not have a critical angle but instead have an angle of intromission at about 6 deg. The reflection coefficient curves, shown in Dwgs. AS-71-216, AS-71-217, AS-71-218, and AS-71-219, are relatively smooth because the angle of intromission is actually below the lower limit of the range of grazing angles of interest. It is expected that an angle of intro-mission will produce the same kind of fluctuacions in the reflection coefficient as that observed near the critical angles. Again the forward scatter curves were omitted because they were very nearly constant.

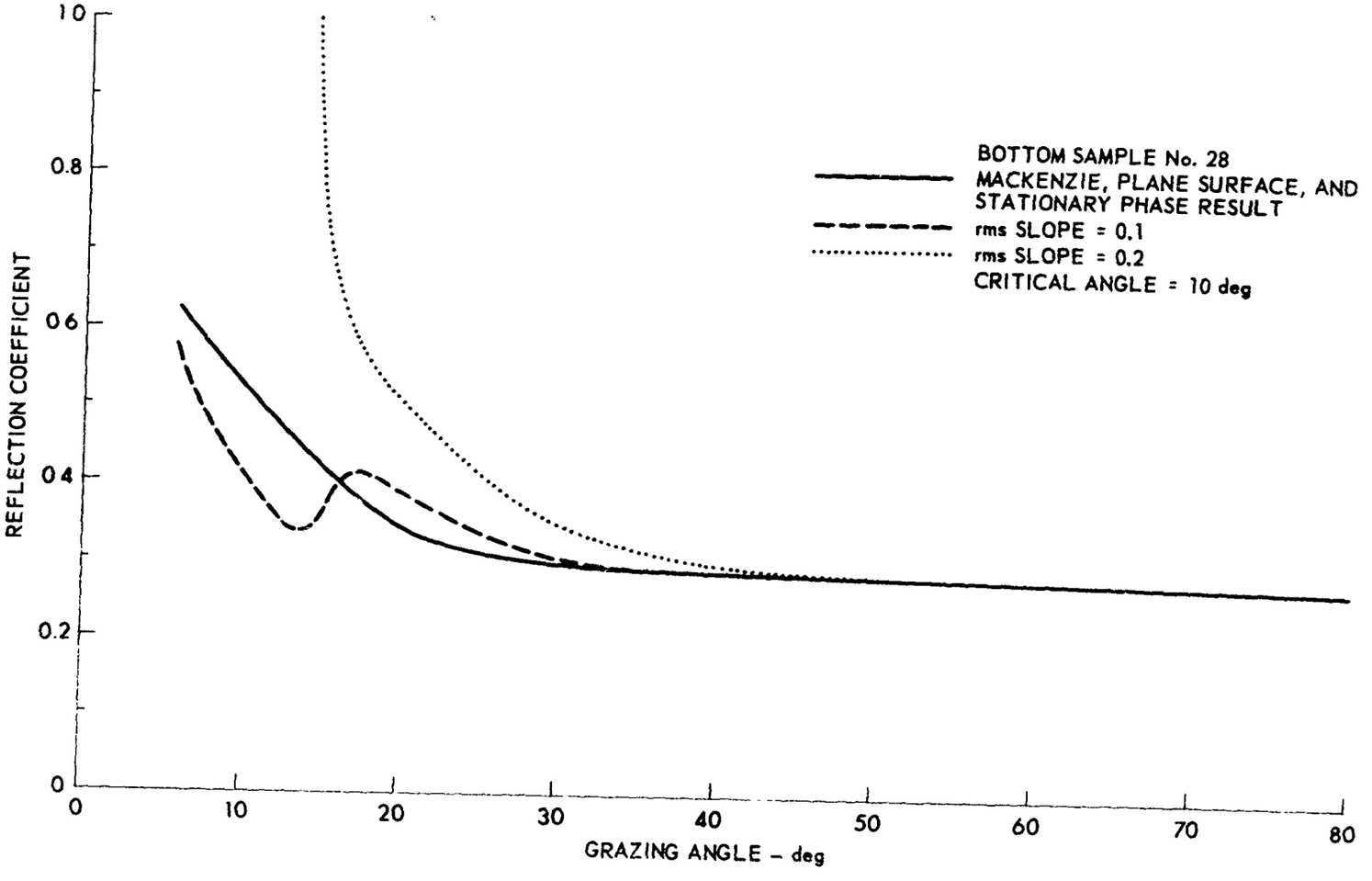

ARL - UT
AS-71-214
MLB - RFO
3 - 30 - 71

REFLECTION COEFFICIENT vs INCIDENT GRAZING ANGLE
FOR SPECULAR SCATTERING GEOMETRY

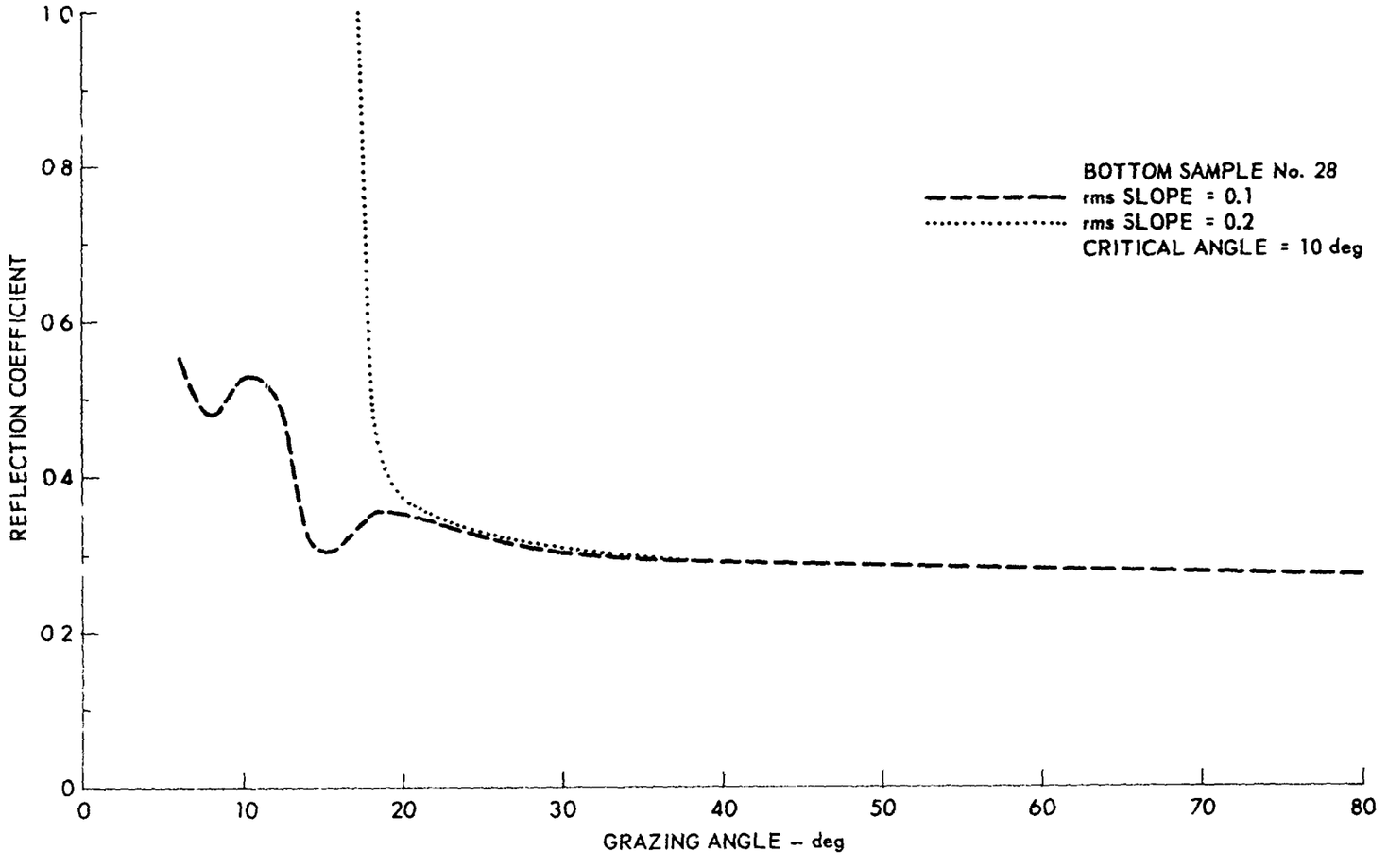

ARL - UT
AS-71-215
MLB - RFO
3 - 30 - 71

REFLECTION COEFFICIENT vs INCIDENT GRAZING ANGLE
FOR BACKSCATTERING GEOMETRY

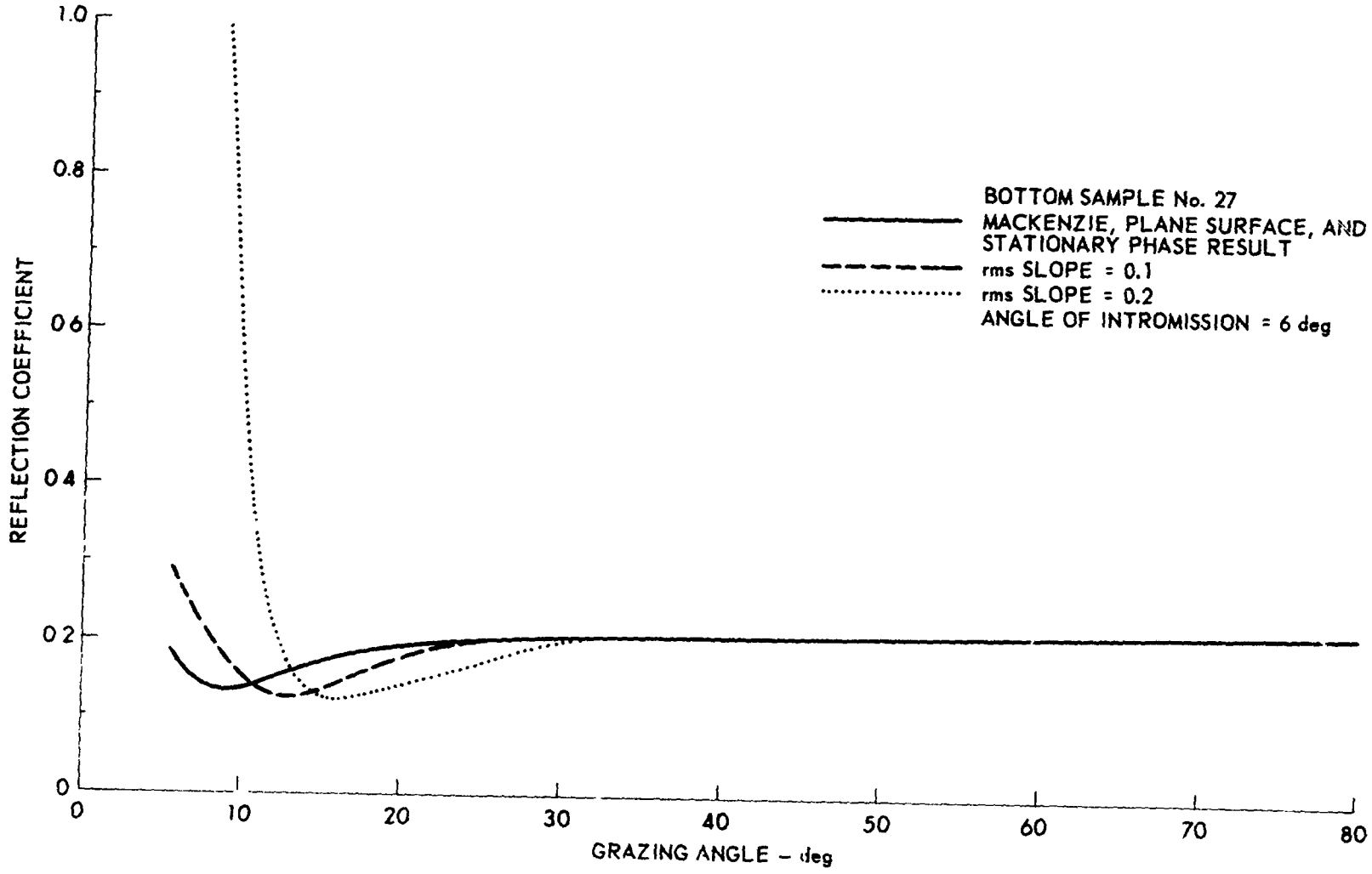

ARL - UT
AS-71-214
MLB - RFO
3 - 30 - 71

REFLECTION COEFFICIENT vs INCIDENT GRAZING ANGLE
FOR SPECULAR SCATTERING GEOMETRY

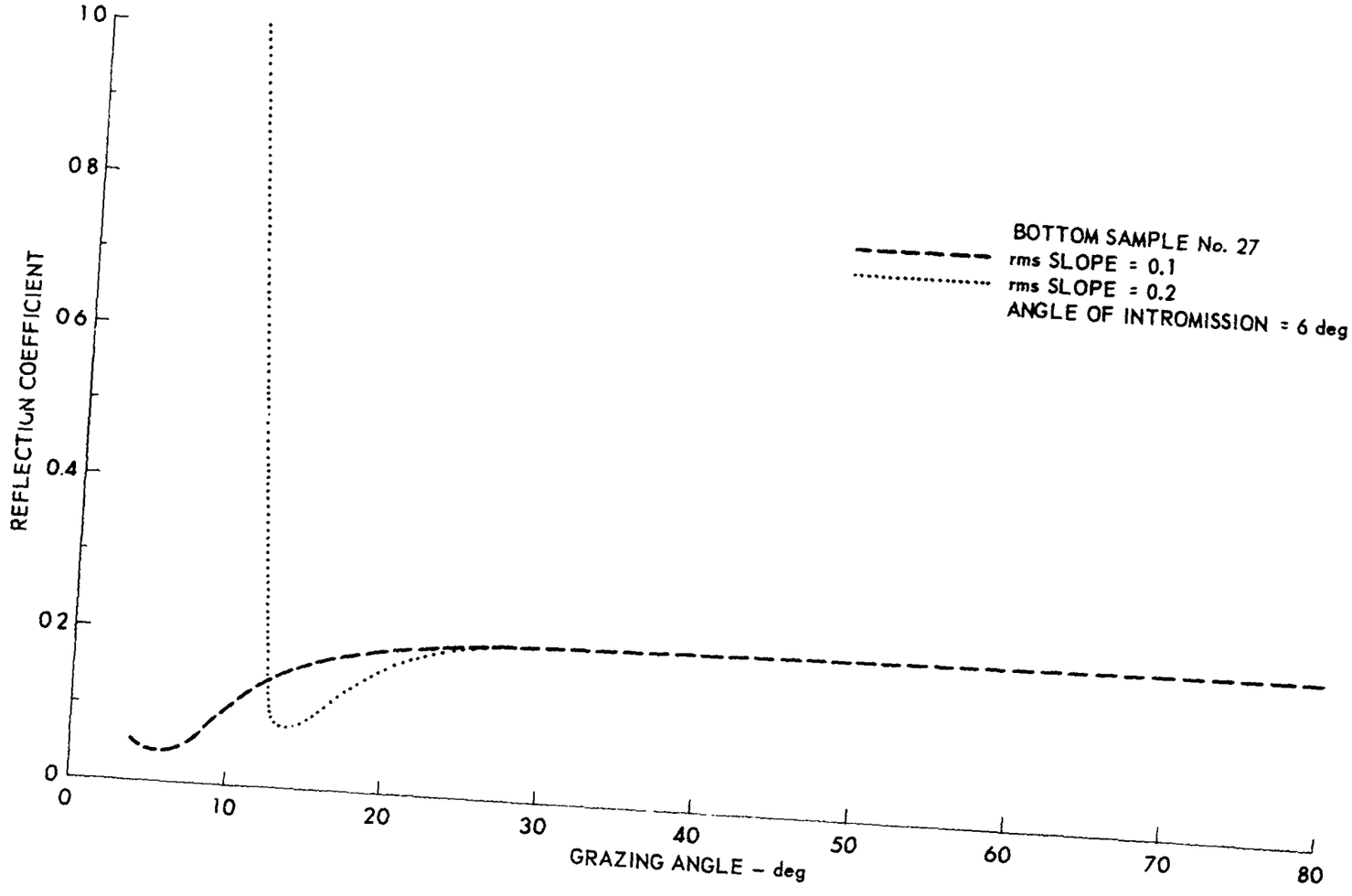

ARL - UT
AS-71-217
MLB - RFO
3 - 30 - 71

REFLECTION COEFFICIENT vs INCIDENT GRAZING ANGLE
FOR A BACKSCATTERING GEOMETRY

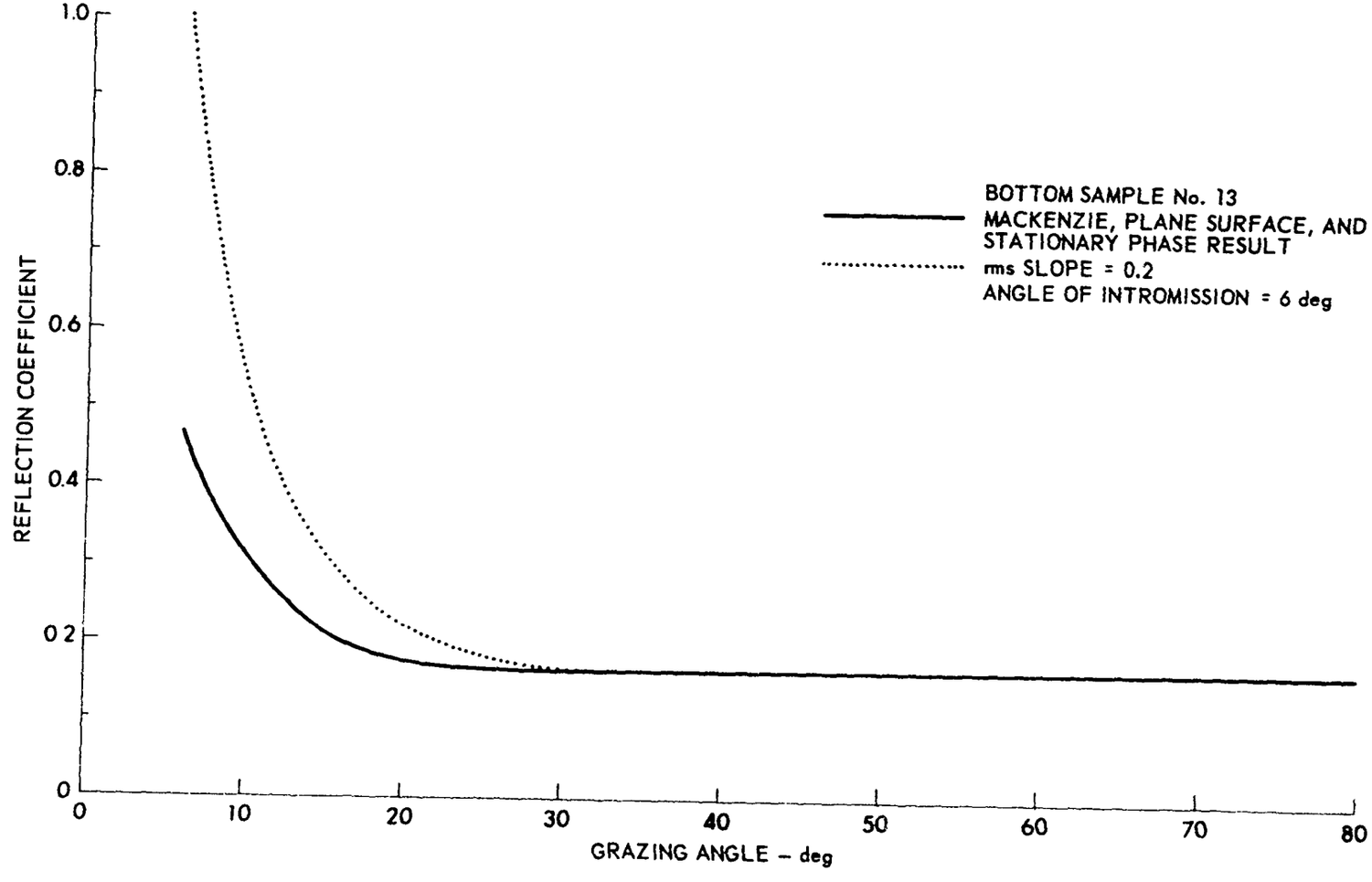

45

ARL - UT
AS-71-218
MLB - RFO
3 - 30 - 71

REFLECTION COEFFICIENT vs INCIDENT GRAZING ANGLE
FOR SPECULAR SCATTERING GEOMETRY

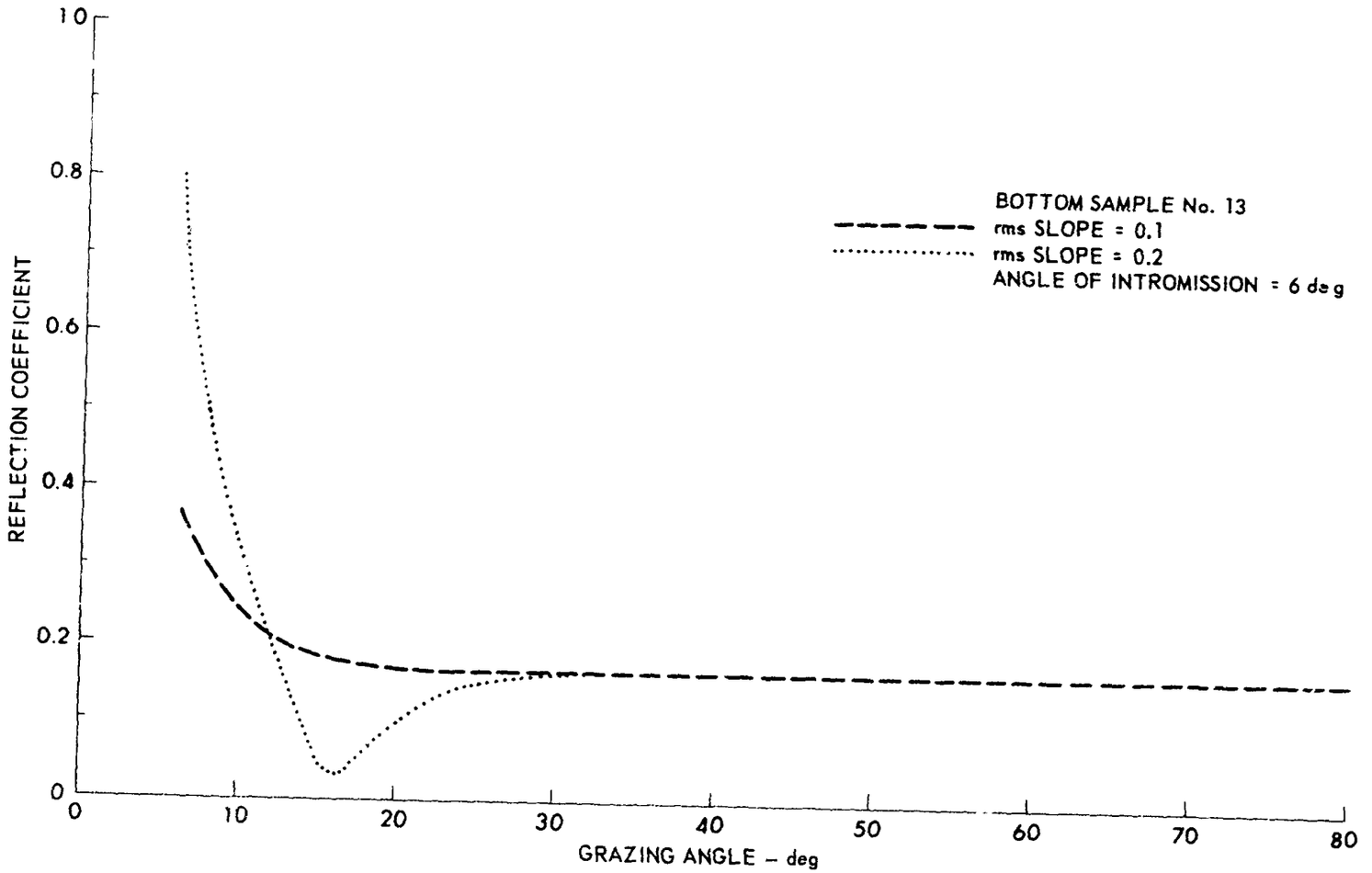

46

REFLECTION COEFFICIENT vs INCIDENT GRAZING ANGLE
FOR BACKSCATTERING GEOMETRY

ARL - UT
AS-71-219
MLB - RFO
3 - 30 - 71

It was first thought that the fluctuations near the critical angle were simply the result of not retaining an adequate number of terms in the series expansion given by Eq. (25). However, a partial sum decomposition of the series shows that this is not the case and that the series is actually diverging in this region. This indicates that the problem is inherent in the formulation of the method. The presence of fluctuations near the critical angle points out several similarities between this approach and the method used by Brekhovskikh to treat the reflection of spherical waves from a plane interface, which suffers similar difficulties.[15] Brekhovskikh uses a plane wave decomposition of a spherical incident wave, and saddle point integration to arrive at an effective reflection coefficient given by

$$\left[R(\theta_o) - \frac{iN}{kR_1} + \ldots\right] \quad ,$$

where

$$N = \frac{1}{2}\left[R''(\theta_o) + R'(\theta_o)\cot\theta_o\right] \quad .$$

Here $R'(\theta_o)$ and $R''(\theta_o)$ are the derivatives of the reflection coefficient with respect to θ. The reflection coefficient itself is of the same form as Eq. (17). In the derivation of this spherical wave reflection coefficient, it is assumed that $R(\theta)$ is slowly varying. Near the critical angle this is no longer true and the derivatives of R with respect to θ become large. Thus, as Brekhovskikh shows, the series is no longer valid near the critical angle.

The application of these ideas to the series given by Eq. (27) is straightforward. It was initially assumed that the first term of Brekhovskikh's series was an adequate approximation to the spherical wave reflection coefficient. This approximation is quite

good because kR_1 is very large for the scattering geometries being considered. At this point the failure of the series development presented in this section is difficult to understand because the terms that cause Brekhovskikh's coefficient to be invalid near the critical angle have simply been neglected on geometrical grounds. However, when the effects of roughness are included, the reflection coefficient takes on the form $R(\theta+\beta)$, where β is the random angle associated with the slope of the local tangent. In order to evaluate R it is necessary to expand it in the Maclaurin series given by Eq. (25). Since the reflection coefficient is of the form $R(\theta+\beta)$, it can easily be shown that

$$\frac{\partial R}{\partial \theta} = \frac{\partial R}{\partial \beta} = \frac{\partial R}{\partial \eta}\frac{\partial \eta}{\partial \beta} = \frac{\partial R}{\partial \eta}\sec^2\beta \quad .$$

Thus, the derivatives of R with respect to η which appear in the Maclaurin series behave in much the same manner as the derivatives of R with respect to θ which had previously been eliminated from Brekhovskikh's formula. Consequently, the effective reflection coefficient given by Eq. (27) suffers the same fluctuations at grazing angles near the critical angle. If Eq. (24) could be evaluated directly, then the fluctuations associated with the expansion could be avoided. Direct evaluation of Eq. (24) might be accomplished using numerical integration techniques although this approach is complicated by the fact that $R(\theta_1,\eta)$ is a complex function of real arguments. An alternate method utilizing the complex nature of R would be to express $\langle R(\theta_1,\eta)\rangle$ and $\langle \eta R(\theta_1,\eta)\rangle$ as contour integrals. The evaluation of these contour integrals, however, is not straightforward because of the presence of branch cuts. These ideas are being investigated at the present time.

To summarize the results of this subsection, it was shown that an effective reflection coefficient, for a single interface, which

could be removed from the integral for the scattered pressure in an averaged form was given by

$$\left[\langle R\rangle - \cot\theta_r \langle \eta R\rangle\right] \quad .$$

It was also shown that, for small values of the rms slope, the scattering contribution to this expression could be neglected and that the effective reflection coefficient represented the change in the scattered pressure due to the penetrability of the surface. For larger slope values the true reflection coefficient was given by Eq. (49) and can be easily calculated from the effective reflection coefficient. In order to calculate the effective reflection coefficient for penetrable rough surfaces, $R(\theta_1,\eta)$ was expanded in a Maclaurin series in η. This technique made the evaluations of $\langle R\rangle$ and $\langle \eta R\rangle$ quite simple but introduced fluctuations near the critical angle, or angle of intromission. It was shown that these fluctuations were a result of using the Maclaurin expansion in a region where the function was not slowly varying. The closed form expression for the effective reflection coefficient, $[\langle R\rangle - \cot\theta_r \langle \eta R\rangle]$, is, however, the result of a rigorous derivation, and so the Maclaurin expansion can be expected to give the correct results in the regions where R is slowly varying. This gives a reflection coefficient which is valid over all angles for surfaces where R varies slowly and is valid over a large range of angles for surfaces that exhibit a critical angle or an angle of intromission. In addition, if the rms slope is very small, as it often is for realistic ocean bottoms, the fluctuations in the derivatives of R in the Maclaurin series are insignificant because the derivatives are multiplied by expectation values of powers of η which are extremely small. Thus, good results can be obtained near the critical angle if the slopes are small enough. This aspect is illustrated by Dwg. AS-71-24, where good results are obtained for $s=0.05$ but fluctuations occur when $s=0.1$.

The results given in this subsection are derived specifically for a single interface. The double interface problem, however, can be treated in a similar manner and will also result in an expression that fluctuates near the critical angle because the expression will still involve the derivatives of R_{12}. It is expected that the effective reflection coefficient for a double interface will be valid over approximately the same range of angles and slopes as the single interface reflection coefficient. However, it should again be pointed out that these expressions are valid for a large number of the combinations of slopes, angles, and bottom parameters of practical interest.

4. Stationary Phase Evaluation of the Reflection Coefficient

As seen in the previous subsection on the series evaluation of the reflection coefficient for the single interface case, accurate results can be obtained for certain special cases. In the event that the source grazing angle is near the critical angle (or angle of intromission, depending on whether the index of refraction N is greater than or less than 1) and that the rms slope is moderate, the series evaluation fails because of the behavior of the derivatives of R. A series evaluation of the double interface reflection coefficient would fail for identical reasons.

A method of evaluating the reflection coefficient which is valid for the case where both the rms heights and slopes are moderate or large is given by the stationary phase evaluation. This method avoids the difficulties encountered in the series method. In the stationary phase method the reflection coefficient is evaluated at the angle Φ which is the local grazing angle at the stationary phase points. If φ is the angle between the plane of incidence and the scattering plane, the assumption $\varphi=0$ implies that only the scattering in the

plane of incidence will be of interest. The local angle Φ is then given by

$$\sin\Phi = \frac{\sin\theta_i - \zeta_x\cos\theta_i}{\left(1+\zeta_x^2+\zeta_y^2\right)^{1/2}} \quad , \tag{51}$$

where at the stationary phase points

$$\zeta_y = -\frac{v_y}{v_z} \quad , \quad \zeta_x = -\frac{v_x}{v_z} \quad ,$$

and

$$v_x = k(\cos\theta_i - \cos\theta_r\cos\varphi) = k(\cos\theta_i - \cos\theta_r) \quad ,$$

$$v_y = -k(\cos\theta_r\sin\varphi) = 0 \quad ,$$

$$v_z = -k(\sin\theta_r + \sin\theta_i) \quad .$$

This gives

$$\sin\Phi = \frac{1}{\sqrt{2}}\left(1 - \cos\theta_i\cos\theta_r + \sin\theta_i\sin\theta_r\right)^{1/2} \quad , \tag{52}$$

$$= \sin\left(\frac{\theta_i + \theta_r}{2}\right) \quad ,$$

where θ_i is the source grazing angle and θ_r is the receiver angle. If $\theta_i+\beta$ instead of Φ is used in the reflection coefficients given by Eqs. (17) and (19), then for the single interface case the reflection coefficient becomes

$$R(\theta_i,\eta) \rightarrow R\left(\frac{\theta_i + \theta_r}{2}\right) \quad , \tag{53}$$

and for the double interface case the reflection coefficient becomes

$$R(\theta_i,\eta) \rightarrow \frac{R_{12}\left(\frac{\theta_i+\theta_r}{2}\right) + \Delta R_{23} e^{-i2k_2 \sin\theta_2 h}}{1 + \Delta R_{23} R_{12}\left(\frac{\theta_i+\theta_r}{2}\right) e^{-i2k_2 \sin\theta_2 h}} \quad . \tag{54}$$

It should be noted that R given by Eq. (53) is identical to the R_{12} contained in Eq. (54). The other terms in Eq. (54) are constants with respect to the stationary phase calculation; consequently, in the following chapter only Eq. (53) will be discussed.

For the backscatter case, $\theta_r = \pi - \theta_i$, so $\Phi = \pi/2$. Thus at all incident grazing angles, the reflection coefficient for backscatter geometry is a constant. In the specular direction, $\theta_r = \theta_i$, so $\Phi = \theta_i$. This simply reproduces Mackenzie's original curves for the reflection coefficient from a smooth penetrable surface. For the forward scatter case, $\Phi = (\theta_i+\theta_r)/2$. The curves for this case are given in Dwg. AS-71-28. These results are particularly easy to interpret in that each point on the surface is assumed to reflect in the specular direction with respect to the local tangent plane at that point. Thus, the reflection coefficient depends only upon the scattering geometry. Once the position of the receiver is specified, the only points which can contribute to the field at the receiver are the stationary phase points.

Examination of Eq. (37) reveals that the results given in Eqs. (53) and (54) are not yet complete. According to Eq. (37), the slope dependence is contained in both R and the scattering integrand as

$$R(\theta_i,\eta)[\sin\theta_r - \eta\cos\theta_r] \quad . \tag{55}$$

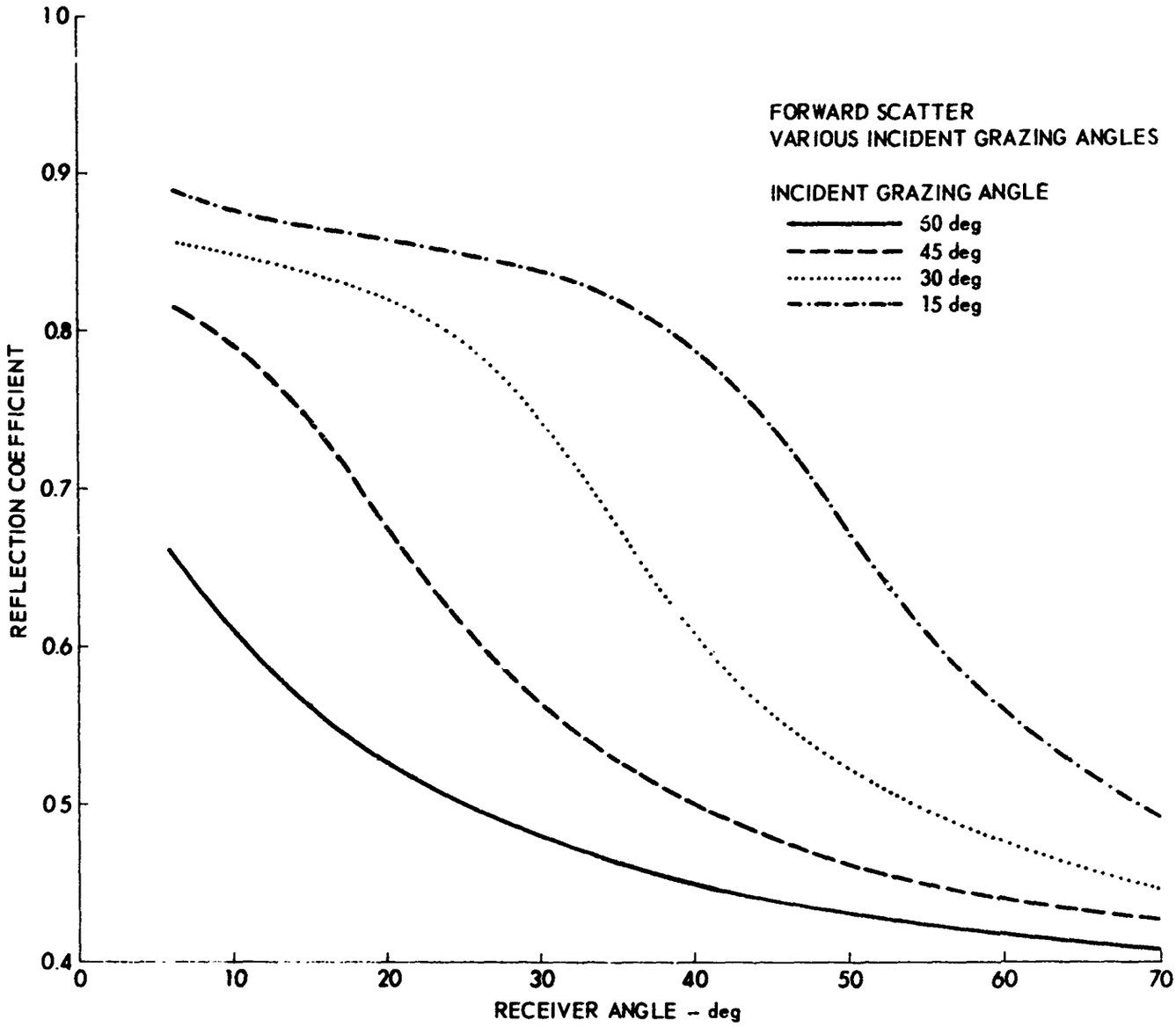

REFLECTION COEFFICIENT EVALUATED BY THE STATIONARY PHASE METHOD FOR FORWARD SCATTERING GEOMETRY WITH VARIOUS INCIDENT GRAZING ANGLES

ARL - UT
AS-71-28
MLB - RFO
1 - 15 - 71

Considering the complete slope dependence contained in Eq. (55), the stationary phase result then becomes

$$R(\theta_i,\eta)[\sin\theta_r - \eta\cos\theta_r] = R\left(\frac{\theta_i + \theta_r}{2}\right) F(\theta_i,\theta_r) \quad , \qquad (56)$$

where R is given by either Eq. (53) or Eq. (54), and F is Beckmann's[12] F and is given by

$$F(\theta_i,\theta_r) = \frac{1 - \cos(\theta_i + \theta_r)}{\sin\theta_i + \sin\theta_r} \quad .$$

Previously, it was pointed out that because both R and the scattering term given in the brackets in Eq. (55) are slope dependent, the acoustic penetrability of the surface interacted with the scattering. This same effect occurs when a stationary phase calculation is made since the term which is then obtained is not just R but rather RF given by Eq. (56).

The stationary phase calculation presented here is a generalization of the results of Hagfors[16] and Stogryn.[17] On the basis of a stationary phase calculation, they obtained a reflection coefficient which, in the case of backscattering, was simply a constant factor equal to the Rayleigh reflection coefficient evaluated at normal incidence.

III. THE EFFECT OF A ROUGH, PENETRABLE LIQUID BOTTOM ON SONAR OPERATION

The motivation for the theoretical work presented in the previous section, and in previous final reports, has been to develop realistic models of sonar operation in the ocean environment. Prior studies have verified the mathematical models which apply to an ocean boundary composed of plane layered sediments or a pressure release sinusoidal surface. More recent work has resulted in the development of a model of forward and backward scattering at the sea surface. The previous theoretical work was somewhat simpler than the present case, since the scattering effects were due only to topography. In developing a model for a rough ocean bottom, an additional complication is introduced, since now both the topography and the physical composition of the bottom affect the scattering behavior.

The model that will be presented in this report is incomplete in several aspects. First, the model is restricted to liquid bottom types; that is, the shear mode of propagation must be insignificant in comparison to the compressional or longitudinal mode of propagation. Second, this model has not as yet been experimentally verified. Special aspects of the simplest case (single interface case) have been discussed in the literature (Hagfors[16] and Stogryn,[17] for example), but a general verification will not be completed until the end of the next contract year. The preliminary experimental work is reported in Appendix A, however.

The effects of a rough bottom are encountered in a number of situations. In general sonar operation the presence of a rough penetrable bottom will degrade the effective range of the sonar and

also give rise to a reverberation return which may mask the presence of a target. For a sonar which operates in a bottom bounce mode the type of bottom present in the area of operation is of critical importance. If the bottom is smooth but penetrable, then the sonar system will suffer only a loss in signal level. Where the bottom is rough but relatively impenetrable, the sonar system will be degraded in several respects. The scattering effect of the bottom will be observed as a general beam broadening with consequent loss of bearing accuracy. Further, a rough bottom will give rise to fluctuations in the returned signal. Obviously, a rough, penetrable bottom will give rise to a combination of the effects just mentioned.

It is important to determine the dominant effect of the bottom; that is, whether penetration or roughness is the dominant loss factor. The importance of this point is best illustrated by an example. Assume that the perpendicularly measured bottom loss in two regions was -20 dB. If, in one region, this loss was primarily due to roughness, then at the grazing angles for which a bottom bounce sonar is operated the loss will still be large and significant signal fluctuation and beam degradation will also occur. Suppose that in the other region the loss was due mainly to penetration. Then at the usual operating angles the loss will perhaps be only -5 dB (assuming $c_{BOTTOM} > c_{WATER}$), and associated beam broadening and signal fluctuations will be insignificant. Consequently, in the second region the bottom bounce mode may be effectively employed at low grazing angles. These considerations take on added weight when it is realized that it is impossible to acoustically map the entire ocean; hence, the local sonar operator will occasionally have to make a determination of the suitability of the bottom for the bounce mode.

A. Physical Description of Some Ocean Bottoms

To be worthwhile, the effects of the bottom presented in this report should represent some fairly typical bottom types. However, those bottoms which are composed of rock or compacted sediments must be excluded since the shear mode will be an important propagation mechanism. Essentially, these regions are centered near the midoceanic ridges which are generally considered to be topographically unsuitable for bottom bounce operation anyway.

The other major physiographic provinces that are of interest, which are also thought to be usually good reflectors, are the continental margins and the ocean basin floor.[18] The continental margins are usually found at moderate depths (100 - 1000 fathoms), have thick sediment layers, and the topography may consist of a small average gradient (1:200 - 1:600) with small local relief (10 - 20 meters).[18] An even smaller scale relief may be due to strewn rocks and boulders[19] or to the characteristic sinusoidal ridges resulting from turbidity currents.[18,20] The principal reflections from the continental margin may then either be due to the bottom itself or to a sub-bottom that is 2 to 10 meters deep.[21] These features are characteristic of the Atlantic Ocean and particularly the North Atlantic Ocean.

The ocean basin floors are generally found at deeper depths (1000 - 4000 fathoms), have a nonexistent or thin (0.2 - 4 meter) organic sediment layer overlying a fairly dense bottom,[19] and the topography may consist of an average gradient less than 1:1000 and, except for isolated hills and sea mounts, relative relief of less than 1 meter.[18] The ocean basin is thought to be quite smooth, and where it is not, the organic sediment tends to smooth over the small scale features. The principal reflections from the ocean basin floors are due either to the bottom or a very near lying sub-bottom. These features are characteristic of large areas of the Pacific and

Indian Oceans, and to a lesser extent to certain portions of the Atlantic Ocean.

In addition to the fact that the physical description of the ocean bottom is well correlated with the type of physiographic province, the acoustic parameters are also moderately well correlated with the physiographic provinces. A consequence of these relationships is that acoustic domains in the ocean largely coincide with physiological provinces.

Table I gives the parameters and the physical description of the four ocean bottom models which will be used in the study of the effects of a rough, penetrable bottom on bottom bounce sonar operation. The velocity and density parameters used in these models are based primarily on the data presented in Hamilton, et al.,[3] Sutton, et al,[22] Shumway,[23] Hamilton,[24] Nafe and Drake,[25] and Hampton[26] for different physiographic provinces in both the Atlantic and Pacific Oceans. Note that in the two layer models given here, the upper layer is a low speed layer; i.e., $c_{BOTTOM} < c_{WATER}$. The shear velocity has been omitted since it is assumed that the bottoms behave as liquid layers.

The absorption used in Table I is based on the data in Shumway,[23] Wood and Weston,[27] Cole,[28] and Hampton.[26] The absorption is based on an assumed first-power frequency dependence, which allows the wave number, k, to be written as

$$k = k_o\left(1 + i\,\frac{\alpha'}{2\pi}\right) \quad ,$$

where the absorption per wavelength, α', given in Table I is then related to the usual absorption α given in the sonar equation by

$$\alpha' = \lambda\alpha \quad .$$

TABLE I

THE PARAMETERS OF SOME REALISTIC OCEAN BOTTOMS

Bottom Province/ Model	Depth to Bottom - ft	Speed of Sound ft/sec	Density g/cm^3	Absorption per Wavelength - α'	Thickness of Layer
1. Continental Margin, Single Interface	1000-6000 ft	$c_1 = 5200$ ft/sec	$\rho_1 = 1.8$ g/cm^3	$\alpha_1' = 0.090$	Not Applicable
2. Continental Margin, Double Interface	1000-6000 ft	$c_1 = 4950$ ft/sec $c_2 = 5200$ ft/sec	$\rho_1 = 1.4$ g/cm^3 $\rho_2 = 1.8$ g/cm^3	$\alpha_1' = 0.180$ $\alpha_2' = 0.090$	$h_1 = 10$ ft
3. Ocean Basin, Single Interface	6000-24000 ft	$c_1 = 5800$ ft/sec	$\rho_1 = 2.05$ g/cm^3	$\alpha_1' = 0.036$	Not Applicable
4. Ocean Basin, Double Interface	6000-2400 ft	$c_1 = 4850$ ft/sec $c_2 = 5800$ ft/sec	$\rho_1 = 1.3$ g/cm^3 $\rho_2 = 2.05$ g/cm^3	$\alpha_1' = 0.220$ $\alpha_2' = 0.036$	$h_1 = 2.5$ ft

Sound Speed in Water at Bottom — 5060 ft/sec

Density — 1.03 g/cm^3 Absorption in Water @ 3.5 kHz ~ 0 dB

The advantage of writing α' instead of α is that α' is a nondimensional quantity, and if the frequency does obey a first-power law, then the absorption at any frequency is easily obtained using the simple relation given.

B. The Theoretical Prediction of the Forward Reflection and Scattering of a Sonar Beam by a Penetrable Bottom

It has been postulated by Kuo[1] and assumed by Clay[4,5] that the scattering behavior of a penetrable, rough bottom is given very simply by

$$\sigma_s^{pen} = |R(\theta_i)|^2 \sigma_s \quad , \tag{57}$$

where σ_s is just the scattering coefficient for an impenetrable rough surface and is defined as the ratio of the intensity scattered by the impenetrable rough surface in the direction of interest to the intensity reflected in the specular direction by an impenetrable plane surface. According to Clay, $R(\theta_i)$ is the Rayleigh reflection coefficient defined at the given incident angle, θ_i, for perfectly plane layers with parameters identical to the rough layers. Hence, $R(\theta_i)$ is defined by Eq. (33) with the local slope angle β set to zero. According to Kuo, $R(\theta_i)$ is given by his $\mathfrak{R}(\gamma)$ [Eq. (1)] for the case of backscattering.

The viewpoint implicit in the expressions given by both Kuo and Clay is that the scattering features due to the physical properties of the bottom and the scattering features due to the acoustical properties of the bottom are completely separable and may be independently expressed by the terms σ_s and $R(\theta_i)$, respectively. In general this viewpoint is <u>incorrect</u> since both $R(\theta_i)$ and the scattering factor depend on the local rough surface slope value. These terms must be combined when the average over the slopes is to be taken.

When extended to multiple layer media, the breakdown of Clay's viewpoint is even more severe since, as seen in Eq. (19), the reflection coefficient now depends on both the local slope and the local separation of the layers [which depends on the local height $\zeta(x,y)$]. Hence, the effects of the physical and acoustical properties of the bottom are now bound together in both the average over the surface slopes and the average over the surface heights.

These arguments may be mitigated under several circumstances, but only for the case of a single interface. If the slopes are small, then for many scattering configurations they may be ignored. Or in cases where the slopes are significant, they may still be ignored in forward scattering if the grazing angles are not too small. In these two cases Eq. (57) as given by Kuo or Clay will give good results (provided σ_s is correctly calculated). However, for backscatter, or low grazing angle forward scatter in the case of one interface, or any type of scattering in the case of multiple layers, Eq. (57) will not hold.

For the ocean bottom models to be used in this section, the scattered intensity is given by

$$\left\langle I_s \right\rangle = \left(\frac{k}{2\pi}\right)^2 \iint_S \iint_{S'} R(\theta_i,\eta) R^*(\theta_i,\eta') D_o^* D_o \frac{e^{ik\left[(R_o-R_o') + (R_1-R_1')\right]}}{R_o R_o' R_1 R_1'}$$

$$\times \left\langle e^{-ik\gamma(\zeta-\zeta')} \left[\left(\zeta_x \hat{e}_x + \zeta_y \hat{e}_y - \hat{e}_z\right) \cdot \hat{e}_1\right] \right. \tag{58}$$

$$\left. \times \left[\left(\zeta_x' \hat{e}_x' + \zeta_y' \hat{e}_y' - \hat{e}_z'\right) \cdot \hat{e}_1'\right] \right\rangle dx\,dy\,dx'\,dy' \quad ,$$

where the notation is identical to the notation used in Eq. (26), and the source strength has been normalized to unity. This equation is the extension to acoustically penetrable rough surfaces of the potential formulation given in the Final Report under Contract N00024-69-C-1275. The boundary value has been modified by the inclusion of $R(\theta_i,\eta)$, the pressure density coefficient (or reflection coefficient). $R(\theta_i,\eta)$ is given by either Eq. (17) or Eq. (19) according to whether the bottom contains a single or double interface.

Upon making the stationary phase calculation given in Section II, Eq. (58) becomes

$$\left\langle I_s \right\rangle = \left|F(\theta_i,\theta_r)R(\theta_i,\theta_r)\right|^2 \left(\frac{k}{2\pi}\right)^2 \iint_S \iint_{S'} D_o^* D_o \frac{e^{ik\left[(R_o-R_o')+(R_1-R_1')\right]}}{R_o R_o' R_1 R_1'} \times \left\langle e^{-ik\gamma(\zeta-\zeta')} \right\rangle dxdydx'dy' \quad . \tag{59}$$

The integrals given in Eq. (59) have been calculated in the previously mentioned final report for a surface with a normal (Gaussian) bivariate height distribution and Gaussian correlation function, and they included a realistic insonification function and the Fresnel phase approximation.

The intensity scattered by an acoustically penetrable rough surface is then given by [recall $F(\theta_i,\theta_r)$ is defined by Eq. (56)]

$$\left\langle I_s \right\rangle_o = \frac{k^2\left|F(\theta_i,\theta_r)R(\theta_i,\theta_r)\right|^2}{8\pi r_{oo}^2 r_{1o}^2} e^{-g} \frac{A}{K} \sum_{n=o}^{\infty} \frac{g^n}{n!} \frac{e^{-\left[\frac{k^2a^2}{4\left(M+\frac{n}{L^2}\right)}\right]}}{\sqrt{\left(N+\frac{n}{L^2}\right)\left(M+\frac{n}{L^2}\right)}} \quad , \tag{60}$$

where

$g = k^2\gamma^2h^2$,

A is the insonified area defined by the -3 dB down points,

$M = \dfrac{k^2\alpha^2}{2KR_2^2}$,

$N = \dfrac{k^2\beta^2}{2KR_1^2}$,

$K = \dfrac{3\log_{10}(e)}{20}$ is a beam function constant,

L is the correlation length of the upper surface,

$a = \cos\theta_i - \cos\theta_r$,

$R_1 = 2r_{oo}r_{lo}/(r_{oo}+r_{lo})$,

$R_2 = 2r_{oo}r_{lo}/(r_{oo}\sin^2\theta_r + r_{lo}\sin^2\theta_i)$, and

α and β are the semimajor and semiminor axes, respectively, of the elliptical insonified area, $A = \pi\alpha\beta$.

Since the important features of Eq. (60) are rather difficult to discover in its present form, let us investigate these formulas for the case where the receiver is in the specular direction. Using the definitions of M, N and a, and some algebraic manipulation gives

$$\langle I_s\rangle_o = \frac{|F(\theta_i,\theta_r)R(\theta_i,\theta_r)|^2e^{-g}}{\sin^2\theta_r\left(r_{oo}+r_{lo}\right)^2}\sum_{n=o}^{\infty}\frac{g^n}{n!}\left[\left(1+\frac{n}{NL^2}\right)\left(1+\frac{n}{ML^2}\right)\right]^{-1/2} . \qquad (61)$$

One significant but often misunderstood aspect of reflection and scattering phenomena, demonstrated in Eq. (61), is the range dependence. The n=o term is just the coherently scattered intensity; since this term can be considered to be the reflection by a lossy plane, the geometrical acoustics (optics) range dependence, $(r_{oo}+r_{lo})^{-2}$, is

obtained as expected. For n=1, . . . , ∞, the terms in Eq. (61) represent the incoherently scattered intensity. Clearly, for N and M very large (recall that M and N depend on R_1 and R, respectively), the range dependence of the incoherently scattered intensity will also be given by geometrical acoustics. The condition of M and N large is obtained when the insonified area is many wavelengths in dimension and the roughness is not too great. When M and N are small, Eq. (60) becomes

$$\langle I_s \rangle = \langle I_s \rangle_{\text{coherent}} + \frac{k^2 |F(\theta_i,\theta_r)R(\theta_i,\theta_r)|^2 e^{-g}}{8\pi\, r_{oo}^2 r_{1o}^2} \frac{A}{K} \sum_{0=1}^{\infty} \frac{g^n}{n!n} \quad . \quad (62)$$

Here, the incoherently scattered pressure is now area dependent and has Fraunhofer range dependence, $(r_{oo}r_{1o})^{-2}$. The condition of M and N small which leads to the above equation is obtained when the insonified area is small with respect to a wavelength and/or when the roughness features are quite large. Even for a large insonified area it is interesting to note that Eq. (62) will be obtained for quite rough surfaces. The physical interpretation of this result is that for a fairly rough surface the individual surface features behave as independent scatterers with dimensions on the order of a wavelength. Equation (62) is also obtained if the insonified area is only a few wavelengths in diameter.

Equation (60) thus has two important consequences. In addition to its ability to predict the correct shape of the forward scattered field, it also predicts that the range behavior of the scattered field makes a transition from $(r_{oo}+r_{1o})^{-2}$ for a very smooth surface to $(r_{oo}r_{1o})^{-2}$ for a very rough surface or for a very small insonified area. The transition in the range dependence is obtained strictly as a result of using the Fresnel phase approximation. This situation should be contrasted with the range dependence by all of the other

scattering theories (see, for example, Refs. 5,6,7,8,9,10,11,12,13,14, 16,17) which use only the Fraunhofer phase approximation, and consequently obtain only a range dependence of $(r_{oo}r_{lo})^{-2}$. Obviously, in the limit as the surface approaches a plane this result will fail (unless, it can be shown that a real source at infinity still insonifies only an area of a few wavelengths).

To obtain the scattering coefficient generally used in field work, the source strength and the total travel path are usually divided out. Since the source strength has already been normalized to unity, the scattering coefficient of an acoustically penetrable, rough surface is given by

$$\sigma_s^{pen} = \langle I_s \rangle (r_{oo}+r_{lo})^2 \quad , \tag{63}$$

where $\langle I_s \rangle$ is given by Eq. (60). This result will be used in the next subsection in conjunction with the parameter values listed in Table I to demonstrate the effects of an acoustically penetrable bottom on bottom bounce sonar operation.

C. Discussion of Results

The acoustic parameters given in Table I will be used in Eq. (63) to study the effects of some typical rough, acoustically penetrable bottoms on bottom bounce sonar operation. The only additional quantities which must be supplied are the rms heights and slopes which might be encountered in the different physiographic provinces. In the interests of brevity, only two bottom provinces are considered. On a shallow bottom (continental margin), greater roughness can be expected than on a deep bottom (ocean basin) due to the presence of turbidity currents and much greater depositional activity. Due to the great variability to be found in the bottom structure, it will be possible to investigate the scattering for

only a few typical but arbitrarily chosen roughness values. The values of the rms height and slope which will be used here are given in Table II. For the single interface case, the values of σ and s represent the rough parameters at the water-sediment interface. For the double interface case the subscript 1 indicates the water-sediment roughness parameters, while the subscript 2 indicates the sub-bottom roughness parameters. Notice that the sub-bottom roughness is here the same for both deep and shallow bottoms.

In Dwg. AS-71-389 the effect of roughness alone on a sonar beam reflected from an acoustically impenetrable bottom in the plane of incidence is illustrated. The sonar has a conical beamwidth of 8 deg measured with respect to the half-power points and is operating at a frequency of 3.5 kHz ($\lambda \approx 18$ in.).

TABLE II

SOME TYPICAL ROUGHNESS PARAMETERS FOR

REALISTIC OCEAN BOTTOMS

Bottom Province/ Model	RMS Height, σ	RMS Slope, $s = \sigma/L$
1. Continental Margin, Single Interface	$\sigma = 12$ in.	$s = 0.1$
2. Continental Margin, Double Interface	$\sigma_1 = 12$ in. $\sigma_2 = 9$ in.	$s_1 = 0.1$ $s_2 = 0.05$
3. Ocean Basin, Single Interface	$\sigma = 1$ in.	$s = 0.0085$
4. Ocean Basin, Double Interface	$\sigma_1 = 1$ in. $\sigma_2 = 9$ in.	$s_1 = 0.0085$ $s_2 = 0.05$

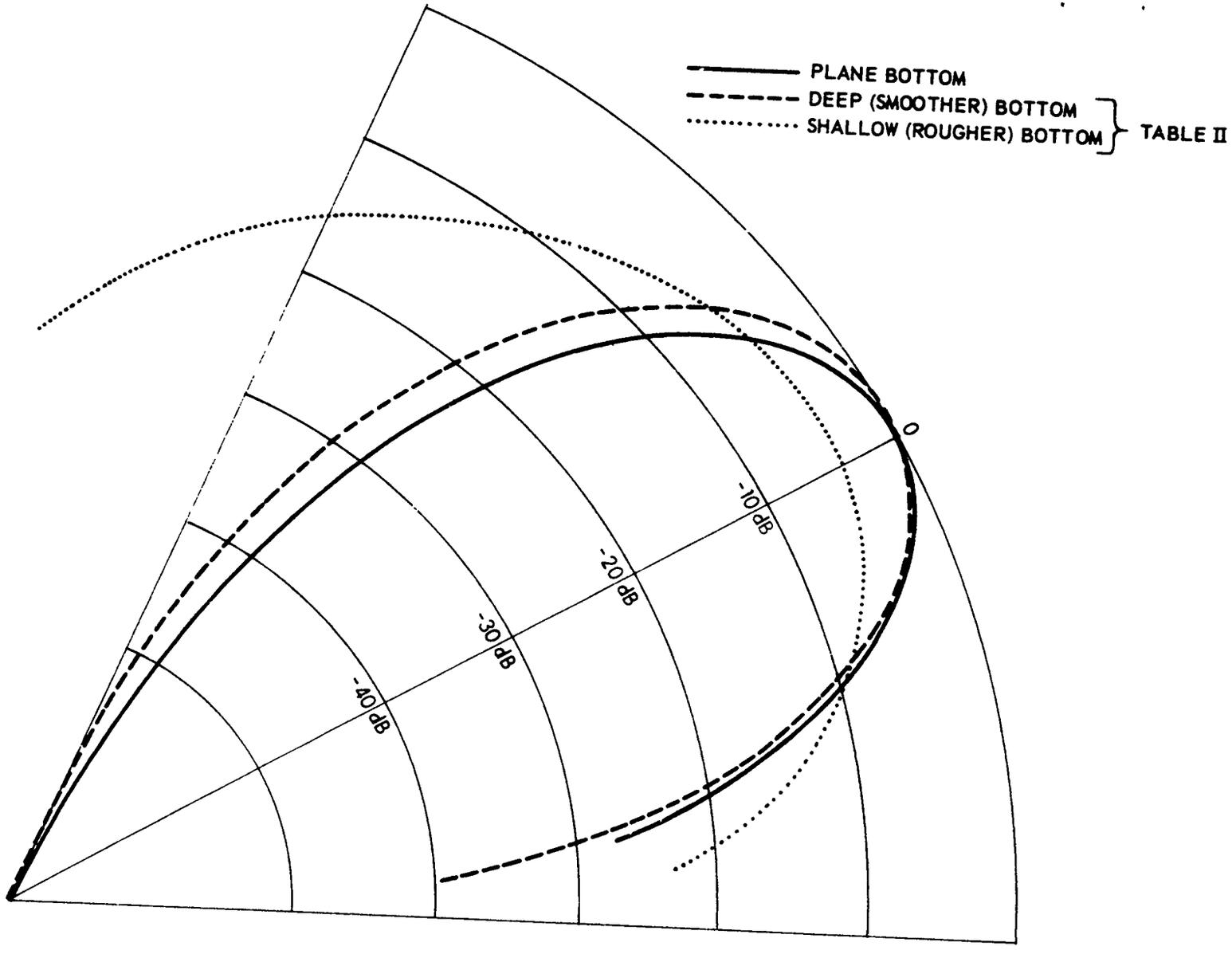

THE EFFECT OF AN IMPENETRABLE ROUGH BOTTOM
ON A BOTTOM BOUNCE SONAR BEAM
AT 30 deg GRAZING ANGLE

ARL - UT
AS-71-389
PJW - ORS
4 - 20 - 71

The beam reflected by a perfectly reflecting plane bottom is included for comparison. The beamwidth of the beam reflected by a plane appears to be broader than 8 deg for the simple reason that the angles shown in the drawing are measured with respect to the point where the beam axis intersects the surface. This makes the beam appear to be about twice as broad as it would be if the angles were measured with respect to the image point where the source can be thought of as actually being located. The slight roughness assumed for a deep bottom has resulted in a beamwidth increase from 8 deg to 9 deg at 30 deg grazing incidence with no other perceptible effects. The greater roughness assumed for the shallow bottom has resulted in a beamwidth increase from 8 deg to 12 deg at 30 deg grazing incidence and the loss of about 4 dB from the specular portion of the beam. It should be emphasized that the beam broadening is given with respect to the source, i.e., the ship; it appears to be larger in Dwg. AS-71-389 because of the way the angles are referenced.

The curves given in Dwg. AS-71-390 represent the effect of the single and double interface shallow bottom model on a bottom reflected sonar beam at 15 deg grazing angle. The beam which would be reflected by an acoustically impenetrable plane is also included for reference. For the single interface case the peak value of the beam is displaced downward by about 3 deg from the beam axis. The reason for this angular displacement of the beam maximum is that the portions of the beam which are incident at higher grazing angles have greater penetration into the bottom if $c_{BOTTOM} > c_{WATER}$. For a low speed bottom the peak would be displaced to the opposite side of the beam axis or the beam would have a null at the angle of intromission. There is also a 4 dB loss in the specular direction due to penetration, in addition to the 4 dB scattering loss. When an intermediate depositional layer is present that provides a good impedance match between the water and bottom, then the penetration losses increase drastically. Ordinarily, for a smooth sub-bottom and little absorption the peaks of the multiple lobes due to the sub-bottom interference would be

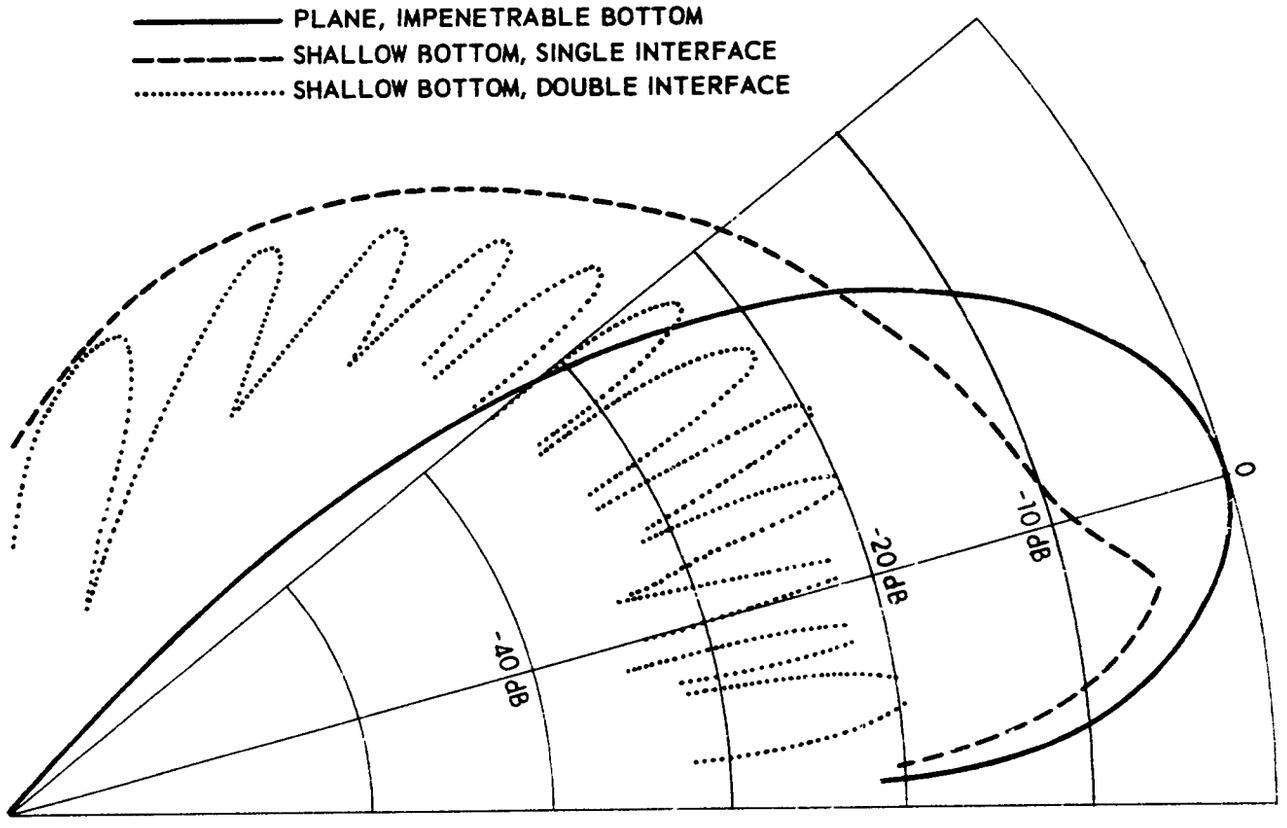

THE EFFECT OF A ROUGH, ACOUSTICALLY PENETRABLE BOTTOM ON A BOTTOM BOUNCE SONAR BEAM AT 15 deg GRAZING ANGLE

ARL - UT
AS-71-390
PJW - ORS
4 - 20 - 71

very close to the level of the single interface scattering. However, since the sub-bottom can also scatter acoustic waves, the sub-bottom is a source of scattering interference with the waves reflected by the bottom itself. The amount of lobing that occurs depends on how many wavelengths the sub-bottom lies below the bottom. For the assumed shallow bottom model, the sub-bottom lies about 7 wavelengths below the bottom, and consequently there is considerable lobing due to interference. Drawing AS-71-391 shows the effect of the shallow (rough) bottom on a sonar beam incident at 30 deg grazing.

Drawings AS-71-392 and AS-71-393 show the effect of the typical deep ocean bottom model on a sonar beam incident at 15 deg and 30 deg grazing, respectively. Since the water-sediment interface was assumed to be quite smooth, little beam broadening has taken place. Again the main effects of the bottom at 15 deg grazing have been the displacement of the beam peak and some penetration losses. In the case of an impedance matching intermediate layer, there is some additional penetration loss with very little lobing. The lobing effect is much less here since the sub-bottom lies only one and one-half wavelength below the bottom. At 30 deg grazing, the main effect of a smooth, acoustically penetrable bottom has been to produce a slightly narrower beam with about 10 dB loss near specular angles and only minor lobing.

It must be emphasized that the descriptions of shallow and deep bottoms given here are strictly arbitrary; there is no rule which states that a deep bottom must be smoother and have thinner sediment deposits than a shallow bottom. On the average these descriptions might hold, and at the very least they can be considered reasonably representative of ocean bottoms.

In summary, several general comments can be made on the effects of rough, acoustically penetrable bottoms on bottom bounce sonar

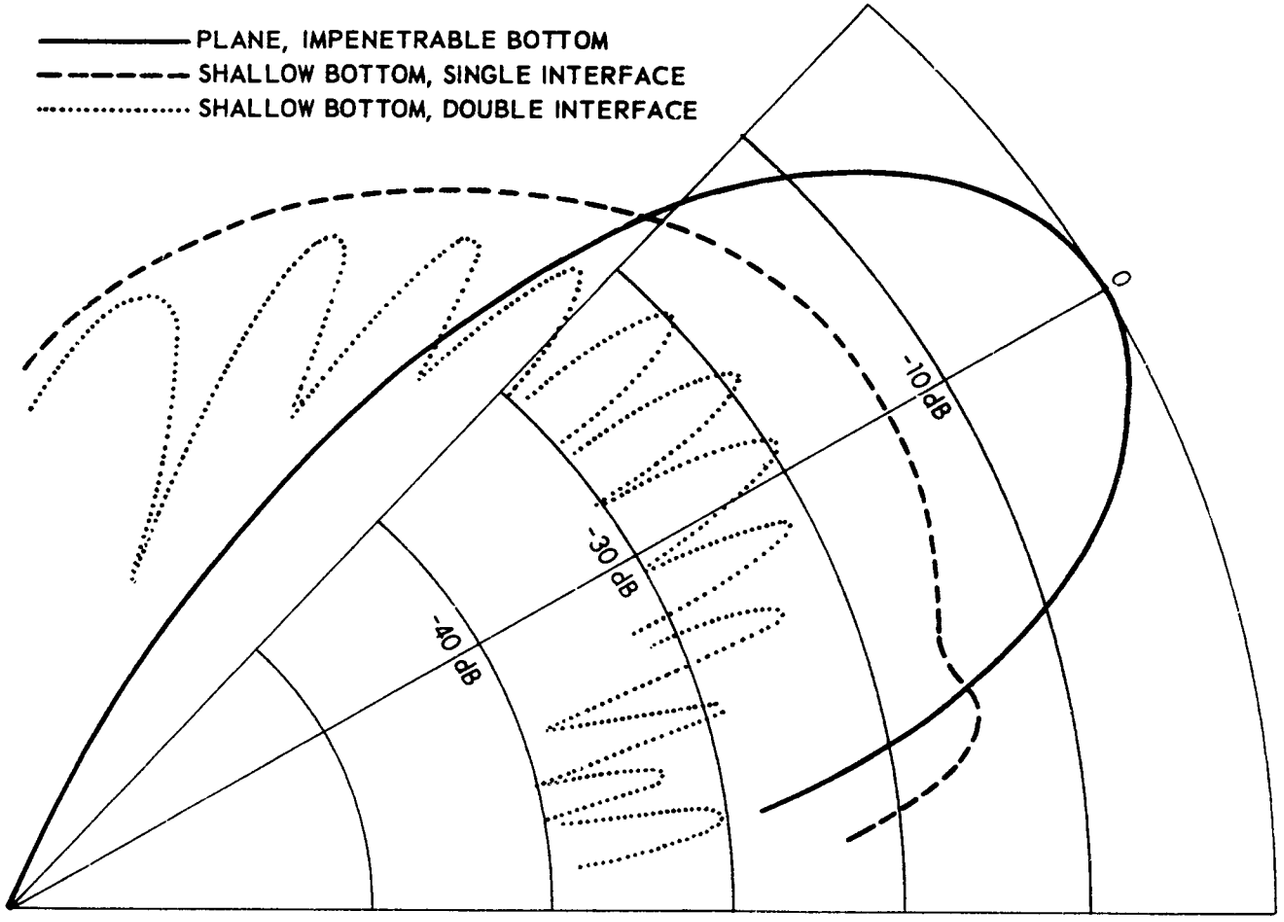

THE EFFECT OF A ROUGH, ACOUSTICALLY PENETRABLE BOTTOM ON A BOTTOM BOUNCE SONAR BEAM AT 30 deg GRAZING ANGLE

ARL - UT
AS - 71 - 391
PJW - ORS
4 - 21 - 71

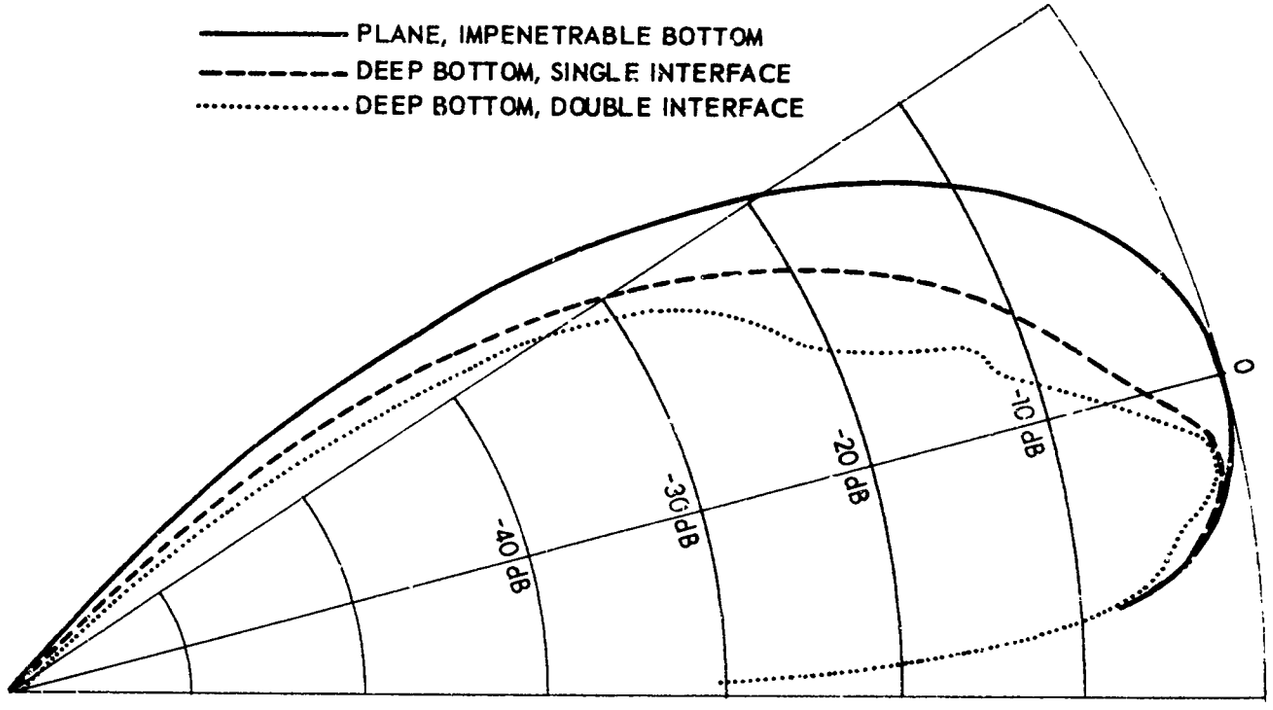

THE EFFECT OF A ROUGH, ACOUSTICALLY PENETRABLE BOTTOM ON
A BOTTOM BOUNCE SONAR BEAM AT 15 deg GRAZING ANGLE

ARL - UT
AS-71-392
PJW - ORS
4-21-71

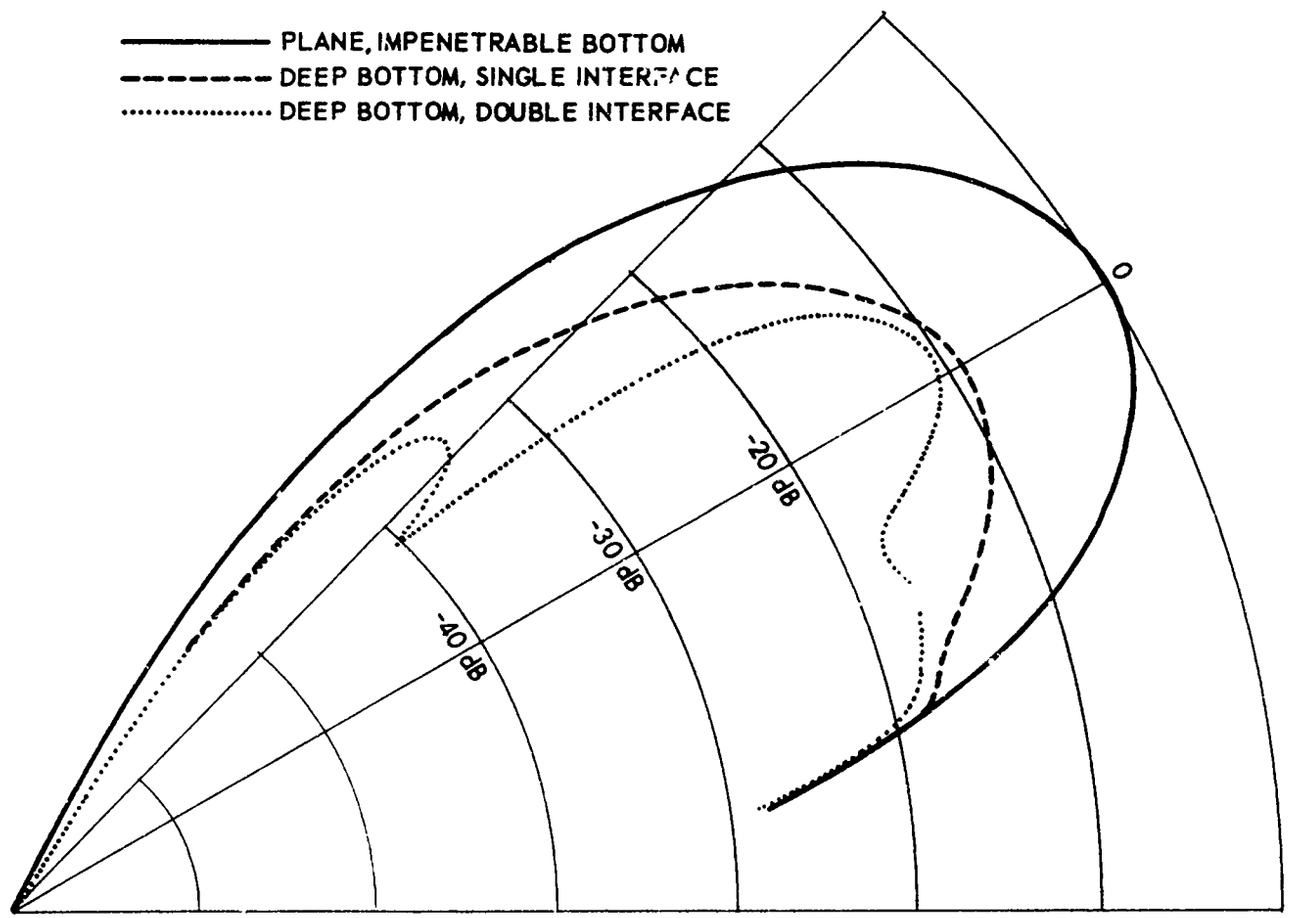

THE EFFECT OF A ROUGH, ACOUSTICALLY PENETRABLE BOTTOM ON A BOTTOM BOUNCE SONAR BEAM AT 30 deg GRAZING ANGLE

ARL - UT
AS-71-393
PJW - ORS
4 - 21 - 71

operation. If the bottom is rough, then directional ambiguity is introduced into the target location due to the beam broadening caused by scattering. Further, if the bottom is both rough and penetrable, then considerable beam distortion, or lobing, and level decrease due to penetration may occur on bouncing a signal from the bottom. Also, some of the secondary effects would become more important. For example, volume reverberation would increase in duration and possibly level since scattering would increase the insonified ocean volume. In addition, broad scattered beams would contribute to mutual interference among several sonar systems operating in the same vicinity. Finally, a rough bottom introduces fluctuations into the scattered sound field as the insonified area moves along the bottom. Of course, the fluctuations depend on the density of scatterers in the insonified area. If there are very many scatterers in the insonified area, then the fluctuations will be small as the insonified area moves along the bottom, since each return will represent a large statistical sample. For this reason the fluctuations in a signal scattered by a deep bottom will be less than in a signal scattered by the identical bottom at a shallower depth, since the insonified area increases with depth.

IV. THE IN SITU DETERMINATION OF THE SUITABILITY OF THE OCEAN BOTTOM FOR BOTTOM BOUNCE SONAR OPERATION

There are many operational circumstances in which one would like to use the bottom bounce mode, but knowledge of the suitability of the bottom for such sonar operation is lacking. Regional acoustic atlases have been compiled, but at best these can supply only very broad outlines as to the usefulness of the bottom bounce mode at a given location. Ideally, what a shipboard sonar operator desires would be a very simple method to determine the characteristics of the bottom using readily available equipment.

If there is only one ship available, then the bottom measurements must be made in the backscattering configuration. The question then naturally reduces to: What can be predicted about the forward scatter behavior from measurements of the backscattering? To be able to answer this question requires that the theoretical foundations of forward and backscattering be well understood.

The theoretical formulation of scattering developed at Applied Research Laboratories (ARL) predicts forward scattering accurately if the rms height and slope of the scattering surface are known. Also, backscattering predictions are quite good from normal incidence down to 50 deg grazing angles. Below 50 deg, the typical flattening out of the backscattering curves, which is observed in all backscatter measurements (acoustic, radar, and laser), is not predicted by the usual theories. It was first postulated by Kur'yanov[29] that the correct agreement between measured and predicted backscattering could be obtained if it were assumed that the surface

was composite in nature; that is, in addition to the roughness features which are easily measured, there occurs on most natural surfaces a small scale roughness which is usually characterized by a much larger rms slope than that of the large scale roughness. The concept of scattering due to large scale and small scale roughness features has received additional theoretical and experimental support in the papers of Beckmann,[30] Fuks,[31] Fung and Chan,[8] Volovova and Zhitkovskiy,[32] Zhitkovskiy and Lysanov,[33] and Schmidt.[34] Some natural examples for this type of feature would be ripple on swell, boulders strewn on a hill, etc. The first theories developed using the composite surface concept gave good predictions of backscattering after all of the parameters had been adjusted, but in many cases for the same parameter values only nonsense could be obtained for forward scattering. The reason for these failures can be traced directly to the approximations made in the treatment of the surface slopes.

The composite theory developed at ARL utilizes an exact slope treatment and can, consequently, predict both forward and backscattering from the same set of parameters. Unfortunately, the small scale features usually cannot be measured; hence, they can only be determined by adjusting the parameters until the theory fits experiment. This requires a certain amount of faith on the part of the theoretician. It should be noted that this procedure is not as weak as it sounds. Since the large scale roughness is well known, only the small scale parameters must be guessed. However, the guess obtained for one surface at one frequency gives a good fit for all the other surfaces and frequencies, which instills considerable faith in the procedure.

The most surprising aspect of the small scale roughness features is that their effect is only evident in low grazing angle backscattering; forward scattering and high angle backscatter are largely determined by the large scale roughness features.

The backscattering by an impenetrable surface, which has small scale roughness ($\lambda/\sigma \approx 100$) with large rms slopes, is shown in Dwg. AS-71-355. Notice the almost constant level from 75 deg on down to 20 deg grazing. The backscattering level seen in this curve can be adjusted to any arbitrary level by merely changing the values of the rms height and/or slope. Examination of the forward scattering curve for the same parameter values reveals that the relatively large change in the distribution of energy seen in the backscatter direction is obtained at a cost of only 1/3 dB in the forward specular direction. While the curve given in Dwg. AS-71-355 was derived from theoretical considerations, experimental curves of like shape have been obtained by Nolle et al.[35] for a very similar experimental situation. No attempt was made in Dwg. AS-71-355 to match the physical parameters of Nolle's experiments.

If the backscattering for impenetrable surfaces composed of the single small scale roughness but various large scale roughnesses is plotted, one obtains the curves shown in Dwg. AS-71-356. If the small scale parameters are adjusted slightly, but the large scale parameters held fixed, the curves shown in Dwg. AS-71-357 are obtained. The only change seen is that the limiting level at low grazing angles has been adjusted upward 5 dB.

The significance of Dwg. AS-71-357 is that at grazing angles less than 45 deg no information on the large scale roughness features is retained, since the backscattering at those angles is controlled by small scale roughness. Consequently, if only the backscattering data for a single frequency and at grazing angles less than 45 deg were available, no conclusions about the large scale roughness could be reached, and hence no prediction of forward scatter could be made. (Remember, it is only the large scale roughness which affects forward or specular scattering.) In Dwg. AS-71-356, it is seen that no information on the large scale roughness is retained at grazing

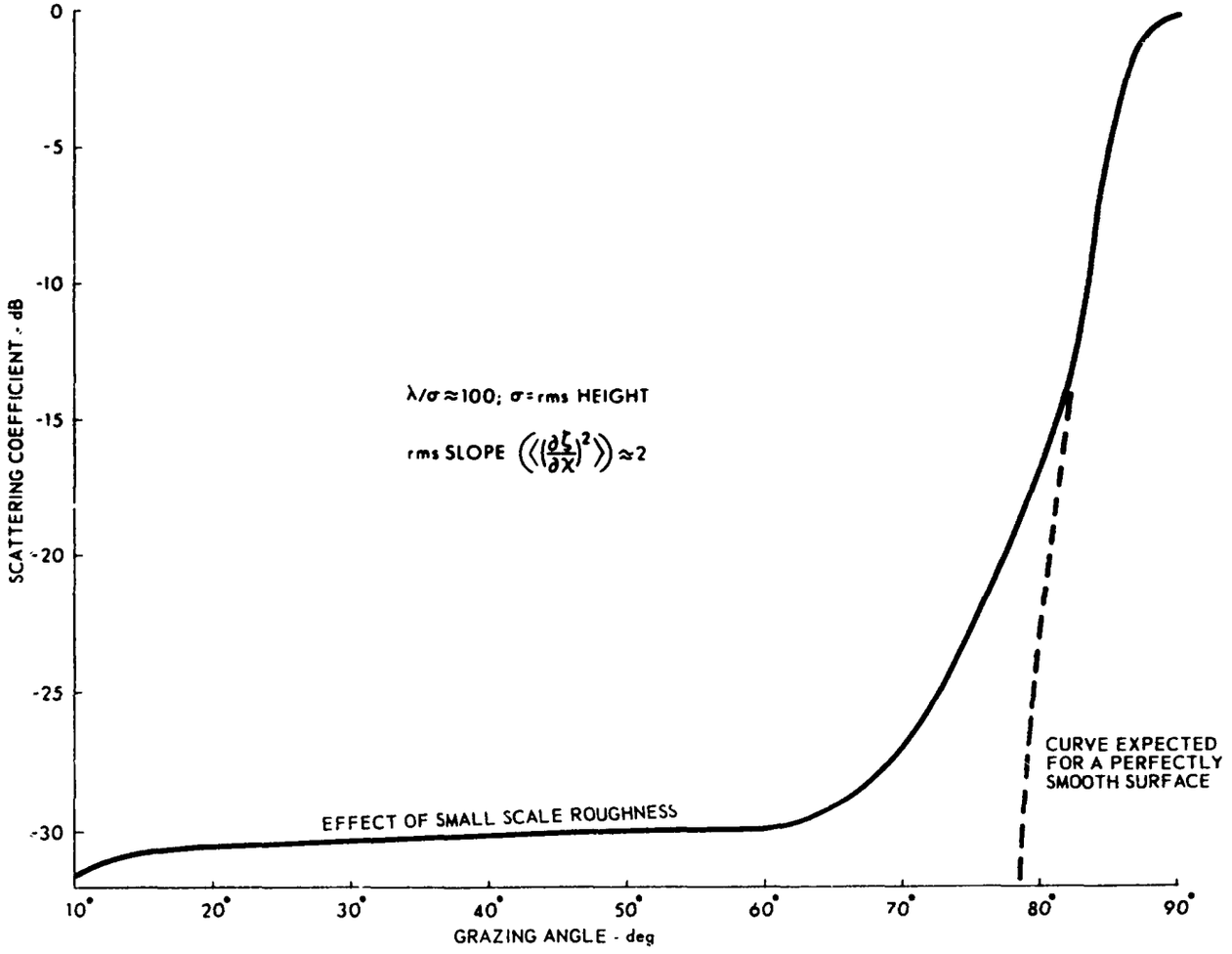

ARL - UT
AS-71-355
PJW - RHC
4 - 20 - 71

BACKSCATTERING BY A SURFACE
WITH SMALL SCALE ROUGHNESS

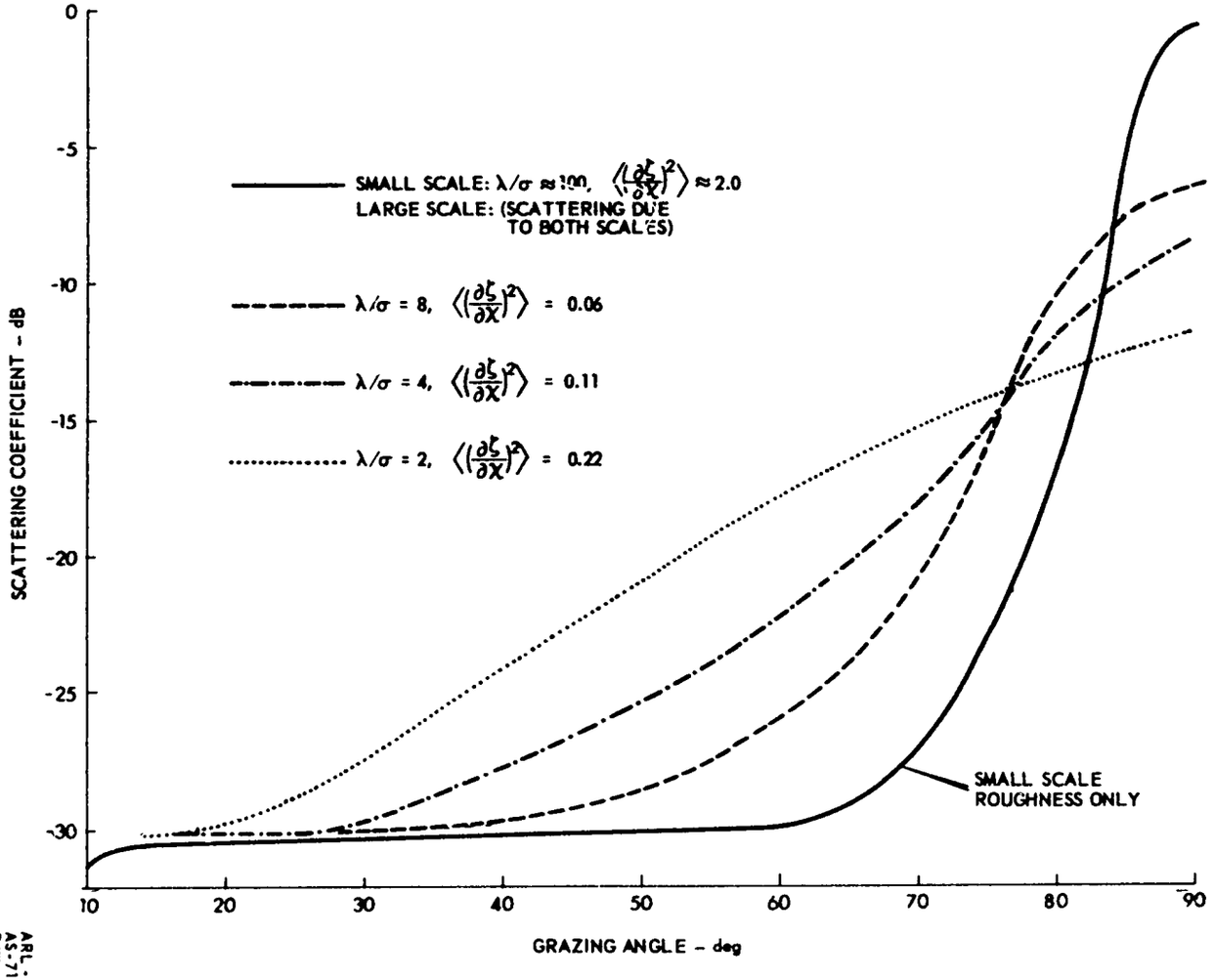

ARL - UT
AS-71-356
PJW - ORS
4 - 22 - 71

BACKSCATTERING BY A COMPOSITE ROUGH SURFACE

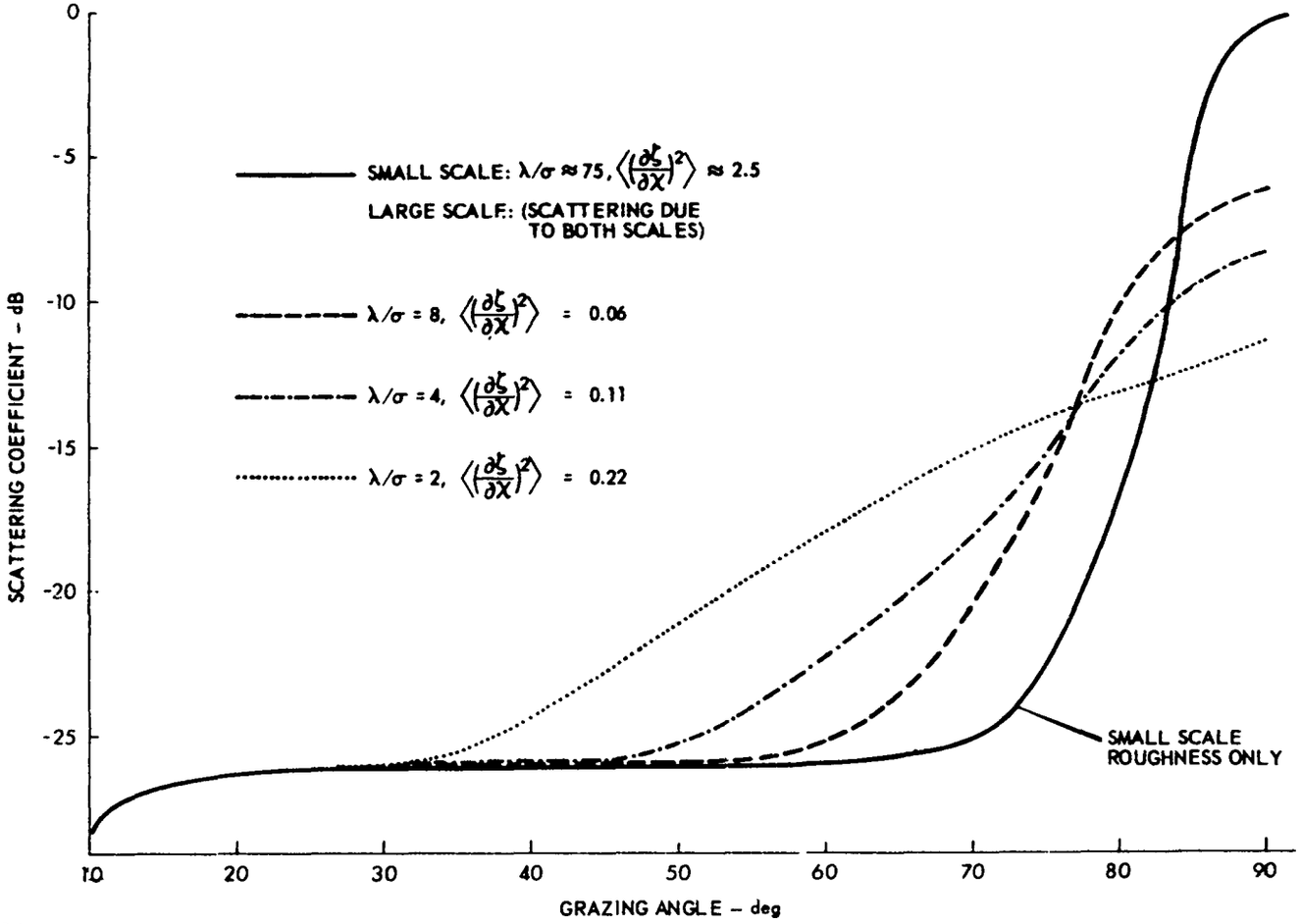

ARL:UT
AS-71-357
PJW-ORS
4-22-71

BACKSCATTERING BY A COMPOSITE ROUGH SURFACE

angles less than 30 deg. It should be noted that the scattering due to the small scale roughness is frequency dependent, in some cases varying as frequency to the fourth power; therefore, the masking effect of the low grazing angle backscatter may not be as pronounced at other (principally lower) frequencies. The effects due to the large scale features appear to be largely frequency independent;[32,33] hence, the information about the large scale features will be retained if frequency adjustments are made to reduce the small scale scattering.

In view of the difference in the levels at normal incidence for the different roughnesses in Dwg. AS-71-356 and AS-71-357, the obvious question might then be asked: Suppose the data for normal incidence (90 deg grazing) were available, could anything be inferred from these data? First, recall that the surfaces considered in these figures are acoustically impenetrable. For an ocean bottom the return at normal incidence will depend on both the penetrability and the roughness of the surface as given in Eqs. (61) and (63). If the acoustic parameters of the bottom are unknown, then it is impossible to determine the relative influence of the topography and the acoustic penetrability on the scattering. Consequently, it will not be known if the loss measured at normal incidence was due primarily to scattering or to penetration. The importance of this point was discussed in the example given in the introduction to Chapter III.

It was pointed out in Chapter II, in the discussion of the stationary phase evaluation of $R(\theta_1)$, that for backscattering, $R(\theta_1)$ is given by a constant ($|R(\theta_1)| \leq 1$) for the single interface case. Consequently, the shape of the backscattering curve from a penetrable surface remains constant, with only the level shifted downward. Therefore, for a fixed frequency, it is necessary to have the backscattering curve for the entire range of grazing angles from 90 deg to 10 deg (or, at least from 90 deg to 40 deg) if any inferences about the large scale roughness are to be drawn. The implication of these facts is rather severe if

it was hoped that forward scattering performance of a bottom bounce sonar could be predicted from simple observations of the backscattering return level from the sonar and the on-board depth sounder since these pieces of equipment will not cover the requisite angles or frequencies.

At present, it seems that the only way to obtain data on the bottom roughness from backscatter measurements using present ships' equipment will require some fairly sophisticated signal processing. Even this method will require that the return from a very small region of the bottom (fractions of a correlation length) must be resolved by the receiver.

If a wideband source, for example an explosive charge, is used, then the ability to differentiate between the bottom losses arising because of scattering and acoustic penetration increases. This technique is complicated by the necessity of using wideband, multichannel filtering and recording equipment.

The separation of the losses due to scattering and bottom penetration is based on a presumed difference in the frequency dependence of the two effects. The scattering is assumed to be frequency dependent while the acoustic penetration is not. It is well known experimentally and theoretically that if the bottom features are large with respect to the wavelength, then the scattering is frequency independent and varies only as the slopes of the scatterer and not the heights. This effect is associated with the high frequency [in reality, large $g(g = k^2\gamma^2h^2)$] limit of scattering. To obtain roughness information from a wideband source requires that the frequencies present should represent both the high frequency limit and the low frequency limit. The data recorded using explosive sources are usually contained in the 5 octave band from 1 to 30 kHz. These frequencies represent wavelengths of 2 to 60 in.

Based on the rather incomplete knowledge of the roughnesses to be found in the ocean (see Chapter III), the frequency band of 1 to 30 kHz adequately represents the high frequency limit but is only marginally close to a low frequency limit. However, for many ocean regions the 1 to 30 kHz band provides sufficient frequency dependence to determine the relative effects of roughness.[32,34]

The assumption that the acoustic penetration of the bottom is frequency independent holds only for a bottom from which the return comes primarily from a single interface. If the bottom consists of several layers with different acoustical properties, the angular dependence of the reflection coefficient will be complex and in every instance will be associated with the parameters of the layers and the frequency of the sound wave. Similarly, if the absorption is strongly frequency dependent, interpretation of the bottom returns is again rendered difficult.

Considerable qualitative data are, however, provided by the short pulses which are associated with explosive sources. Zhitkovskiy[36] describes a method of measuring the distances between irregularities on the ocean floor. Brekhovskikh[37] shows data from which much qualitative information on the character of the bottom can be determined by a fairly inexperienced operator after only a cursory inspection.

In summary, the feasibility of <u>in situ</u> determination of ocean bottom characteristics depends on the available measurement apparatus. The bottom characteristics of interest have been shown to be the large scale topography of the bottom and the acoustic penetrability (which depends on the physical composition and structure of the bottom). To adequately determine these characteristics from simple measurements of the backscattered signal level requires at least the range of

grazing angles from 90 deg to 40 deg. The confidence in this determination will be substantially increased if the data for several different frequencies are also available. The equipment presently available in tne form of on-board sonars and depth sounders is not adequate for this determination. If additional equipment in the form of wideband, multichannel filtering and recording equipment is available, then explosive sources may be used to obtain the necessary angular and frequency measurements. However, in many cases, the reduction of these raw data and the subsequent prediction of forward scattering require sophisticated analysis by experienced personnel.

The ideal situation would be to have a profilometer which has a sufficiently narrow beam so that the insonified area of the bottom would be a few correlation lengths. The time record of this return would then represent a bottom profile with sufficient resolution to determine the topographical features of interest in forward scattering. Further, if the source were calibrated, then the level of the returned signal could be used to determine the acoustic penetrability of the bottom. Under these circumstances the forward scattered signal could be predicted.

V. ACOUSTIC FIELD IN A SURFACE DUCT WITH A ROUGH SURFACE

A. Introduction

The acoustic field is derived for a cw point source located in an inhomogeneous medium with a rough surface. Application is made to the case of a surface duct, and examples are given for two cases (bilinear and Epstein). The effects of surface roughness are introduced by means of an effective reflection coefficient. Lapin[38-40] and Lysanov[41-43] show that a statistically rough boundary can be approximated by a flat boundary with some effective reflection coefficient in the case of waveguide propagation, but the form of this coefficient will, in general, be different from the expression for reflection from a single uneven surface. Lysanov[43] explicitly carries out the calculations for the case of a Gaussian surface overlying a bilinear surface duct.

Recently Bucker[44] has given an excellent treatment of propagation in a layered waveguide with lossy boundaries. Bucker, however, gives the effect of roughness in terms of a plane wave reflection coefficient S, which does not allow for the variable nature of the medium. The reflection is assumed to take place from a pseudoisovelocity layer which is allowed to shrink to zero. Bucker makes no attempt to drive S from the statistical nature of the surface. He assumes various values for the dB loss per surface reflection SL_n and then calculates the reflection coefficient S from the equation

$$SL_n = -20 \log_{10} |S| \quad . \tag{64}$$

The propagation model that Bucker formulates assumes an impedance boundary condition. The value for the impedance is determined from the plane wave reflection coefficient. In order to find initial approximate eigenvalues, Bucker relates each mode to a ray and arrives at a boundary attenuation in the form of an imaginary component to the eigenvalues. Specifically, he obtains

$$\frac{SL_n + BL_n}{H_n} = -20 \log_{10} e^{-k_n''} \quad , \tag{65}$$

where BL_n is the bottom loss of the ray associated with mode n, H_n is the ray horizontal cycle distance, and k_n'' is the approximate imaginary part of the eigenvalue which is due to the lossy boundaries. Bucker[45] assumes various values for SL_n since the values for SL_n given by Marsh[46] seem to be too high for the experimental cases he treats.

The rough surface propagation problem has also been treated by Clay.[47] Clay shows that surface scattering produces an increase in mode attenuation and a decrease in coherence of the signal. Ray theory has been applied to this problem by various authors.[48-53] A useful survey of both ray theory and wave approaches has been given by Schulkin.[54] The present report will follow the treatment given by Bucker, but will use Green's functions and attempt to arrive at expressions for the surface loss per bounce which relate directly the ray angle, frequency, and peak to trough heights.

B. Green's Function Solution

The wave equation for a point source, with angular frequency ω, located in a layered inhomogeneous medium is given by

$$\nabla^2 P - \frac{1}{c^2(z)} \frac{\partial^2 P}{\partial t^2} = -i\omega Q_o \delta(\bar{r}-\bar{r}_o)\, e^{-i\omega t} \quad , \tag{66}$$

where P represents the pressure, $c(z)$ is the sound velocity (variable in the coordinate z), and $\delta(\bar{r}-\bar{r}_o)$ is the three-dimensional Dirac delta function. The strength Q_o of the source is equal to the density times the volume velocity, that is, mass flow per second. If cylindrical coordinates (r,θ,z) are assumed with azimuthal symmetry and a time factor of $\exp(-i\omega t)$ is suppressed, the following equation is obtained:

$$\frac{1}{r}\frac{\partial}{\partial r}\left(r\frac{\partial P}{\partial r}\right)+\frac{\partial^2 P}{\partial z^2}+k^2(z)P=\frac{-i\omega Q_o\,\delta(r)\,\delta(z-z_o)}{2\pi r} \quad , \tag{67}$$

where P now represents the time independent pressure. The wave number $k(z)$ is defined as $\omega/c(z)$ and the source is located at $z = z_o$ and $r = o$, as indicated in Dwg. AS-70-767. The vertical depth coordinate z varies from $0 \leqq z \leqq \infty$, and the range coordinate r varies from $0 < r < \infty$. The boundary conditions imposed on Eq. (67) are that

a) P must satisfy a radiation condition for $r \to \infty$ and $z \to \infty$

b) $$\left.\frac{\partial P/\partial z}{P}\right|_{z=o} = \gamma \tag{68}$$

c) P and $\frac{\partial P}{\partial z}$ be continuous across any discontinuities in the velocity-depth profile (such as the bilinear profile).

The statistical nature of the surface at $z = o$ will be introduced by means of an effective reflection coefficient which then determines γ.

In the Green's function approach, Eq. (67) is separated into the following forms:

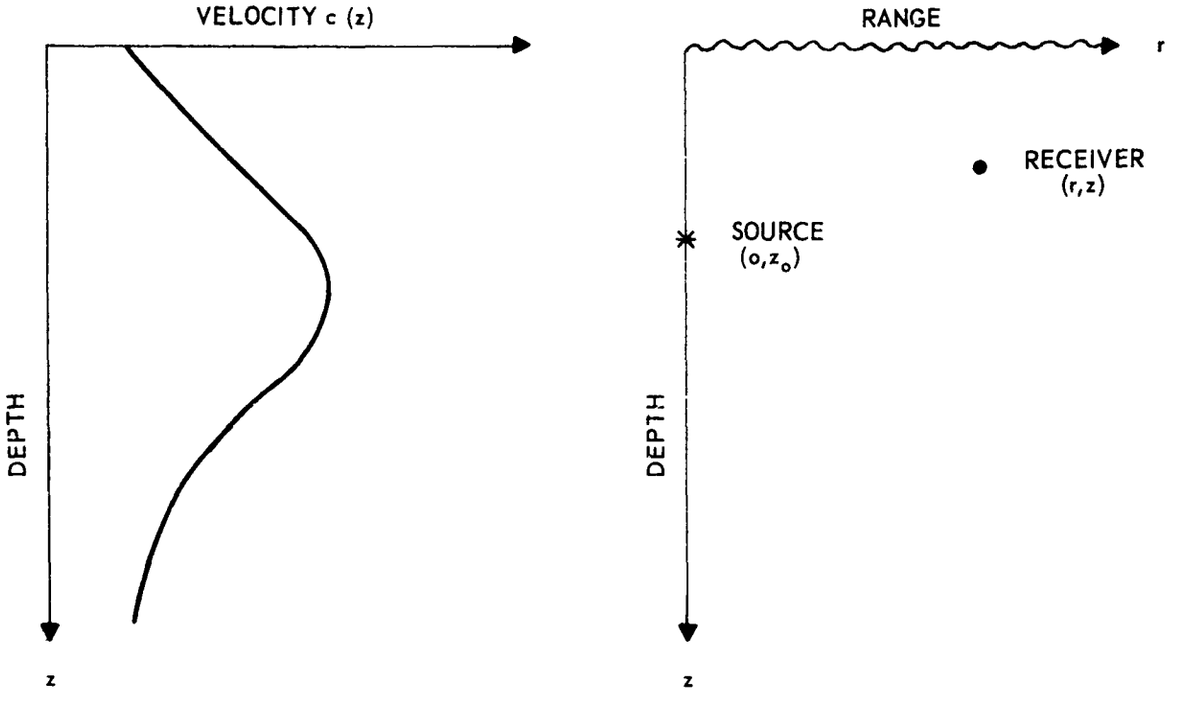

DIAGRAM OF WAVEGUIDE SHOWING LOCATION
OF SOURCE AND RECEIVER

ARL - UT
AS-70-767
RLD - WDC
6 - 29 - 70

$$\left[\frac{d}{dr}\left(r\frac{d}{dr}\right) + \lambda r\right]G_1(r,\lambda) = \frac{-\delta(r)}{2\pi} \tag{69}$$

$$\left[\frac{d^2}{dz^2} + k^2(z) - \lambda\right]G_2(z,z_o,-\lambda) = -i\omega Q_o\delta(z-z_o) \quad , \tag{70}$$

where λ is the separation constant. By the resolvent Green's function technique, the solution of Eq. (67) is given by a complex convolution of G_1 and G_2:

$$P(r,z,z_o) = \frac{1}{2\pi i}\int_C G_1(r,\lambda)G_2(z,z_o,-\lambda)d\lambda \quad , \tag{71}$$

where the contour C separates the singularities of the Green's functions.

The solutions of Eq. (69) and Eq. (70) that satisfy the required boundary conditions are given by

$$G_1(r,\lambda) = \frac{i}{4}H_o^1(\xi r)(\xi = \lambda^{1/2}, o < \arg\lambda < 2\pi) \quad , \tag{72}$$

$$G_2(z,z_o,-\lambda) = \frac{n_2(z,\xi)[n_1(z_o,\xi) - X^- n_2(z_o,\xi)]}{W(n_2,n_1)} \quad z_o < z < \infty \quad , \tag{73}$$

$$G_2(z,z_o,-\lambda) = \frac{n_2(z_o,\xi)[n_1(z,\xi) - X^- n_2(z,\xi)]}{W(n_2,n_1)} \quad o < z < z_o \quad ,$$

where $H_o^1(\xi r)$ is the Hankel function of the first kind, and

$$X^- = \frac{n_1'(0,\xi) - \gamma n_1(0,\xi)}{n_2'(0,\xi) - \gamma n_2(0,\xi)} \quad . \tag{74}$$

The Wronskian of n_2 and n_1 is represented by $W(n_2,n_1)$, where n_2 is a solution to the homogeneous part of Eq. (70) and has outgoing waves at $z \to +\infty$, and where n_1 has outgoing waves at $z \to -\infty$. The primes indicate differentiation with respect to z.

When Eq. (72) and Eq. (73) are used in Eq. (71), the solution for Eq. (67) is obtained as

$$P(r,z,z_o) = \frac{\omega Q_o}{4\pi} \int_C \frac{n_2(z_<,\xi)[n_1(z_>,\xi) - X^- n_2(z_>,\xi)]H_o^1(\xi r)\xi d\xi}{W(n_2,n_1)} \quad , \quad (75)$$

where $z_<$ and $z_>$ denote the smaller or larger, respectively, of the variables z and z_o.

When Eq. (75) is integrated by Cauchy's residue theorem, the normal modes (plus any branch line integrals) are obtained. The poles yielding the normal modes are given by the zeroes of the expression

$$[n_2'(0,\xi) - \gamma n_2(0,\xi)] \quad . \quad (76)$$

The normal mode expansion can be written as

$$P(r,z,z_o) = \frac{\omega Q_o}{2} \sum_{n=o} \frac{n_2(z,\xi_n)n_2(z_o,\xi_n)H_o^1(\xi_n r)}{N_n} \quad , \quad (77)$$

where

$$N_n = \int_o^\infty n_2^2(z,\xi_n)dz + \frac{n_2^2(0,\xi_n)}{2\xi_n} \frac{\partial\gamma}{\partial\xi}\Big|_{\xi_n} \quad , \quad (78)$$

or

$$N_n = \frac{-n_2(0,\xi_n)}{2\xi_n} \left\{ \frac{\partial}{\partial \xi} \left[n_2'(0,\xi) - \gamma n_2(0,\xi) \right] \right\}_{\xi_n} \quad .$$

Equation (77) can also be written as

$$P(r,z,z_o) = \left(\frac{\omega^2 Q_o^2}{2\pi r} \right)^{1/2} \sum_{n=o} \frac{n_2(z,\xi_n) n_2(z_o,\xi_n) e^{i\xi_n r}}{N_n(\xi_n)^{1/2}} \quad . \tag{79}$$

In general the eigenvalues ξ_n will be complex. The lossy boundaries add an extra imaginary component k_n'' to the complex eigenvalue ξ_n. (In the surface duct case, boundaries mean the surface and any velocity-depth discontinuities.) Approximate values for k_n'' can be found in the following manner (Bucker,[44] Urick,[55] and Watt[56]):

$$\frac{SL_n}{H_n} \equiv -20 \log_{10} e^{-k_n''} \quad , \tag{80}$$

or

$$k_n'' = \frac{SL_n}{8.686\ H_n} \quad , \tag{81}$$

where SL_n is the surface loss per bounce, and H_n is the ray horizontal cycle distance. SL_n is defined by

$$SL_n = -20 \log_{10} |S| \quad , \tag{82}$$

where S is the plane wave reflection coefficient from a pseudoisovelocity surface layer that is allowed to shrink to zero.

Explicitly, S is related to the boundary condition at the surface through the formula

$$\gamma = \frac{i\xi_n a(S-1)}{S+1} \quad , \tag{83}$$

where $(\xi_n a)^2 = (\omega/v_s)^2 - \xi_n^2$, and v_s is the sound velocity at the surface. Therefore, if either S or γ is a known quantity, it is possible to find the attenuation (k_n'') from Eq. (76). In this report the plane wave reflection coefficient will be assumed to be known. The mode attenuation factor k_n'' is approximately given by

$$k_n'' = \frac{-20 \log_{10} |S|}{8.686\, H_n} \quad . \tag{84}$$

From classical scattering theory the coherent reflection coefficient for a Gaussian surface is given by

$$S = -e^{-2(k \sin\theta_n \sigma)^2} \quad , \tag{85}$$

where θ_n is defined by the condition $\cos\theta_n = [v_s \mathrm{Re}(\xi_n)/\omega]$, and σ is the rms height value for the rough surface. If a peak to trough height h is known, then a good approximation (Longuet-Higgins) for σ is given by the equation

$$\sigma = \frac{h}{2\sqrt{2}} \quad . \tag{86}$$

Equation (82) will now be calculated for one of the cases Bucker considered. He found that a reasonable value for SL_n was between zero and one dB per bounce, yielding a value of S between -1 and -0.8913. For a peak to trough height of 2 ft and an average grazing angle of 3 deg, Eq. (85) yields a value of S equal to -0.92 for a frequency of

1.5 kHz. Therefore, Eq. (85) appears to be a valid method for introducing the surface roughness into waveguide problems.

Marsh[46] and Marsh, Schulkin and Kneale[57] have arrived at another expression for the surface loss per bounce using the Neumann-Pierson spectrum. Their expression for SL_n is given by

$$SL_n = -10 \log_{10}(1 - 0.0013\, b^{3/2} h^{1/10} L) \quad , \tag{87}$$

where h is the average trough to crest height in feet, L is the isothermal layer depth in feet, and $b = fh$ is the frequency-wave height product in kHz × ft. Since Marsh's formula for SL_n does not depend on the grazing angle θ_n, Eq. (87) is not believed to be a valid formula for introducing the losses due to surface scattering.

Computer programs for propagation loss versus range are presently being completed for two surface duct profiles. The profiles (Epstein and bilinear) are shown in Dwg. AS-71-188. (The figure has been taken with permission from the paper by Bucker and Morris.[58]) Various surface conditions are being considered for these two velocity-depth profiles, and propagation loss curves will be published as soon as the computer programs are completed. The Epstein profile is a five-parameter velocity function which has been examined for ray theory solutions and normal mode solutions. Explicitly, the Epstein profile is given by

$$\frac{1}{c^2(z)} = A\, \mathrm{sech}^2\left(\frac{z-z_1}{H}\right) + B \tanh\left(\frac{z-z_1}{H}\right) + D \quad , \tag{88}$$

where the quantities A, B, D, z_1, and H are parameters.

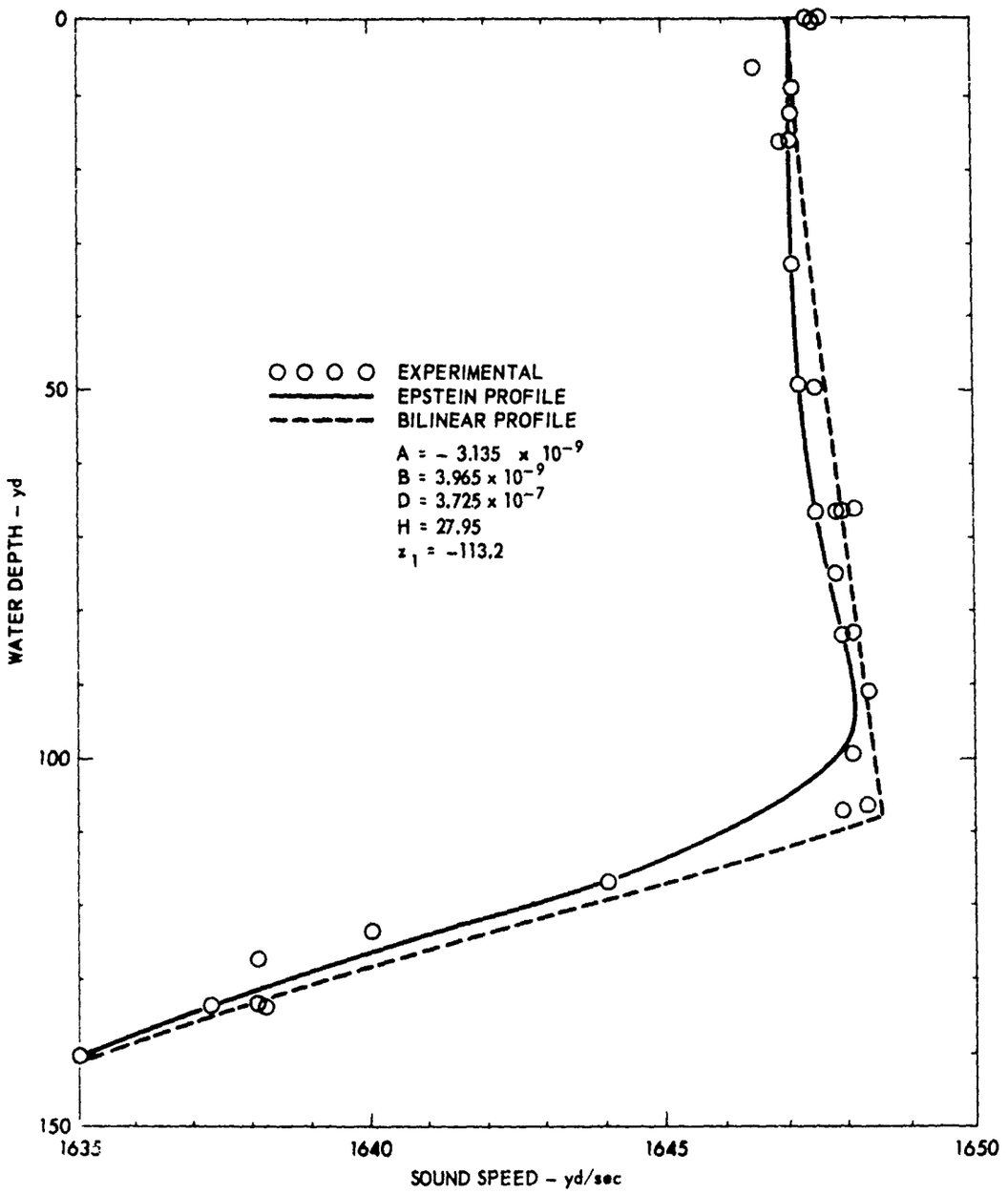

ARL - UT
AS-71-188
MLB - RFO
3 - 30 - 71

VELOCITY DEPTH PROFILES FOR SURFACE DUCT

The bilinear profile is also a well known, extensively treated, velocity function.[50] It is given by

$$c(z) = \frac{c_o}{\left(1 - \frac{2\gamma_o}{c_o} z\right)^{1/2}} \quad 0 \leqq z \leqq z_a \quad , \tag{89}$$

$$c(z) = \frac{c_o}{\left[1 - \frac{2\gamma_o}{c_o} z_a - \frac{2\gamma_1 (z - z_a)}{c_o}\right]^{1/2}} \quad z_a \leqq z < \infty \quad .$$

In Dwg. AS-71-188 the parameters are given by $c_o = 4940.94$ ft/sec, $z_a = 326.67$ ft, $\gamma_o = 0.0144$, and $\gamma_1 = -0.438$. These values were taken directly from Pedersen's article.[50]

Table II illustrates the effects of surface roughness on the first three modes of the Epstein surface duct considered by Bucker and Morris. The values for $\mathrm{Re}(c_n)$ in column two do not correspond to the roots obtained from

$$[n_2'(z_1, \xi_n) - \gamma n_2(z_1, \xi_n)] = 0 \quad ,$$

but correspond to the pressure release condition

$$n_2(z_1, \xi_n) = 0 \quad .$$

However, for the first few modes the values of $\mathrm{Re}(c_n)$ will nearly be the same. In column three the peak to trough heights are given from zero to 6 yd. The values for the rms heights, calculated from Eq. (86), then range from zero to 2.12 yd. Column four gives the surface loss per bounce as found from Eq. (82). The grazing angles

TABLE II

SURFACE LOSSES FOR FIRST THREE MODES

1	2	3	4	5	6	7	8
Mode No.	$Re(c_n)$ (yd/sec)	Peak to Trough Height h (yd)	Surface Loss SL_n (dB)	Grazing Angle θ (deg)	Reflection Coefficient S	Horizontal Range H_n (kyd)	Mode Attenuation k_n''
1	1647.31	0	0.000	0.46	-1.00	14.826	0.0
	1647.31	2	0.009	0.46	-0.999	14.826	6.7×10^{-8}
	1647.31	4	0.034	0.46	-0.996	14.826	2.7×10^{-7}
	1647.31	6	0.077	0.46	-0.991	14.826	6.0×10^{-7}
2	1647.59	0	0.000	1.15	-1.00	6.816	0.0
	1647.59	2	0.054	1.15	-0.994	6.816	9.2×10^{-7}
	1647.59	4	0.217	1.15	-0.975	6.816	3.7×10^{-6}
	1647.59	6	0.487	1.15	-0.945	6.816	8.2×10^{-6}
3	1647.93	0	0.000	1.64	-1.00	5.123	0.0
	1647.93	2	0.110	1.64	-0.988	5.123	2.5×10^{-6}
	1647.93	4	0.438	1.64	-0.951	5.123	9.8×10^{-6}
	1647.93	6	0.985	1.64	-0.893	5.123	2.2×10^{-5}

for the equivalent rays are given in column five. In column six the reflection coefficients as calculated from Eq. (85) are given. Column seven gives the horizontal range values in kiloyards as calculated from the following expression given by Pedersen and White:[60]

$$H_n = Ha^{-1/2}\left[\frac{1}{2}\ln|d| - \ln|2(aX_i)^{1/2} + \alpha_i|\right]$$

$$- Hc^{-1/2}\left[\frac{1}{2}\ln|d| - \ln\left(\frac{2(cX_i)^{1/2} + \delta_i}{u_i}\right)\right] \quad ,$$

where all quantities on the right of the equation are defined in Ref. 60, and where the subscripted quantities are evaluated at the surface. The mode attenuation factor k_n'' is calculated from Eq. (84) and is given in column eight. The reason for the low losses due to surface roughness is because of the small grazing angles and the fairly low frequency.

APPENDIX A

MODELING A PENETRABLE SURFACE: SELECTION OF MATERIALS AND PARAMETER MEASUREMENT

by

Helge Wieder* and Pat Welton

The use of model surfaces in experimental scattering measurements is a well established procedure. The models heretofore used in scattering work at Applied Research Laboratories have been made of pressure release materials. These scattering surfaces are representative of the ocean surface or an extremely gaseous ocean bottom. The scattering by the pressure release model surfaces is influenced only by the topography of the surface. The roughness of the topography of the models varies from quite smooth to very rough, and by using different frequencies the models can be scaled to represent regions of the ocean bottom ranging from abyssal plain areas to the midocean ridges.

In modeling acoustically penetrable ocean bottoms, not only should the expected topography be well modeled, but also the physical parameters and structure of the model should bear a reasonably direct relationship to realistic ocean values. While it is easy to obtain the topography desired by simply making molds of the pressure release models, the scaling of the physical parameters required considerable effort in the selection and measurement of the various materials available. In this appendix the selection criteria of a modeling material and the actual measurement of the physical parameters of this material will be discussed.

---

*Visiting Exchange Scientist from the Federal Republic of Germany

A. Selection Criteria

Recall that the experimental work which is to be performed under this program is the measurement of scattering by an acoustically penetrable liquid bottom of known statistical description as a function of angle and frequency. If the statistical parameters are to remain constant, then the model material must be permanently moldable. This requirement eliminates the use of the actual muds and unconsolidated sediments found on the ocean bottom in the making of the models, since the statistics would be unstable. When considering a permanently moldable material the first criteria which must be applied is the approximation of this material to a liquid. Essentially, this implies that the shear velocity must be small with respect to the compressional velocity. Some of the first materials which come to mind are transducer window materials. The agents are polyurethane compounds which behave like rubber in that they will only support a very small shear wave component, and hence very little conversion from compressional to shear mode occurs. These materials have the further advantage of having a ρc product (ρ is the density, and c is the speed of sound in the material) which is very close to that of water and which allows these materials to be used as a binding agent for sedimentary materials. In this manner a moldable compound can be made which has ρc values very close to those actually encountered in the ocean bottom but for which the binding agent is practically acoustically invisible.

The binding agent is Scotchcast 221 polyurethane, while the filler material is No. 5 sandblasting sand. The acoustic characteristics of the penetrable material can be altered by varying the proportion of filler material to binding agent. Number 5 sandblasting sand was selected as a filler material because it is the finest sand commercially available. A very fine sand is necessary to prevent settling of the filler during the curing of the binding agent. The only disadvantage of using sand as a filler material is that a ρc product less than that

of water cannot be obtained. However, this defect can be remedied by using the very fine, commercially available plastic beads which are used to make reflective paint.

It should be noted that as the proportion of filler material to binding agent is increased, the rigidity and hence the shear velocity of the compound increases, and the approximation to a liquid bottom is diminished.

B. Measurement of the Acoustic Parameters

Appropriate samples were made for each of the separate parameter measurements. Each sample was placed in a vacuum chamber prior to curing to remove any air bubbles entrained during the thorough mixing of filler material and binding agent. The measurements described in this section were made for pure Scotchcast 221 or for Scotchcast and sand. No samples of Scotchcast and plastic beads have been prepared as yet.

1. Shear Velocity in Pure Scotchcast

The shear velocity was determined by measuring the Lamé constant, μ, and by using the equation

$$c_s = \sqrt{\frac{\mu}{\rho}} \quad . \tag{A1}$$

The value of μ was determined according to two standard mechanical tests. The first determination was made by the method of the torsional pendulum.

A cylindrical sample of Scotchcast 221 of length 8 in. and radius 1/8 in. was rigidly clamped at the upper end, while a metal

weight of moment of inertia θ was rigidly fixed at the lower end. The metal weight was displaced a small angular distance from equilibrium and was released so that it described torsional oscillations. The period of the oscillations was measured. The value of μ is obtained from

$$\mu_T = \frac{2\omega^2 l\theta}{\pi r^4} \quad , \tag{A2}$$

where ω is the angular frequency of the oscillations, l and r are the length and radius of the sample, and θ is the moment of inertia of the suspended weight, which can be easily determined from standard formulas.

The second method of determining μ was a standard deformation test. A cylindrical sample of Scotchcast (diameter 3 in., length 4.5 in.) was deformed in a hydraulic press by a force in the direction of the axis. Length and diameter of the sample were measured as a function of force. From these measurements Young's modulus E and Poisson's ratio σ were determined. Then

$$\mu_D = \frac{E}{2(1+\sigma)} \quad . \tag{A3}$$

The values of μ determined from the two methods were very close:

$$\mu_T = 1.33 \times 10^6 \frac{N}{m^2}$$

$$\mu_D = 1.31 \times 10^6 \frac{N}{m^2} \quad .$$

If the density of Scotchcast 221 is 1.06 g/cm^3, then the shear velocity is

$$c_s = 35.3 \text{ m/sec} \simeq 115 \text{ ft/sec} \quad .$$

Subsequent error analysis indicated the values of μ were probably accurate to within ±2%.

2. Density and Porosity Measurements of Mixtures of Scotchcast 221 and Sand

The No. 5 sand used in these measurements consisted of pure quartz sand (the density of quartz is 2.65 g/cm^3). The grain size distribution was checked in standard sieves and the sand was found to be distributed as shown in Table A1. The sand is very well sorted, since approximately 70% of the sand grains are between 0.250 and 0.177 mm in diameter.

Three disk-like samples (diameter 5.5 in., thickness ≈ 1 in.) were made using different proportions of Scotchcast 221 and sand. The measured and computed values of the density and porosity are given in Table A2.

3. Velocity of Sound in Mixtures of Scotchcast 221 and Sand

Next the sound velocity in each of the three samples given above was measured. Since the sound velocity is fairly difficult to measure, three different techniques were used to determine the sound velocity.

METHOD I: The travel time differences between a source and a receiver are measured when the sample is in place between the source and receiver and when it is removed. The sound velocity in the sample is then given by

TABLE A1

DISTRIBUTION OF GRAIN SIZE

BY WEIGHT OF NO. 5 SAND

Sieve No.	ø mm	% by weight
45	0.350	5.2%
60	0.250	69.8%
80	0.177	18.8%
120	0.125	4.4%
170	0.088	1.8%
others		

TABLE A2

DENSITY AND POROSITY VALUES

OF SCOTCHCAST-SAND MIXTURE

Mixing Ratio by Weight Scotchcast:Sand	Measured Density g/cm^3	Computed Porosity %
Pure Scotchcast	1.06	100%
1:1	1.51	71.5%
1:3	1.86	45.6%

$$c = c_{water} \frac{1}{1 - c_{water} \frac{\Delta t}{d}} \quad , \tag{A4}$$

where c_{water} is the velocity of sound in water measured when the sample is removed, d is the sample thickness, and Δt is the travel time difference. While this method is not particularly accurate, it does have the advantage of allowing c to be measured for a wide range of frequencies to determine dispersion. The velocity of sound in water at 72°F was found to be

$$c_{water} = 1463 \text{ m/sec} \quad .$$

The velocity of sound as a function of frequency for the three different samples measured is given in Dwg. AS-71-358. In the range of frequencies measured, the sound velocity in pure Scotchcast was independent of frequency, while in the mixtures the velocity appears to be slightly frequency dependent. Error analysis of the measurement technique indicated that error for mixture 1:1 was about

$$\Delta c_{1:1} = \pm 36 \text{ m/sec} \quad ,$$

while for mixture 1:3 the error was probably

$$\Delta c_{1:3} = \pm 70 \text{ m/sec} \quad .$$

These error bounds are indicated in Dwg. AS-71-358 by the vertical extensions about the measured point.

METHOD II: If the frequency is varied and the frequency difference of neighboring maxima of the reflected signal (steady state part of a long pulse) is measured when the source and receiver are on the same side of the sample, then the sound velocity can be calculated from

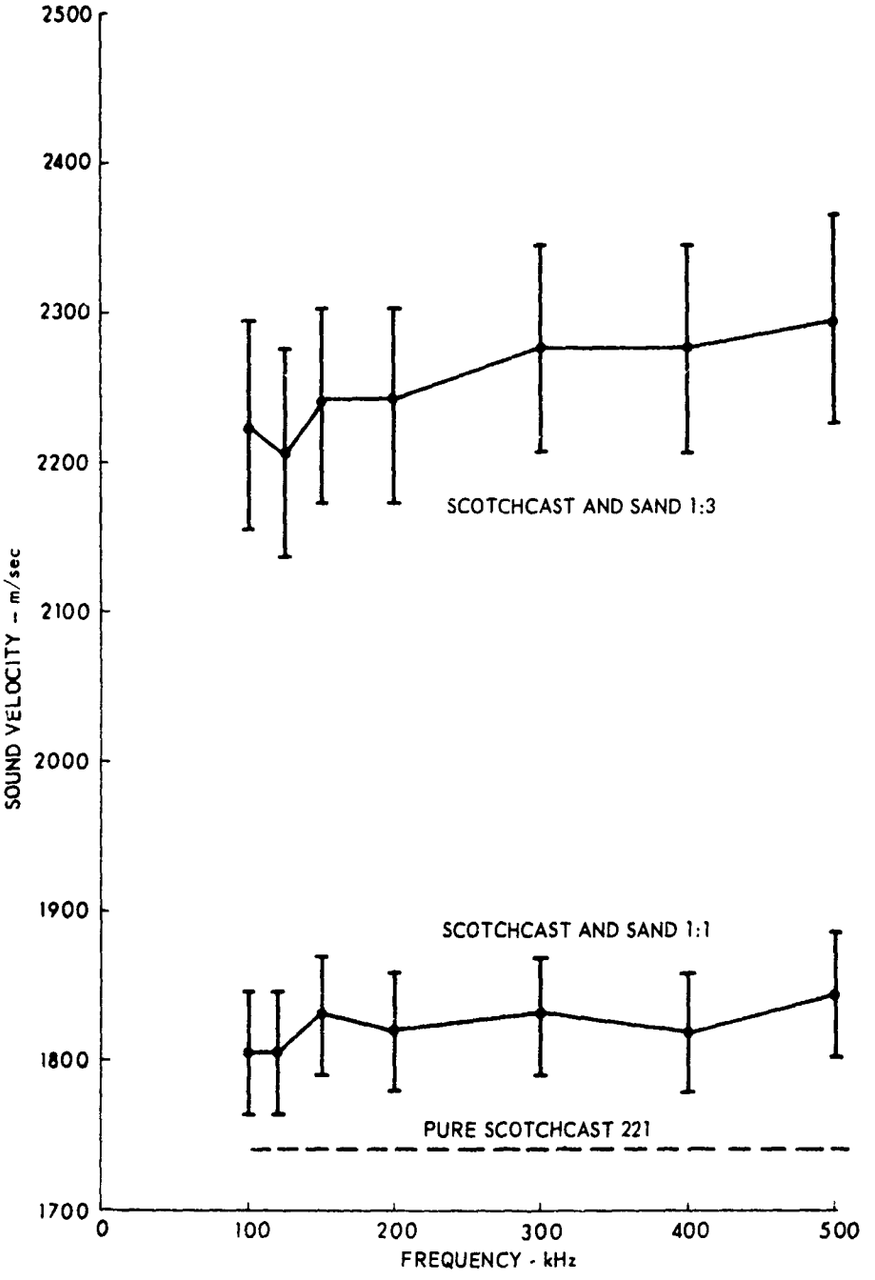

SOUND VELOCITY AS A FUNCTION OF FREQUENCY
MEASURED BY METHOD 1

ARL - UT
AS-71-358
PJW - RHC
4 - 20 - 71

$$c = 2\, d\Delta f \quad . \tag{A5}$$

Of the three methods used, this method should give the most accurate measurement of the sound velocity if the absorption is not too great. However, at the frequencies used here, the absorption was large enough that pulse distortion did occur, and consequently the accuracy of the results were reduced somewhat. The average value of four measurements for each of three samples is shown in Table A3.

METHOD III: The time difference between the very short pulses (shorter than $2d \cdot c$) reflected from the front and the rear interface of the sample was measured. This method has the advantage of measuring the velocity over twice the thickness instead of just over one thickness, as Method I. However, care must be taken to allow for the phase change which occurs upon reflection at the rear interface, and the correct portion of the two pulse returns must be compared. The average value of four measurements for each of three samples is given in Table A3 under the heading Method III.

TABLE A3

THE VALUES OF THE SPEED OF SOUND IN
MIXTURES OF SCOTCHCAST AND SAND

MIXTURE	METHOD I	METHOD II	METHOD III	MEAN VALUE
Pure Scotch-cast	1743 m/sec	1800 m/sec	1789 m/sec	1777 m/sec
1:1	1826 m/sec	1959 m/sec	1925 m/sec	1903 m/sec
1:3	2253 m/sec	2401 m/sec	2346 m/sec	2333 m/sec

The values of the speed of sound listed in Table A3 under Method I are the average values of the speed of sound measured in the frequency range 100 - 500 kHz.

4. Measurement of the Absorption

The absorption of a medium is generally identified as the imaginary part of the complex wave number

$$k = k_o + i\alpha \quad .$$

Absorption is usually measured by varying the source-receiver distance while maintaining a constant source output; the signal loss after spherical spreading has been removed is then the absorption loss (assuming a homogeneous medium).

In the case at hand, the determination of the absorption is not so simple since only one sample of absorbing material of fixed thickness was available. The absorption can be determined, however, by measuring the reflected level of a short pulse and the front interface and the transmitted level of this pulse through the disk. The transmitted pressure is given by

$$Tp_i = T_{12}T_{21}e^{-\alpha d}p_i \quad , \tag{A6}$$

where Eq. (A6) represents the transmitted pressure for pulselengths $L < 2d \frac{c_{material}}{c_{water}}$. T_{12} is the single interface transmission coefficient from water into the material, T_{21} is the single interface reflection coefficient from the material into water, and d is the thickness of the sample. Consideration of the boundary conditions gives

$$1 + R_{12} = T_{12} \quad ,$$

$$1 + R_{21} = T_{21} \quad , \tag{A7}$$

and

$$R_{12} = -R_{21} \quad ,$$

where R represents the reflection coefficient, and the subscripts indicate the same interfaces as those of the transmission coefficients. Substituting Eqs. (A7) into (A6) gives

$$T = (1 - R_{12}^2)\, e^{-\alpha d} \quad . \tag{A8}$$

The experimental quantities which have been measured are the magnitudes $|T|$ and $|R_{12}|$, and the absolute value of Eq. (A8) is

$$|T| = \left[1 - |R_{12}|^2\right] e^{-\alpha d} \quad . \tag{A9}$$

Consequently, α is given by

$$\alpha = \frac{\ell n \left\{ \left[1 - |R_{12}|^2\right] / |T| \right\}}{d} \quad . \tag{A10}$$

Both $|R_{12}|$ and $|T|$ have been measured as a function of frequency in the range 150 to 500 kHz for each of the three samples. From these measurements α can be determined according to Eq. (A10). In Chapter III of this report, it was pointed out that if α has a first power frequency dependence, then k could be written as

$$k = k_o\left(1 + i\,\frac{\alpha'}{2\pi}\right) \quad , \tag{A11}$$

where

$$\alpha' = \lambda\alpha \quad , \tag{A12}$$

and λ is the wavelength in the material.

The values of α and α' for each of the mixtures are given in Table A4. The value of α' is also plotted in Dwg. AS-71-359 as a function of frequency. From the drawing it appears that α' is a constant, and consequently α does indeed have a first-power frequency dependence.

TABLE A4

THE MEASUREMENT OF THE ABSORPTION COEFFICIENT VERSUS FREQUENCY

Frequency	Pure Scotchcast α (in.$^{-1}$)	α'	Mixture 1:1 α(in.$^{-1}$)	α'	Mixture 1:3 α(in.$^{-1}$)	α'
150	0.34/in.	0.159	0.39/in.	0.194	0.49/in.	0.300
200	0.37/in.	0.129	0.38/in.	0.142	0.52/in.	0.239
250	0.46/in.	0.129	0.64/in.	0.192	0.45/in.	0.165
300	0.65/in.	0.152	0.83/in.	0.207	0.68/in.	0.208
350	0.73/in.	0.146	0.77/in.	0.165	0.84/in.	0.220
400	0.81/in	0.142	0.97/in.	0.182	0.95/in.	0.218
450	0.98/in.	0.152	1.17/in.	0.195	1.07/in.	0.218
500	1.29/in.	0.180	1.46/in.	0.219	1.16/in.	0.213
	0.149 ± 0.016 Mean		0.187 ± 0.023 Mean		0.223 ± 0.034 Mean	

If the mean value of the absorption is scaled to a frequency of 3.5 kHz, it is found that the absorption in dB per foot for each of these materials is

Pure Scotchcast — 0.85 dB/ft
Mixture 1:1 — 1.09 dB/ft
Mixture 1:3 — 1.29 dB/ft .

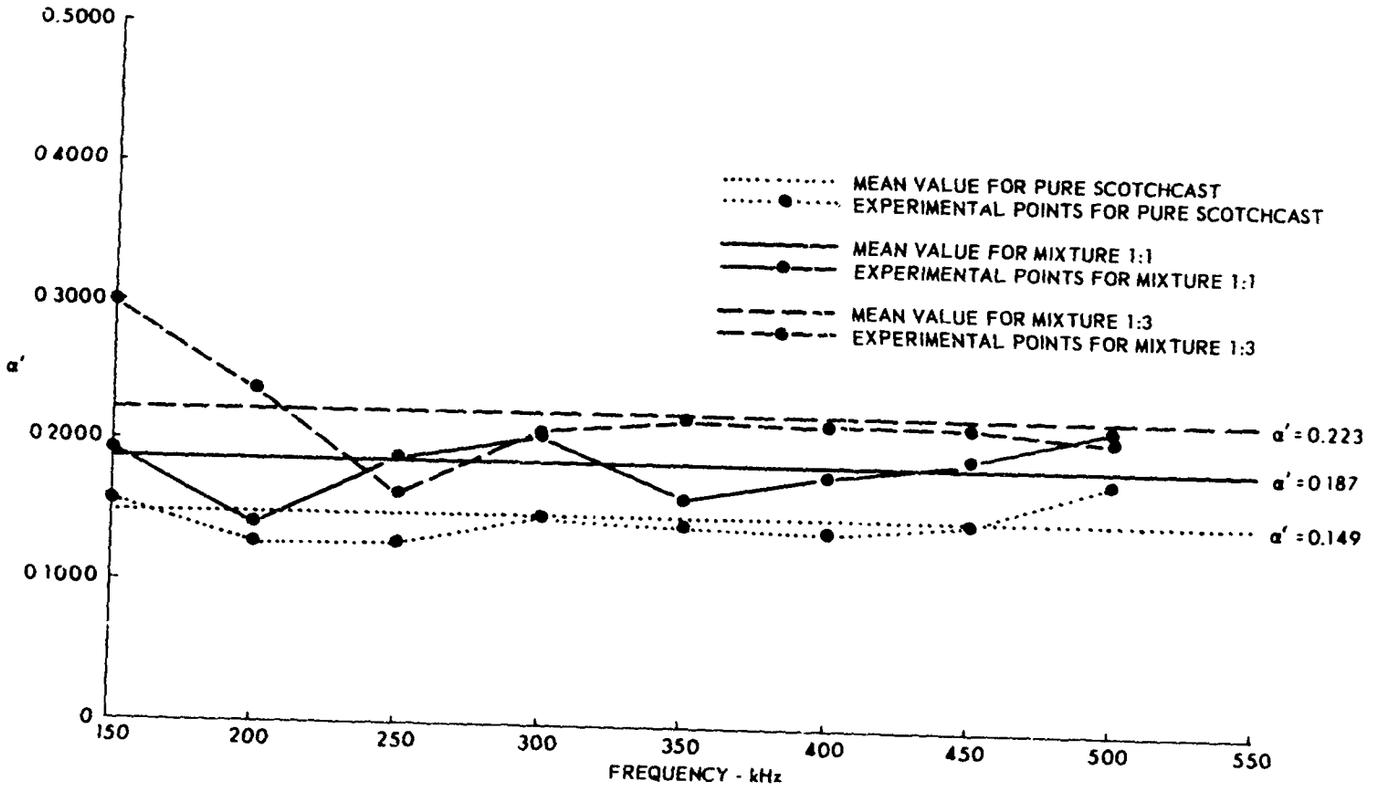

ARL - UT
AS-71-359
PJW - RHC
4 - 20 - 71

THE ATTENUATION PER WAVELENGTH *vs* FREQUENCY

These values are quite typical of those actually occurring in ocean bottoms.

5. Summary

The mean or best values of the data presented in Tables A1 - A4 are collected into Table A5. On the whole, the errors in the measurements are on the order of 3% or less except for the absorption coefficient, for which the error is about 10%. The greater dispersion in the absorption coefficient values arises because of the difficulty of measuring the reflection coefficient at normal incidence. The difficulty was simply geometrical; the precision of the positioning system used was not good enough to be certain that the transducer beam was perpendicular to the sample at each measurement.

The most striking feature of the physical parameters given in Table A5 is the excellent modeling obtained. The values are quite typical of higher speed bottoms ($c_{bottom} > c_{water}$) and are also completely consistent for modeling purposes (that is, none of the parameter values are anomalous with respect to the other values).

TABLE A5

SUMMARY OF THE PHYSICAL PARAMETERS

OF SCOTCHCAST-SAND MIXTURES

	Density (g/cm^3)	Porosity (Percent)	Shear Velocity (m/sec)	Compressional Velocity (m/sec)	Absorption Coefficient α'
Pure Scotchcast 221	1.06 ± 0.01	100%	35.3 ± 1.4	1777 ± 28	0.149 ± 0.016
Mixture 1:1	1.51 ± 0.02	71.5%	—	1903 ± 56	0.187 ± 0.023
Mixture 1:3	1.86 ± 0.06	45.6%	—	2333 ± 61	0.223 ± 0.034

APPENDIX B

Personnel on Contract N00024-70-C-1279

Name	Degree	Period
M. L. Boyd	B.S. in Physics	April 1970 - March 1971
R. L. Deavenport	M.A. (Math)	April 1970 - March 1971
H. G. Frey	M.S. in Physics	April 1970 - March 1971
P. J. Welton	B.A. (Math/Physics)	April 1970 - March 1971

REFERENCES

1. E. Y. T. Kuo, "Wave Scattering and Transmission at Irregular Surfaces," J. Acoust. Soc. Am. 36, 2135-2142 (1964).

2. K. V. Mackenzie, "Reflection of Sound from Coastal Bottoms," J. Acoust. Soc. Am. 32, 221-231 (1960).

3. E. L. Hamilton, et al.,"Acoustic and Other Physical Properties of Shallow Water Sediments," J. Acoust. Soc. Am. 28, 1-15 (1956).

4. C. S. Clay, "Estimation of the Statistical Properties of the Ocean Bottom," Hudson Laboratories Technical Report No. 138 (December 1967).

5. I. Tolstoy and C. S. Clay, Ocean Acoustics (McGraw-Hill Book Co., Inc., New York (1966).

6. K. Krishen and W. W. Koepsel, "Analysis of Acoustic Wave Scattering from a Rough Layer," J. Acoust. Soc. Am. 46, 617-622 (1969).

7. C. Eckart, "The Scattering of Sound from the Sea Surface," J. Acoust. Soc. Am. 25, 566-570 (1953).

8. A. K. Fung and Hsiao-Lien Chan, "Backscattering of Waves by Composite Rough Surfaces," IEEE Ant. Propagat. AP-17, 590-597 (1969)

9. B. E. Parkins, "Omnidirectional Scattering of Acoustic Waves by Rough Imperfectly Reflecting Surfaces," J. Acoust. Soc. Am. 41, 126-134 (1967).

10. A. A. Kovalev and S. I. Pozdnyak, Radiotekn 16, 28-33 (1961).

11. A. K. Fung, R. K. Moore, and B. E. Parkins, "Notes on Backscattering and Depolarization by Gently Undulating Surfaces," J. Geophys. Res. 70, 1559-1562 (1965).

12. P. Beckmann, "Depolarization of Electromagnetic Waves Backscattered from the Lunar Surface," J. Geophys. Res. 73, 649-655 (1968).

REFERENCES (Cont'd)

13. D. E. Barrick and W. H. Peake, "Scattering from Surfaces with Different Roughness Scales; Analysis and Interpretation," Research Report BAT-197A-10-3, Battelle Memorial Institute, Columbus Laboratories, 1 November 1967.

14. T. Hagfors, "Scattering and Transmission of Electromagnetic Waves at a Statistically Rough Boundary between Two Dielectric Media," in Electromagnetic Wave Theory Part 2 (Pergamon Press, New York, 1967), pp. 997-1012.

15. L. M. Brekhovskikh, Waves in Layered Media (Academic Press, London and New York, 1960), Chapter 4.

16. T. Hagfors, "Backscattering from an Undulating Surface with Applications to Radar Returns from the Moon," J. Geophys. Res. 69, 3779-3783 (1964).

17. A. Stogryn, "Electromagnetic Scattering from Rough, Finitely Conducting Surfaces," Radio Science 2, 415-428 (1967).

18. B. C. Heezen, et al., "Physiographic Provinces and Acoustic Domains" JUA(USN) 17, 15-24 (January 1967).

19. R. M. Pratt, "The Ocean Bottom," Science 138, 492-495 (1962).

20. R. B. Patterson, "Relationships between Acoustic Backscatter and Geological Characteristics of the Deep Ocean Floor," J. Acoust. Soc. Am. 46, 756-761 (1969).

21. W. B. Randlett and N. J. DiPiazza, "Bottom Reflection Loss Measurements in the Western North Atlantic," Proceedings of the 22nd Navy Symposium on Underwater Acoustics, Washington, D. C., ONR Symposium Report ACR-110 (1964).

22. G. H. Sutton, et al., "Physical Analysis of Deep Sea Sediments," Geophysics 24, 779 (October 1957).

23. A. Shumway, "Sound Speed and Absorption Studies of Marine Sediments by a Resonance Method," Parts I and II, Geophysics 25, 451, 659 (1960).

24. E. Hamilton, "Thickness and Consolidation of Deep Sea Sediments," Bull. Geop. Soc. Am. 70, 1399 (November 1959).

REFERENCES (Cont'd)

25. J. Nafe and C. Drake, "Variation with Depth in Shallow and Deep Water Marine Sediments of Porosity, Density, and the Velocities of Compressional and Shear Waves," Geophysics 22, 523 (July 1957).

26. L. Hampton, "Acoustic Properties of Sediments," J. Acoust. Soc. Am. 42, 882 (1967).

27. A. Wood and D. Weston, "The Propagation of Sound in Mud," Acustica 14, 156 (1964).

28. B. Cole, "Marine Sediment Attenuation and Ocean-Bottom Reflected Sound," J. Acoust. Soc. Am. 38, 291 (1965).

29. B. F. Kur'yanov, "The Scattering of Sound at a Rough Surface with Two Types of Irregularity," Sov. Phys.-Acoust. 8, 252-257 (1963).

30. P. Beckmann, "Scattering by Composite Rough Surfaces," Proc. IEEE 53, 1012-1015 (1965).

31. I. M. Fuks, "Theory of Radio Wave Scattering at a Rough Sea Surface," Radiofizika 9, 876-887 (1966).

32. L. A. Volovova and Yu. Yu. Zhitkovskiy, "Acoustic Determination of Some Irregularities of the Ocean Floor," Oceanology (USSR) 6, 867-871 (1966).

33. Yu. Yu. Zhitkovskiy and Yu. P. Lysanov, "Reflection and Scattering of Sound from the Ocean Bottom (Review)," Sov. Phys.-Acoust. 13, 1-13 (1967).

34. P. B. Schmidt, "Bottom Reverberation Measurements in the Norwegian Sea and North Atlantic Ocean," Informal Report No. 69-38, Naval Oceanographic Office (1969).

35. A. W. Nolle, et al., "Acoustical Properties of Water-Filled Sands," J. Acoust. Soc. Am. 35, 1394-1408 (1963).

36. Yu. Yu. Zhitkovskiy, "An Acoustic Method for Measuring Distances Between Irregularities on the Ocean Floor," Oceanology (USSR) 6, 874-875 (1966).

37. L. M. Brekhovskikh, "On the Role of Acoustics in Exploring the Ocean," Atmospheric and Ocean Phys. Series 1, 1050-1064 (1965).

REFERENCES (Cont'd)

38. A. D. Lapin, "Scattering of Sound Waves in Irregular Waveguides," Sov. Phys.-Acoust. 4, 272-279 (1958).

39. A. D. Lapin, "Sound Scattering in an Irregular Waveguide at the Normal Mode Critical Frequencies," Sov. Phys.-Acoust. 15, 490-493 (1970).

40. A. D. Lapin, "Sound Propagation in Inhomogeneous Waveguides," Sov. Phys.-Acoust. 13, 198-200 (1967).

41. Yu. P. Lysanov, "On the Field of A Point Radiator in a Laminar-Inhomogeneous Medium Bounded by an Uneven Surface," Sov. Phys.-Acoust. 7, 255-257 (1962).

42. Yu. P. Lysanov, "Influence of Inhomogeneity of the Medium on Wave Scattering by an Uneven Surface," Sov. Phys.-Acoust. 13, 66-70 (1967).

43. Yu. P. Lysanov, "Mean Coefficient of Reflection from an Uneven Surface Bounding an Inhomogeneous Medium," Sov. Phys.-Acoust. 15, 340-344 (1970).

44. H. P. Bucker, "Sound Propagation in a Channel with Lossy Boundaries," J. Acoust. Soc. Am. 48, 1187-1194 (1970).

45. H. P. Bucker, "Normal Mode Solution for Sound Propagation in a Surface Duct with a Rough Surface" (U), JUA(USN) 19, 13-28 (January 1969). (CONFIDENTIAL)

46. H. W. Marsh, "Sound Reflection and Scattering from the Sea Surface," J. Acoust. Soc. Am. 35, 240-244 (1963).

47. C. S. Clay, "Effect of a Slightly Irregular Boundary on the Coherence of Waveguide Propagation," J. Acoust. Soc. Am. 36, 833-837 (1964).

48. W. C. Meecham, "Propagation of Radiation in an Inhomogeneous Medium Near an Irregular Surface," J. Acoust. Soc. Am. 25, 1012(L) (1953).

49. J. G. Parker and R. W. Bryant, "A Statistical Ray Theory of Sound Propagation in Oceanic Isothermal Surface Layers," Naval Research Laboratory Report No. 4196 (20 July 1953).

50. B. J. Schweitzer, "Sound Scattering into the Shadow Zone Below an Isothermal Layer," J. Acoust. Soc. Am. 44, 525-530 (1968).

REFERENCES (Cont'd)

51. H. N. Van Ness, "Calculation of the Scattered Field in the Shadow Zone," JUA(USN) 19, 47-54 (January 1969).

52. A. D. Seifer and N. J. Jacobson," Ray Transmissions in an Underwater Acoustic Duct with a Pseudorandom Bottom," J. Acoust. Soc. Am. 43, 1395-1403 (1968).

53. Yu. P. Lysanov, "Average Decay Law in a Surface Sound Channel with an Uneven Boundary," Sov. Phys.-Acousts. 12, 425-427 (1967).

54. M. Schulkin, "The Propagation of Sound in Imperfect Ocean Surface Ducts," U.S. Navy Underwater Sound Laboratory Report No. 1013 (22 April 1969).

55. R. J. Urick, "Intensity Summation of Modes and Images in Shallow-Water Sound Transmission," J. Acoust. Soc. Am. 46, 780-788 (1969).

56. A. D. Watt, VLF Radio Engineering (Pergamon Press, Oxford, 1967), pp. 244-255.

57. H. W. Marsh, M. Schulkin, and S. G. Kneale, "Scattering of Underwater Sound by the Sea Surface," J. Acoust. Soc. Am. 33, 334-340 (1961).

58. H. P. Bucker and H. E. Morris, "Epstein Normal-Mode Model of a Surface Duct," J. Acoust. Soc. Am. 41, 1475-1478 (1967).

59. M. A. Pedersen and D. F. Gordon, "Normal Mode Theory Applied to Short-Range Propagation in an Underwater Acoustic Surface Duct," J. Acoust. Soc. Am. 37, 105-118 (1965).

60. M. A. Pedersen and D. White, "Ray Theory of the General Epstein Profile," J. Acoust. Soc. Am. 44, 765-786 (1968).